

**STUDIES ON SOME SIMPLE AND ZEOLITE-Y ENCAPSULATED  
3d-TRANSITION METAL COMPLEXES OF  
SCHIFF BASES DERIVED FROM 2-AMINOBENZOTHAZOLE**

**THESIS SUBMITTED TO THE  
COCHIN UNIVERSITY OF SCIENCE AND TECHNOLOGY  
IN PARTIAL FULFILMENT OF THE  
REQUIREMENTS FOR THE DEGREE OF**

**DOCTOR OF PHILOSOPHY**

**IN**

**CHEMISTRY**

**UNDER THE FACULTY OF SCIENCE**

**BY**

**P. JELAJA**

**DEPARTMENT OF APPLIED CHEMISTRY  
COCHIN UNIVERSITY OF SCIENCE AND TECHNOLOGY  
KOCHI - 682 022, KERALA**

**FEBRUARY 2003**

## CERTIFICATE

This is to certify that the thesis entitled “Studies on some simple and zeolite-Y encapsulated 3d-transition metal complexes of Schiff bases derived from 2-aminobenzothiazole” submitted by Mrs. P. Jelaja is a bonafide record of research work carried out by the author under my supervision, in partial fulfillment of the requirements for the degree of Doctor of Philosophy of Cochin University of Science and Technology, and further that no part of this has been presented before for any other degree.



Prof. (Dr). K.K. Mohammed Yusuff,  
Department of Applied Chemistry,  
Cochin University of Science and Technology

Kochi-22.  
25-02-2003

## PREFACE

In recent years considerable amount of work has been devoted to synthesize transition metal complexes. In this regard Schiff base complexes have attracted wide attention. Furthermore, such complexes are found to play important role in analytical chemistry, organic synthesis, metallurgy, refining of metals, electroplating and photography. Many Schiff base complexes are reported in literature. Their properties depend on the nature of the metal ion as well as on the nature of the ligand. By altering the ligands it is possible to obtain desired electronic environment around the metal ion. Thus there is a continuing interest in the synthesis of simple and zeolite encapsulated Schiff base complexes of metal ions.

Zeolites have a number of striking structural similarities to the protein portion of natural enzymes. Zeolite based catalysts are known for their remarkable ability of mimicking the chemistry of biological systems. In view of the importance of catalysts in all the areas of modern chemical industries, an effort has been made to synthesize some simple Schiff base complexes, heterogenize them by encapsulating within the supercages of zeolite Y cavities and to study their applications.

The thesis deals with studies on the synthesis and characterization of some simple and zeolite Y encapsulated Mn(II), Fe(III), Co(II), Ni(II) and Cu(II) complexes and on the catalytic activity of these complexes on some oxidation reactions. The thesis is divided into eight chapters. Chapter I of the thesis presents a general introduction to the simple and zeolite Y encapsulated Schiff base complexes and the development in the field of homogeneous and heterogeneous catalytic systems. Chapter II deals with the experimental techniques used for the preparation and purification of ligands, simple

complexes and encapsulation procedure of zeoliteY complexes. The various physico-chemical techniques used for the characterization of simple and zeoliteY encapsulated complexes are also presented in this chapter. In Chapter III, details regarding the studies on the synthesis and characterization of Mn(II), Fe(III), Co(II), Ni(II) and Cu(II) complexes of the Schiff base derived from 2-aminobenzothiazole and salicylaldehyde (SBT) are provided. Chapter IV is on the synthesis and characterization of Mn(II), Fe(III), Co(II), Ni(II) and Cu(II) complexes of the Schiff base derived from 2-aminobenzothiazole and vanillin (VBT),. Studies involving the preparation and characterization of zeoliteY encapsulated SBT and VBT complexes of these metal ions are presented in Chapter V and Chapter VI respectively. In Chapter VII, the details regarding the preparation and characterization of zeoliteY encapsulated 2-aminobenzothiazole complexes of Mn(II), Fe(III), Co(II), Ni(II) and Cu(II) are presented. Chapter VIII of the thesis describes the studies on application of all the above mentioned complexes as catalysts for the decomposition of hydrogen peroxide, oxidations of benzaldehyde, benzyl alcohol, 1- propanol and 2-propanol by acid potassium permanganate and for the oxidation of cyclohexanol by hydrogen peroxide. Summary and conclusions are provided at the end of the thesis. References are provided at the end of appropriate chapters.



## CONTENTS

|  | Page No. |
|--|----------|
| <b>CHAPTER. I. Introduction.</b>   | 1        |
| 1.2. Schiff base complexes.  | 2        |
| 1.3. Synthesis of zeoliteY encapsulated complexes.                                     | 7        |
| 1.3.1 Flexible ligand method.  | 11       |
| 1.3.2. Ship-in - the - bottle (the template synthesis) method.                         | 12       |
| 1.3.3. Zeolite synthesis (crystallization inclusion) method.                           | 13       |
| 1.4. Homogeneous and heterogeneous catalysis.  | 14       |
| 1.5. Schiff base complexes as catalysts.   | 19       |
| 1.6. Zeolite Y encapsulated Schiff base complexes as catalysts.                        | 23       |
| 1.7. Scope of the present investigation.   | 24       |
| References.  | 27       |
| <br>   |          |
| <b>CHAPTER. II. Experimental techniques.</b>   |          |
| 2.1. Introduction.   | 36       |
| 2.2. Reagents.   | 36       |
| <b>2.3. Preparation of Schiff base ligands.</b>  |          |
| 2.3.1. Salicylalidene -2-aminobenzothiazole (SBT).                                     | 37       |
| 2.3.2. 4-Hydroxy-3- methoxybenzalidene-<br>2- aminobenzothiazole (VBT).                | 37       |
| <b>2.4. Synthesis of zeoliteY supported metal complexes.</b>                           |          |
| 2.4.1. Modification of zeoliteY to zeolite NaY.  | 38       |
| 2.4.2. Modification of zeolite NaY to<br>metal exchanged zeoliteY (MY).                | 38       |
| 2.4.3. Encapsulation of metal complexes in zeoliteY.                                   | 39       |
| <b>2.5. Analytical methods.</b>  |          |
| 2.5.1. Estimation of metal content in simple complexes.                                | 39       |
| 2.5.2. Estimation of Si,Al,Na and transition metal ion<br>content in zeoliteY samples. | 40       |
| 2.5.3. C H N analyses.   | 41       |

|             |  |           |
|-------------|--|-----------|
| 2.5.4.      | Estimation of halogen and sulphur.     | 41        |
| <b>2.6.</b> | <b>Physico-chemical methods.</b>       |           |
| 2.6.1.      | Conductance measurements.              | 42        |
| 2.6.2.      | Magnetic susceptibility measurements.  | 42        |
| 2.6.3.      | Surface area and pore volume analyses. | 43        |
| 2.6.4.      | X-ray diffraction studies (XRD).       | 43        |
| 2.6.5.      | Electronic spectra.                    | 44        |
| 2.6.6.      | Diffuse reflectance spectra (DRS).     | 45        |
| 2.6.7.      | FTIR spectra.                          | 45        |
| 2.6.8.      | EPR spectra.                           | 45        |
| 2.6.9.      | Thermogravimetric analysis.            | 46        |
| 2.6.10.     | Scanning electron microscopy (SEM).    | 47        |
| <b>2.7.</b> | <b>Catalytic activity studies.</b>     | <b>47</b> |
|             | References.                            | 49        |

**CHAPTER. III. Mn(II), Fe(III), Co(II), Ni(II) and Cu(II) complexes of the Schiff base derived from salicylaldehyde and 2-aminobenzothiazole.**

|            |                                |           |
|------------|--------------------------------|-----------|
| 3.1.       | Introduction.                  | 50        |
| <b>3.2</b> | <b>Experimental.</b>           | <b>51</b> |
| 3.2.1.     | Materials.                     | 51        |
| 3.2.2.     | Synthesis of the complexes.    | 51        |
| 3.2.3.     | Analytical methods.            | 52        |
| <b>3.3</b> | <b>Results and Discussion.</b> | <b>52</b> |
| 3.3.1.     | Elemental analysis.            | 52        |
| 3.3.2.     | Conductance measurements.      | 54        |
| 3.3.3.     | Magnetic susceptibility.       | 55        |
| 3.3.4.     | Electronic spectra.            | 56        |
| 3.3.5      | FTIR spectra.                  | 59        |
| 3.3.6.     | EPR spectra.                   | 62        |

|        |                             |    |
|--------|-----------------------------|----|
| 3.3.7. | Thermogravimetric analysis. | 63 |
|        | References.                 | 66 |

**CHAPTER. IV. Mn(II), Fe(III), Co(II), Ni(II) and Cu(II) complexes of the Schiff base derived from vanillin and 2-aminobenzothiazole.**

|             |                                |    |
|-------------|--------------------------------|----|
| 4.1.        | Introduction.                  | 68 |
| <b>4.2.</b> | <b>Experimental.</b>           | 69 |
| 4.2.1.      | Materials.                     | 69 |
| 4.2.2.      | Synthesis of the complexes.    | 69 |
| 4.2.3.      | Analytical methods.            | 70 |
| <b>4.3.</b> | <b>Results and Discussion.</b> | 70 |
| 4.3.1.      | Elemental analysis.            | 70 |
| 4.3.2.      | Conductance measurements.      | 71 |
| 4.3.3.      | Magnetic susceptibility.       | 72 |
| 4.3.4.      | Electronic spectra.            | 73 |
| 4.3.5.      | FTIR spectra.                  | 75 |
| 4.3.6.      | EPR spectra.                   | 77 |
| 4.3.7.      | Thermogravimetric analysis.    | 79 |
|             | References.                    | 81 |

**CHAPTER.V. ZeoliteY encapsulated Mn(II), Fe(III), Co(II), Ni(II) and Cu(II) complexes of the Schiff base derived from salicylaldehyde and 2-aminobenzothiazole.**

|             |   |    |
|-------------|---|----|
| 5.1.        | Introduction.                                     | 82 |
| <b>5.2.</b> | <b>Experimental.</b>                              | 82 |
| 5.2.1.      | Materials.  | 82 |
| 5.2.2.      | Synthesis of zeoliteY encapsulated SBT complexes. | 83 |

|             |  |     |
|-------------|--|-----|
| <b>5.3.</b> | <b>Results and discussion.</b>         | 84  |
| 5.3.1.      | Elemental analysis.                    | 84  |
| 5.3.2.      | Surface area and pore volume analysis. | 86  |
| 5.3.3.      | X-ray diffraction studies.             | 88  |
| 5.3.4.      | Magnetic susceptibility.               | 89  |
| 5.3.5.      | Diffuse reflectance spectra.           | 91  |
| 5.3.6.      | FTIR spectra.                          | 94  |
| 5.3.7.      | EPR spectra.                           | 96  |
| 5.3.8.      | Thermogravimetric analysis.            | 98  |
|             | References.                            | 100 |

**CHAPTER.VI. Zeolite Y encapsulated Mn(II), Fe(III), Co(II), Ni(II) and Cu(II) complexes of the Schiff base derived from vanillin and 2-aminobenzothiazole.**

|             |   |     |
|-------------|---|-----|
| 6.1.        | Introduction.                                     | 102 |
| <b>6.2</b>  | <b>Experimental.</b>                              | 103 |
| 6.2.1       | Materials.  | 103 |
| 6.2.2.      | Synthesis of zeoliteY encapsulated VBT complexes. | 103 |
| <b>6.3.</b> | <b>Results and Discussion.</b>                    | 104 |
| 6.3.1.      | Elemental analysis.                               | 104 |
| 6.3.2.      | Surface area and pore volume analysis.            | 105 |
| 6.3.3.      | X-ray diffraction studies.                        | 107 |
| 6.3.4.      | Magnetic susceptibility.                          | 107 |
| 6.3.5.      | Diffuse reflectance spectra.                      | 109 |
| 6.3.6.      | FTIR spectra.                                     | 112 |
| 6.3.7.      | EPR spectra.                                      | 114 |
| 6.3.8.      | Thermogravimetric analysis.                       | 115 |
|             | References.                                       | 116 |

**CHAPTER.VII. Zeolite Y encapsulated  
Mn(II), Fe(III), Co(II), Ni(II) and Cu(II)  
complexes of 2-aminobenzothiazole.**

|             |   |     |
|-------------|---|-----|
| 7.1.        | Introduction.                                     | 118 |
| <b>7.2.</b> | <b>Experimental.</b>                              | 119 |
| 7.2.1.      | Materials.  | 119 |
| 7.2.2.      | Synthesis of zeoliteY encapsulated ABT complexes. | 119 |
| <b>7.3</b>  | <b>Results and Discussion.</b>                    | 120 |
| 7.3.1.      | Elemental analysis.                               | 120 |
| 7.3.2.      | Surface area and pore volume analysis.            | 121 |
| 7.3.3.      | X-ray diffraction studies.                        | 123 |
| 7.3.4.      | Magnetic susceptibility.                          | 123 |
| 7.3.5.      | Diffuse reflectance spectra.                      | 125 |
| 7.3.6.      | FTIR spectra.                                     | 128 |
| 7.3.7.      | EPR spectra.                                      | 130 |
| 7.3.8.      | Thermogravimetric analysis.                       | 131 |
|             | References.                                       | 133 |

**Chapter. VIII. Studies on catalytic activity of simple and  
zeoliteY encapsulated transition metal complexes.**

|                |  |     |
|----------------|--|-----|
| 8.1.           | Introduction.  | 134 |
| <b>VIII.A.</b> | <b>Catalytic activity of the simple and zeoliteY encapsulated<br/>complexes on decomposition of hydrogen peroxide.</b> |     |
| 8.A.1.         | Introduction.  | 136 |
| 8.A.2.         | Experimental.  | 137 |
| 8.A.3.         | Results and Discussion.  | 140 |

|                |   |            |
|----------------|---|------------|
| <b>VIII.B.</b> | <b>Catalytic activity on oxidation of benzaldehyde<br/>by acid potassium permanganate.</b>  |            |
| 8.B.1.         | Introduction.   | 145        |
| 8.B.2.         | Experimental.   | 145        |
| 8.B.3.         | Results and Discussion.   | 148        |
| <b>VIII.C.</b> | <b>Catalytic activity on the oxidation of benzyl alcohol,<br/>propan-1-ol and propan-2-ol by<br/>acid potassium permanganate.</b> |            |
| 8.C.1.         | Introduction.   | 156        |
| 8.C.2.         | Experimental.   | 157        |
| 8.C.3.         | Results and Discussion.   | 160        |
| <b>VIII.D.</b> | <b>Catalytic activity on partial oxidation of cyclohexanol<br/>to cyclohexanone by hydrogen peroxide.</b>                         |            |
| 8.D.1.         | Introduction.   | 166        |
| 8.D.2.         | Experimental.   | 167        |
| 8.D.3.         | Results and Discussion.   | 169        |
|                | References.   | 172.       |
|                | <b>SUMMARY AND CONCLUSIONS.</b>   | <b>177</b> |

\*

# CHAPTER I



## INTRODUCTION

Coordination chemistry has become an exciting field of research rather than a closed body of knowledge. Large numbers of articles on coordination compounds are being published every week. New synthetic techniques allow the identification of enormous numbers of interesting complexes and in the laboratory they continue to provide synthetic challenges. Metal complex catalyzed reactions now constitute another extensive field of chemical research embracing reactions occurring both in living systems and under the conditions of industrial manufacture. Industrially important reactions of this type include liquid phase oxidation of paraffins and alkyl arenes, the oxidation of alkenes to carbonyl compounds, vinyl and aryl esters and numerous alkene epoxidation processes.

A feature of modern coordination chemistry is the increasing number, complexity and variety of new ligands. Schiff bases<sup>1</sup> are the most important and widely studied class of chelating ligands due to the wide possibility of synthesizing a large number of Schiff bases from a single aldehyde or an amine by a mere alteration of the substituents in them. The most common method of obtaining them is the direct condensation of primary amines with aldehydes or ketones and thus it contains an azomethine group ( $>C=N-$ ). Among the enormous numbers of coordination compounds, transition metal complexes of Schiff bases have been extensively studied due to their preparative accessibility, application in catalysis and as models for biologically important species.

## 1.2. Schiff base complexes.

Schiff base complexes have attracted wide attention due to their similarity in nature to the prosthetic part of proteins and enzymes. Furthermore, such types of complexes are found to play important role in analytical chemistry, organic synthesis, metallurgy, refining of metals, electroplating and photography. Pfeiffer and co-workers<sup>2</sup> have made a systematic study on Schiff base complexes. Their properties depend on the nature of the metal ion as well as on the nature of the ligands. By altering the ligands it is possible to obtain desired electronic environment around the metal ion. Thus there is a continuing interest in the synthesis of Schiff base complexes of metal ions due to their preparative convenience<sup>3-5</sup> and applications in catalysis<sup>6,7</sup>. Their ready synthesis and myriad properties have contributed greatly to their popularity and to the study of many biological systems<sup>8</sup>.

A review on metal complexes of Schiff bases by Holm et.al<sup>9</sup> shows that more than half of these reported complexes were derived from salicylaldehyde. Complexes of Schiff base ligands derived from salicylaldehyde was first used by Pfeiffer and Tsumaki<sup>10</sup>. A wide variety of ligands with salicylaldehyde may be obtained through condensation of a primary amine, which vary in denticity, flexibility, nature of donor atoms and in electronic properties. Recently, it has been reported that the metal complexes of ligands containing electron-withdrawing group exhibit improved biological activity. Some of the important classes of ligand derived from salicylaldehyde are shown in Figure.I.1. Alterations in coordinating characteristics can be achieved within each class by variations in the nature of R –groups and in the nature of phenyl ring substituents.

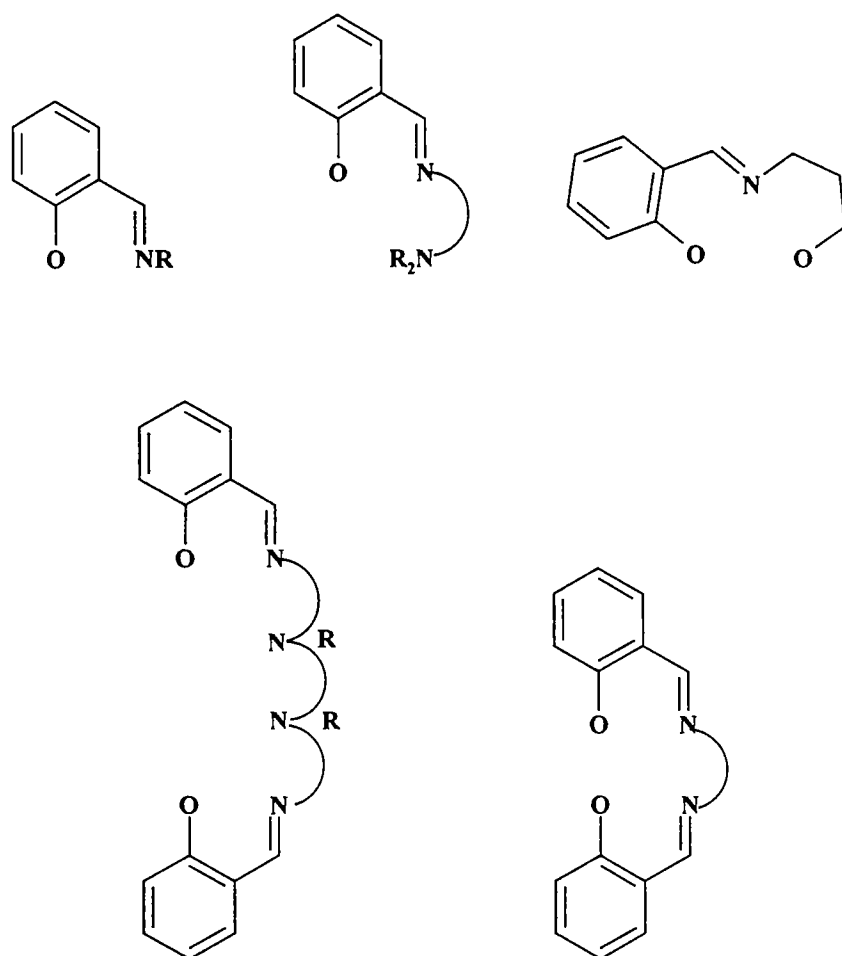


Figure. I.1. Some Schiff base ligands derived from salicylaldehyde.

Condensation of two equivalents of salicylaldehyde with diaminoethane (en), gives tetradentate Schiff base ligand 'salen'. These compounds were reported to act as bidentate ligand through oxygen atoms towards transition and non-transition metals<sup>11</sup>. Different monomeric or dimeric complexes were obtained from salen according to the method of preparation or isolation. The monomeric and dimeric  $\text{Fe}(\text{salen})\text{X}$  ( $\text{X} = \text{Cl} / \text{Br}$ )

complexes and various ring substituted derivatives are reported in which they are readily distinguished on the basis of their magnetic properties<sup>12</sup>. Tetrametallic complexes having four different metals have been prepared by reacting substituted ferrocene with salen<sup>13</sup>.

Sulphur containing Schiff base complexes have found various use in medicines such as antituberculous<sup>14</sup>, hipnotics<sup>15</sup>, local anesthetics<sup>16</sup> rodentisides<sup>17</sup> and antispasmodics<sup>18</sup>. Hypoglycemic activity<sup>19</sup> has also been claimed in some derivatives. Schiff base complexes are well known to have pronounced biological activities<sup>19-22</sup>.

Quinque-dentate Schiff base containing disulphide groups derived from salicylaldehyde and 2-aminophenyldisulphide and 2-aminoethyldisulphide were complexed with Ni(II) ions and the electrochemistry of the complexes so synthesized were reported<sup>23</sup>. Spectroscopic properties and magnetic behaviours of the N-substituted salicylaldimine ligands and their Co(III) and Cu(II) complexes were studied and the molecular structure were determined by three dimensional single crystal X-ray analysis<sup>24</sup>. Biological activity of some N-(salicylidene-glutamato)copper(II) complexes containing imidazole derivatives were reported<sup>25</sup>. The prepared complexes were Cu(sal-L-glu)X, and Cu(sal-DL-glu)X, where X= 2-methylimidazole or 4-ethylimidazole. The complexes adopt square pyramidal arrangement and also exhibit significant efficiency against the bacteria *Staphylococcus aureus*. Three salen type heterocyclic Schiff base complexes of YCl<sub>3</sub> derived from 2-amino-5-phenylazopyridine and salicylaldehyde, 5-nitrosalicylaldehyde or 4-hydroxy-3-methoxybenzaldehyde (vanillin) were synthesized and characterized<sup>26,27</sup>.

A new method for the synthesis of metal complexes with thiolate coordination was described<sup>28</sup>. In this method the reaction of

2,2'-dithiodibenzaldehyde with Ni(II) complexes containing coordinated primary amines in methanol results in the Schiff base condensation. This method was used to synthesize Ni(II) complexes of varying N/S donor sets. Synthesis, characterization and bacterial properties of Ni(II), Cu(II) and Zn(II) metal chelates with some thiazole derived Schiff bases of salicylaldehyde derivatives were reported<sup>29</sup>. They were screened for their bio-activity against *E.Coli*, *S.aureous*, *P.aeruginosa* and *K.pneumonea*. These metal chelates were found to possess more antibacterial activity than the uncomplexed Schiff bases. Manganese salen complexes have recently found use as combined superoxide dismutase/catalase antioxidant mimics with pharmacological use in the treatment of diseases associated with cell or tissue damage produced by reactive oxygen species superoxide ion, H<sub>2</sub>O<sub>2</sub> and the hydroxyl radical.

Schiff bases derived from thiazole derivatives are reported to have significant anticancer activity<sup>30-35</sup>. Many of the anticancer drugs are viable ligands<sup>36</sup>. Some of these drugs exhibit increased anticancer activity when administered as metal complexes<sup>37,38</sup>. Physical characteristics and antifungal activity of several Schiff bases derived from 4-aryl-2-aminothiazoles, substituted 2-aminobenzothiazoles, 4-aryl-2-aminothiazole methiodides, 4-aryl-2-substituted-methylaminothiazoles or 2-(2'-hydroxyphenyl or naphthyl)-3-(4'-arythiazol-2''-yl)-4-thiazolidones and vanillin were extensively studied<sup>39,40</sup>. Sixteen Schiff base complexes of Co, Ni, Cu, and Zn derived from substituted thiazoles and substituted salicylaldehydes were prepared and tested for their antineoplastic potency against L-1210 lymphoid leukemia<sup>41</sup>.

Synthesis and characterization of a series of Hg(II) complexes with substituted aminobenzothiazoles were reported by Guru<sup>42</sup>.et.al. Investigation

on the preparation and characterization of Co(II) and Cu(II) complexes<sup>43</sup> with monodentate 2-amino-6-methylbenzothiazole (L) and 2-amino-6-chlorobenzothiazole (L') of the composition  $[M(L \text{ or } L')_2X_2]$  and  $[ML'_4]Y_2$  where X = Cl<sup>-</sup>, Br<sup>-</sup>, SCN<sup>-</sup>, NO<sub>3</sub><sup>-</sup> or OAc<sup>-</sup> and Y= ClO<sub>4</sub><sup>-</sup> showed that the Co(II) complexes to be tetrahedral and the Cu(II) complexes are square planar in nature.

Many Schiff base complexes have been encapsulated inside the zeolite Y cages and have been used as catalysts for oxidation reactions involving organic compounds. Schiff base salen on treatment with cobalt exchanged zeolite Y in an inert atmosphere results in the formation Co(salen)<sup>44</sup> complex within the  $\alpha$ -cages. The reflectance spectrum of the complexes is almost identical with that of the complex in solution suggesting a retention of the structure of the free complex inside the zeolite cage. The ligand is non-extractable, is also consistent with complex formation. Size exclusion studies have revealed that complex is internally confined in zeolite Y.

Interaction of five different tetra and penta dentate Schiff base chelates with in the Co(II) exchanged zeolite Y were studied and the use of these ligands in the oxygen activation of intrazeolitic Co(II) were compared<sup>45</sup>. Use of these ligands greatly raises the fraction of the Co(II) participating in the oxygen activation even up to 25% of the total Co(II). Mn(III)salen and Fe(III)salen complexes have been entrapped in the supercages of zeolite Y and the redox properties of these complexes were investigated<sup>46</sup> by cyclic voltammetry in acetonitrile and dimethyl sulphoxide solutions. The electroactivity of encapsulated Mnsalen towards the biomimetic activation of molecular oxygen was also studied.

### 1.3. Synthesis of zeolite Y encapsulated complexes.

The polyhedral cavities in zeolite Y inscribes a cavity of substantial dimensions that they could be able to hold clusters of small molecules in addition to the appropriate numbers of exchangeable cations. Proper choice of complex molecule of correct size that fit securely within the  $\sim 13 \text{ \AA}$  supercages of zeolite Y ensures that the molecule cannot escape through the  $\sim 7 \text{ \AA}$  ring opening of the super cage. A wide variety of metal clusters, organometallic compounds and coordination compounds have been encapsulated in a range of different hosts. Such immobilization of known homogeneous complexes on solid supports would combine the advantages of homogeneous and heterogeneous catalysts while minimizing the disadvantages of both. Enhanced selectivity and ease of separation and purification of reactants and products would accompany its activity in solution phase.

Many coordination complexes can be formed within the zeolite pores by simple reaction of the exchangeable cations with various organic molecules. Reviews<sup>47-50</sup> on the early work on mono, bi- and polydentate<sup>51</sup> based complexes are available.

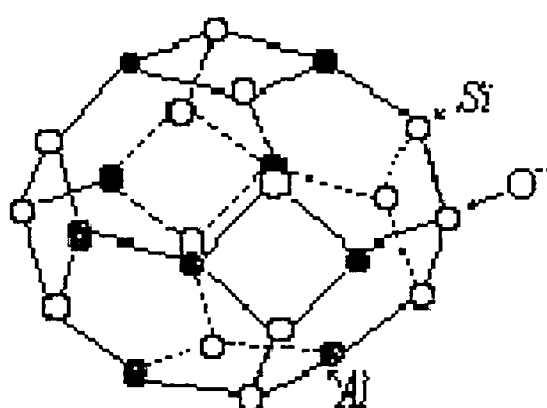
The zeolites<sup>52-60</sup> are built from  $\text{SiO}_4$  and  $\text{AlO}_4$  tetrahedra, which share oxygen atoms at the corners. The crystal skeleton of zeolites consists of aluminium and silicon atoms, each surrounded by four oxygen atoms to form a tetrahedron. These tetrahedra can then be arranged in many ways to form different porous crystal structures. There are 24 such tetrahedra in a sodalite unit (Figure.I.2) which is the basic building block for A-, X-, and Y- type zeolite molecular sieves. A sodalite unit consists of 6 four membered faces and 8 six membered faces. If the sodalite cages are connected to one another at their

hexagonal faces through hexagonal prisms of 6 oxygen atoms, the X- and Y- zeolite structures are formed. The structures of X- and Y- zeolites are identical. These zeolite structures have two types of cavities or pores. The large cavities enclosed within the sodalite framework are referred to as  $\alpha$  - cages with a diameter of 13 Å in X- and Y- zeolites and the smaller cavities are known as  $\beta$ -cages with a diameter 6.5 Å (Figure.I.2). The linking of SiO<sub>4</sub> and AlO<sub>4</sub> tetrahedra always results in lining of the insides of the polyhedron and their polygonal “windows” with anionic oxygens because Al and Si atoms are always buried among the four oxygens of each tetrahedron. The number of tetrahedra forming these windows governs the diameter of channel windows<sup>53</sup>. Zeolites with windows consisting of 6,7,8,9,10,12, and 14 member rings have been synthesized. Size and shape of these windows control the sieving effect of zeolites that result in their adsorption and catalytic performance.

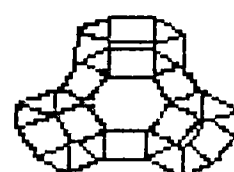
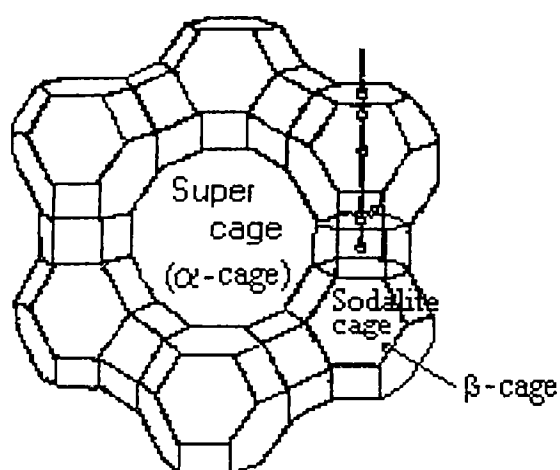
Zeolites with odd membered rings are very rare. Those with even membered rings are usually divided into (i) medium-pore zeolites with 10-membered rings and pore diameter 0.55nm (eg. ZSM-5, ferrierite) (ii) large-pore zeolites with 12-membered rings and pore diameter 0.75nm (eg. zeoliteY, Beta, mordenite) and (iii) extra-large zeolites with 14-membered rings and pore diameter 1nm (eg.CIT-5 and UTD-1). Zeolites also differ in the dimensionality of their channels, with one-dimensional channels without any intersection upto three-dimensional channels. Silicon being tetravalent can take 4 oxygen atoms around it, maintaining electrical neutrality. Trivalent aluminium atom on the other hand when bound to 4 oxygen atoms will have a net negative valency. To provide overall electrical neutrality, as many cationic charges are needed as there are Al atoms in zeolites.



SiO<sub>4</sub> and AlO<sub>4</sub> Tetrahedra



Sodalite Unit



*Projection of idealized sodalite unit and hexagonal prism*

Figure.I.2 Structural units of Zeolite Y

Synthetically zeolites are usually prepared and crystallized as sodium zeolites. Hence, initially, the number of Na and Al atoms will be same in zeolites. The negative charges on the lattice are counterbalanced by exchangeable cations located at well-defined sites. The negative charge may also be compensated by organic cations or protons. The protons represent Bronsted acid sites and participate in acid catalyzed transformations of organic molecules.

Zeolites have the remarkable ability of ion-exchange. The sodium ions can be exchanged by monovalent, bivalent or trivalent ions. The direct replacement of  $\text{Na}^+$  by acids at pH below 4 will cause the removal of aluminium ions resulting in the collapse of structural framework. Therefore,  $\text{Na}^+$  ions are first exchanged with ammonium ions. Ammonia will be removed by heating, leaving behind hydrogen ions in the zeolite. Exchange with other ions is carried out by treating with the corresponding salt solutions.

The main advantages<sup>53</sup> of zeolite and zeotype catalysts include: (a) well defined inorganic crystalline structures differing in channel diameters, geometry and dimensionality, (b) a precisely defined inner void volume providing high surface area, (c) the ability to adsorb and transform molecules in the inner volume, (d) the ability for substitution of cations into the silicate framework enabling the tuning of strength and concentration of catalytic sites, (e) shape selectivity of the reactants, intermediates and products to the dimensions of the channels and (f) environmental tolerance. The following three methods are currently used to prepare the metal complexes with in the supercages of zeolite matrix.

### 1.3.1. Flexible ligand method.

This method was first exploited by Herron<sup>61</sup> to prepare Co(salen) complexes in the supercages of faujasite. It is applied to the free ligands that are flexible enough to pass through the smaller windows to the larger cages of the zeolite host material. The free unfolded ligand is able to enter the pores of the zeolite due to the free rotation around the carbon-carbon  $\sigma$  – bond as depicted in the Figure.I.3 for the Schiff base salen.

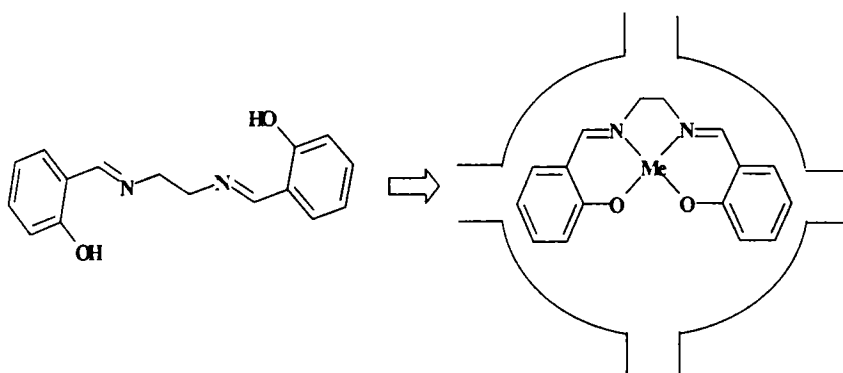


Figure.I.3. Synthesis of zeolite Y encapsulated metal salen complexes via the flexible ligand method.

Ligand, that enters the zeolite cages, complexes with the previously exchanged transition metal ions. The complex so formed adopts a square planar configuration, which is unable to escape from the cavity of zeolite matrix. Thus the metal complex is physically entrapped in the supercages of faujasite. In this method, the ion exchanged and dried zeolite is mixed with the predried ligand, filled in a glass tube, evacuated, sealed and finally heated for several hours at a temperature slightly above the melting point of the ligand until a bright colour is observed. After the reaction, soxhlet extraction with acetone, acetonitrile or dichloromethane is applied to purify the zeolite from the

uncomplexed ligand. This method is generally used for the encapsulation of Schiff base complexes. The transition metal ions as well as the structure of the Schiff base ligands were varied to prepare large numbers of encapsulated complexes. They possess interesting electrochemical properties<sup>62</sup>. The resulting zeolite encapsulated complexes have been used to act as oxygen carriers mimicking haemoglobin<sup>63</sup>, as selective oxidation catalysts<sup>63</sup> or as catalysts for selective hydrogenation<sup>64</sup>.

### **1.3.2. Ship –in – a – Bottle (The template synthesis) method.**

This method was first proposed by Romanovsky and co-workers<sup>65</sup> and later on reported by many workers in this field<sup>66</sup>. The term 'ship – in – a - bottle' was first coined by Herron<sup>67</sup>. This method is generally used for the encapsulation of transition metal-phthalocyanines and porphyrazines in zeolites. Based on molecular graphics analysis, it has been argued that in the case of zeoliteY encapsulated phthalocyanines, the planarity of the complex must be disturbed, since the dimensions of the ligand (14-15Å) exceed the effective diameter of the zeolite super cages(13Å)<sup>66</sup>. Herron proposed that intrazeolitic phthalocyanines have a saddle shaped structure with the benzene groups protruding out of the 7Å windows of the supercages. Clearly, phthalocyanines and porphyrazines cannot be incorporated directly into the 13Å zeolites by flexible ligand method. Thus the most promising method was the template synthesis for them. This method involves assembling of the ligands from smaller species inside the zeolite cavities. Reaction of metal exchanged zeolites or pre-adsorbed labile metal complex such as a carbonyl or a metallocene with 1,2-dicyanobenzene at 250 °C to 350 °C results in phthalocyanine formation and complexation for cobalt, nickel and copper zeolites

(Figure.I.4.). Water is the electron source in this process and hence complexation does not occur if the ion-exchanged zeolite was strongly dehydrated before the complexation step<sup>68</sup>.

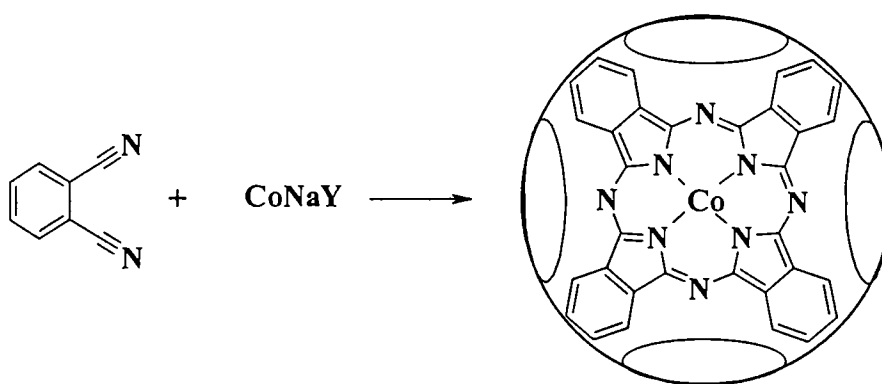


Figure.I.4. Ship-in-a-bottle synthesis of zeolite encapsulated metal phthalocyanine.

Zeolite encapsulated complex was purified by the successive soxhlet extraction for a period of 3-5 days using acetone, pyridine, or dimethylformamide and again by acetone to remove unreacted dicyanobezene and the side products such as phthalimide, phthalocyanine and metal-phthalocyanine, formed on the outer surface of zeolite framework. A “ship-in-a-bottle” approach to entrap the chiral (salen)Mn complexes within the cages of zeoliteY was reported<sup>69</sup>.

### 1.3.3. Zeolite synthesis (crystallization inclusion) method.

This method involves the synthesis of zeolite framework around the preformed complexes. Rankel and Valyocsik<sup>70</sup> reported the synthesis of zeolite mordentite from gels containing bipyridine, phenanthroline or phthalocyanine

complexes. High stability of the complex under the conditions of zeolite synthesis and sufficient solubility in the synthesis medium are the prerequisites for this method. Zeolite synthesis method is restricted to those cases, where the synthesis of zeolite matrix is possible without the use of further organic templates. Recently Wohrle and coworkers<sup>71</sup> reported the successful encapsulation of selected Zn<sup>2+</sup> metalloporphyrins and metalloporphyrazines in molecular sieves using the crystallization inclusion method.

#### **1.4. Homogeneous and heterogeneous catalysis.**

The area of catalysis is sometimes referred to as “fundamental pillar” of green chemistry<sup>72,73</sup>. The challenge before chemists is to develop new pathways for the elaboration of more favourable reaction conditions, solvents for improved selectivity as well as energy minimization and the design of less toxic and safer chemicals. Catalysts are mandatory in the manufacture of a vast array of chemicals and fuels and thus significantly contribute to our economy and high living standards. The 2001 Nobel Prize-winning work<sup>74</sup> on catalytic asymmetric synthesis has been crucial in producing single enantiomer compounds and has met many goals of green chemistry particularly for the pharmaceutical industry. Recently, water has been split into oxygen and hydrogen using a photocatalyst that absorbs light in the visible range<sup>75</sup>. This reaction has the potential to provide hydrogen for use in fuel cells. Hydrogen fuel cells in cars would greatly reduce air pollution, as the oxidation product of it (water) is environmentally benign.

The role of a catalyst in a reaction is to increase the reaction rate by providing a new faster path that had a lower energy of activation through which a reaction can proceed. Catalysis is of two types - homogeneous and heterogeneous. Homogeneous

catalysis is one in which the reactants and the catalyst form a single phase. Acid – base catalysis and enzyme catalysis are the most important examples of homogeneous catalysis. Homogeneous transition metal catalyzed reactions are of utmost importance in organic synthesis. The very positive aspects of homogeneous catalysts are that, they have well-defined reactive centers, which lead to high and reproducible selectivity and operation at low temperatures and pressures. Information regarding their structure, environment of the metal atom, the number of ligands attached and how the coordination changes during a reaction etc can be obtained proficiently. Thus design of catalysts, which lead to better selectivity is possible.

Transition metal complex-catalyzed reactions constitute an extensive field embracing reactions occurring both in living nature and under the conditions of industrial manufacture. An important landmark in the development of homogeneous catalysis by organotransition metal chemistry, was the discovery (in 1959) of the Wacker process reported by Smidt and co-workers<sup>76-78</sup>. This palladium(II) catalyzed oxidation of ethylene to acetaldehyde is with molecular oxygen as terminal oxidant. The commercial success of the Wacker process provided an enormous stimulus for further studies of palladium and other noble metal complexes as homogeneous catalysts<sup>79-82</sup>. This development led to the discovery of a variety of important homogeneous, liquid phase processes involving noble metal catalysts such as hydroformylation, carbonylation, hydrogenation, isomerization and oligomerization. The possibility of multiple oxidation states, accessibility of vacant coordination sites, leeway of tuning the redox potentials by the ligand and the facility to undergo substitutions at the ligands, are one or more be the characters of transition metal complexes to behave as catalysts. But the major problems of homogeneous catalysis are,

the separation of the catalysts from the reaction medium, they get easily poisoned and cannot withstand high temperatures. The procedure for separation of catalysts from reaction mixture generates large volumes of waste eluent and devours a lot of energy.

Heterogenization of the homogeneous catalysts can solve this problem. Heterogeneous catalysis is one in which the reactants form one phase and catalyst form a different phase and has emerged as one of the most important areas in industrial research. General benefits of the heterogenization of homogeneous catalysts include, the easy separation of catalyst from the reaction medium, the reuse of catalyst, possibility of using the catalyst in a continuous process, minimisation of the effluent problems and handling of materials, possibility of using large variety of different solvents and reaction conditions, and high stability and high selectivity or specificity for a given product. Two important disadvantages of heterogeneous catalysts are, that they require rather high temperatures and pressures and frequently lead to mixture of products.

Several attempts have been made to combine the advantages of homogeneous and heterogeneous catalysis. These include supported liquid phase catalysis<sup>83</sup>, biphasic or triphasic catalysis<sup>84,85</sup>, sol-gel processed<sup>86</sup> interphase catalysis and use of ionic liquids as solvents in catalysis<sup>87,88</sup>. The concept of *chemistry in interphases* has been made use of in these catalytic reactions. An interphase is defined as a region within a material in which a stationary and mobile component penetrates each other on a molecular level. The stationary phase is composed of an active center, for example, an organometallic complex, whereas the mobile phase consists of a solvent or a dissolved reactant. Therefore, an interphase is able to simulate homogeneous reaction conditions, and at the same time it has the advantage of a heterogeneous catalyst<sup>86</sup>. The application of

supercritical fluids<sup>89</sup>, dendrimer catalysts<sup>90</sup>, nanofiltration-coupled catalysts<sup>91</sup> and supported catalysts<sup>92,93</sup> are the other methods for heterogenization.

Immobilization of catalysts on inorganic supports has several potential advantages over the immobilization on organic supports. Their chemical stability with regard to oxidizing conditions and mechanical stability are excellent. They have superior thermal stability. Microporous materials such as zeolites and aluminophosphates and mesoporous materials such as oxides of Al, Zr and Ti are available for the immobilization of homogeneous catalysts. Metal complexes in the super cages of zeolites have long been of significance as heterogeneous catalyst systems. The steric and electrostatic constraints that are imposed on the reactants in the channels and cages of zeolite can lead to new reaction pathways. A zeolite encapsulated catalyst species can exhibit properties different from those of analogues of simple complexes. Such modification is obtained from the molecular sieve property of zeolite matrix and from the possibility that three-dimensional environmental aspects of the super cage can influence the substrate-catalyst interaction. Thus these complexes have the potential of being used as industrial catalysts.

Activity, selectivity and stability are the primary requirements of an industrial catalyst, which are met remarkably by zeolites. The nature and degree of exchange of the cation, the silica-alumina ratio, the size of reactant and product molecules are some of the main factors, which determine the catalytic activity of zeolites. The super cages or  $\alpha$ -cages in zeolite are large enough to accommodate most hydrocarbon molecules. The channels interconnecting the supercages provide the molecular sieving action of zeolites. Zeolites are widely accepted as shape selective catalysts<sup>94</sup>.

Shape selective catalysis means the continuous passing and reaction of the molecules of proper dimension through the sieves leaving behind longer, branched or bulky molecules from reactions. Only molecules of proper size and shape are allowed to get out of the cages as products. Thus reactant selectivity and product selectivity occur in zeolite catalysts (Figure.I.5.). Molecular traffic control may occur by which reactant molecules enter the catalyst through one pore system while the products diffuse out by the other.

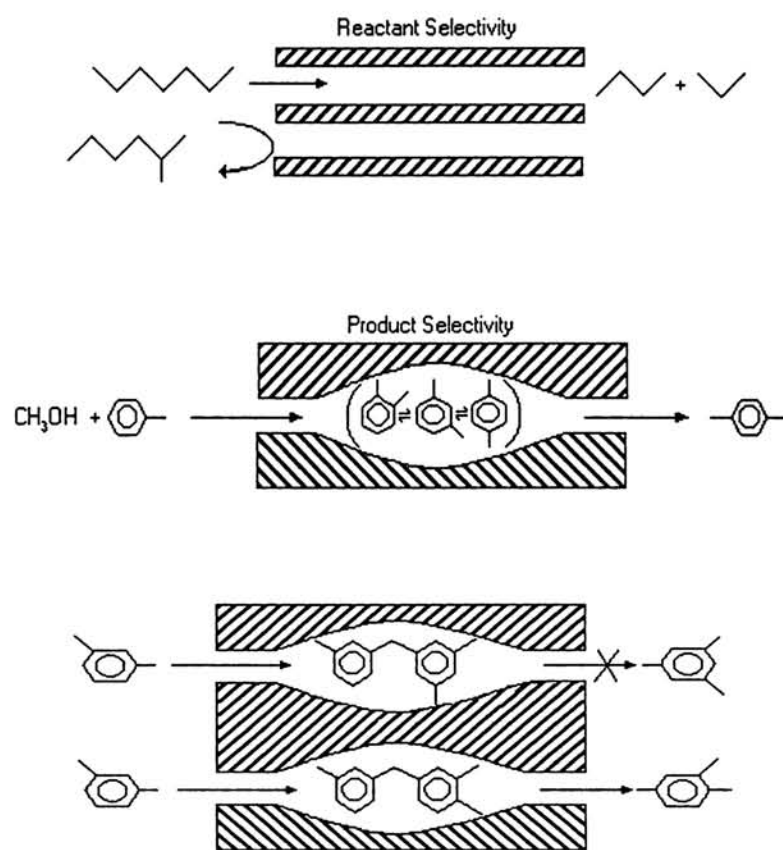


Figure.I.5. Reactant selectivity and product selectivity.

Zeolite encapsulated complexes have also been suggested as model compounds for enzyme mimicking<sup>95</sup>. The term “zeozyme” has been used to describe the catalytic system in which zeolite framework behaves as protein mantle of the enzyme and the entrapped metal complex imitates the active site of the enzyme.

A drawback of supported catalysts is the loss of homogeneity due to minor changes in structure. This leads to a reduced reactivity and selectivity of the immobilized catalysts<sup>86</sup>. The application of surface modified inorganic and organic materials has been less successful because of the short lifetime of these catalysts caused by the leaching of the reactive centers, reduced accessibility of the catalysts, steric effects of the matrix, inhomogeneity of the reactive centers and difficulties in controlling the density of the reactive centers on the surface<sup>96</sup>. However, zeolite encapsulated complexes, especially the zeolite encapsulated Schiff base complexes, continue to be explored as potential catalysts.

### **1.5. Schiff base Complexes as Catalysts.**

Schiff base complexes of transition metal ions have received much attention as oxygen transfer agents to organic compounds<sup>97-99</sup>. Direct participation of dioxygen in the oxidation of organic compounds is effected by such complexes. Reactions of organic compounds with dioxygen are restricted by spin conservation. This may be overcome by forming metal complexes. Salen complexes are known to transfer oxygen atom to alkenes to form epoxides. Schiff base complexes catalyses a large number of organic reactions

such as oxidation of sulphides<sup>99</sup>, redox reactions<sup>100</sup>, hydrolysis<sup>101</sup>, decarboxylation<sup>102</sup>, elimination<sup>103</sup> and aldol condensation<sup>104</sup>.

The oxidation of hydrocarbons using transition metal complexes is of industrial and biological significance. Interest in the study of chemical models that mimic oxygenases is shown for two reasons. Such a study may provide a basis for understanding enzymatic oxidations. It may also develop simple catalytic systems that exhibit high selectivities which are characteristic of enzymatic oxidations. Most studies have concentrated on chemical models for cytochrome P-450 monooxygenases. The cytochrome P-450 family of monooxygenase enzymes, catalyses the reaction of molecular oxygen with various small molecules, including alkanes and alkenes and the epoxidation of alkenes. The active sites of these enzymes contain an iron(III) protoporphyrin IX moiety.

Numerous Co(II)chelates are known to form superoxo or  $\mu$ -peroxo complexes by reaction with dioxygen. The best known of these is Co(II)salen Schiff base complexes studied extensively by Calvin and Martell<sup>105</sup>. The reactions of organic substrates with molecular oxygen in the presence of Co(II)salen and the related complex Co(II)(salpr) were studied by Nishinaga and co-workers<sup>106</sup>. They observed that these complexes reversibly bind the molecular oxygen and Co(II)salen form  $\mu$ -peroxo complexes and a superoxo complex is formed on pyridine or in the presence of imidazole derivatives.

The epoxidation of olefins using tri and tetradentate Schiff base complexes of Fe(III) as catalysts and iodosylbenzene as oxidant have been studied<sup>107</sup>. Cyclohexene gave cyclohexene oxide, cyclohexanol, and cyclohexenone. At higher concentration of catalyst, low yield but high selectivity of epoxide was observed. Similarly the yield of

epoxide increases with increase in concentration of cyclohexene. The addition of pyridine,  $\text{NaH}_2\text{PO}_4$ ,  $\text{NaHCO}_3$  were found to increase the yield of epoxide while addition of cetyltrimethylammonium bromide completely inhibits the epoxidation. The epoxidation of olefins catalysed by dioxotungsten(VI) schiff base complexes have been reported<sup>106</sup> using t-butyl hydroperoxide (TBHP) as the oxidant. Higher rates of epoxidation for cyclooctene, norbornene and cycloheptene have been observed for  $\text{MoO}_2(\text{SALEN}) / \text{TBHP}$  catalyst systems<sup>108</sup>.

Another reaction, which is considered as interesting is the catalytic oxidation of the ascorbic acid to dehydroascorbic acid by metal complexes. The use of first row transition metal complexes of the Schiff bases derived from quinoxaline-2-carboxaldehyde have been reported<sup>109</sup>. A number of other reports on the oxidation of ascorbic acid by metal complexes<sup>110-115</sup> is also seen in literature. A detailed kinetic study of the oxidation of ascorbic acid in methanol-water mixture was carried out and the mechanism of oxidation was proposed<sup>115</sup>. An interesting Cu(I) chiral Schiff base complex for asymmetric cyclopropanation of 2,5-dimethyl-2,4-hexadiene with L-menthylethyl diazoacetate was synthesized<sup>116</sup>. This Schiff base complex was formed in situ by  $\text{Cu}(\text{CH}_3\text{-CN})_4\text{ClO}_4$  and the Schiff base derived from (-)-(1R,2S)-2-amino-1,2-diphenylethanol and substituted salicylaldehyde. This catalytic system was reported to show better enantiomeric excess and higher activity. A series of cobalt complexes prepared<sup>117</sup> from the Schiff bases 2,6-pyridinecarboxaldehyde-bis(imines) and 2,6-diacetylpyridine bis(imines) were shown to catalyze the oligomerization of propylene in the presence of polymethylaluminoxane (PMAO) cocatalyst. Regioselective conversion of epoxides to iodoalcohols and bromoalcohols with elemental iodine and

bromine in presence of some Schiff base complexes of first row transition metals(II) were investigated<sup>118</sup>.The results of the study show that the haloalcohols were produced in high yields. Further more the conversion occurs under mild conditions in various aprotic solvents and the catalysts can be recovered easily and reused several times. The peroxidase-like catalytic activity of Co(II), Ni(II), Cu(II) and Zn(II) complexes of salicylaldehyde-2-amino-4-phenyl thiazole on the oxidation of vitamin C with H<sub>2</sub>O<sub>2</sub> was determined<sup>119</sup>.

Co(II)salen catalyzed oxidation of phenols to the corresponding quinones were first studied by Van Dort and Geursen<sup>120</sup> and later by others<sup>121,122</sup>. The best results are reported to be obtained in DMF as solvent. Alkyl substituted phenols can be effectively oxidized to p-benzoquinones by dioxygen in chloroform or methanol solutions in presence of Co(II)salen as catalyst. Further studies<sup>123</sup> on this reaction showed that the Co(II)salen catalyzed autoxidation of phenols can give high yields of p-benzoquinones or diphenquinones depending on the conditions. High catalyst concentration and low temperature favours the formation of benzoquinones while diphenquinones are formed at low catalyst concentrations and high temperatures. Electron donating group facilitated the formation of benzoquinones. Activated phenols containing a blocked para position can be selectively oxidized to the corresponding o-benzoquinone.

The oxidative cleavage of 3-substituted indoles proceeds at ambient temperatures in presence of Co(II)salen<sup>124</sup> in CH<sub>2</sub>Cl<sub>2</sub> and markedly retarded by strong coordinating solvents such as DMF and pyridine. A biomimetic catalytic system (modeling hydroxylase), [(Fe<sup>III</sup>salen)<sub>2</sub>O] favors the stereoselective oxidation of adamantane<sup>125</sup> at the secondary position. The enantioselective epoxidation<sup>126</sup> of alkenes

over chiral manganese salens incorporated in Zeolites using NaOCl oxidant has also been reported recently.

### **1.6. ZeoliteY encapsulated Schiff base complexes as Catalysts.**

Metal complexes of the Schiff base salens encapsulated in molecular sieves are a novel and promising class of catalysts for the selective oxidation of a variety of substrates. The oxygen binding behaviour of the encapsulated salen complex inside zeoliteY was compared<sup>127</sup> to the behaviour of the free salen complex in solution. The studies have shown that the complex carries oxygen as a cargo and that such a material is much more stable towards irreversible oxidation than the equivalent solution-phase species. ZeoliteY encapsulated Mn-salen, Fe-salen and VO-salen are found to be active redox catalysts<sup>128</sup>. These complexes catalyse hydroxylation of phenol to the extent of 23-28 wt% with more than 99% selectivity to dihydroxybenzenes. The zeolite framework over metal complexes impose size and shape selectivity in the same way as the channels created by protein structure of enzyme. Thus biomimetic activities has been pursued on zeolite encapsulated metal complexes.

ZeoliteY encapsulated Cu and Mn complexes of Schiff base salens and octaza macrocyclic ligand have been investigated for the selective aerobic oxidation of methane at 273 K using TBHP as a promoter and water or acetonitrile as solvent<sup>129</sup>. Methanol and formic acid were the products of conversion when octazamacrocyclic copper complex is employed. Methane conversions are of particular interest due to large reserves of natural gas located in remote areas. Methane is one of the major green house gases considered to be the primary causes of global warming. Technologies are there for the conversion of

methane to more useful chemicals like methanol and formaldehyde. But high temperature is required to activate methane and usually resulted in oxidative coupling reaction<sup>130</sup>. A number of approaches can be seen in literature to activate methane molecule at low temperature, so that the oxidative coupling products can be neglected. Thus there is a significant incentive to develop a one step direct conversion of methane to methanol and formaldehyde. There has been some success in the synthesis of catalysts active for the direct oxidation of methane to methanol.

Salen and substituted salen Schiff base complexes of cobalt(II) encapsulated in the supercages of Na-Y zeolite have been reported for the aerial oxidation of p-cresol under alkaline conditions<sup>131</sup>. The synthesis, physicochemical characterization and catalytic performance of Cu(II) and Mn(III)(X<sub>2</sub>-salen)<sup>132</sup> complexes encapsulated in the cavities of zeolite NaX and NaY have been monitored in the decomposition of H<sub>2</sub>O<sub>2</sub> and tertiary butyl hydroperoxide as well as the peroxidative oxidation of phenol, styrene and para-xylene were investigated.

## **1.7. SCOPE OF THE PRESENT INVESTIGATION.**

There is currently a massive effort in chemical industry to synthesize metal complexes and supported complexes due to the amazing diversity in using them as catalysts. Large-scale industries to small-scale reaction firms are pursuing for the development of new environmentally benign catalysts, which are more efficient, product effective and cost effective. Metal complexes play important role in modifying the prevailing catalytic systems and providing novel catalysts for various applications to

reduce material consumption, energy and wastage. Manipulation of Schiff base ligands, offer considerable scope for designing new complexes of catalytic interest.

Zeolite molecular sieves and the metal complexes entrapped within these sieves have been studied extensively, as these materials are catalytically more active than corresponding simple complexes. ZeoliteY encapsulated Schiff base complexes have been used as catalysts for the oxidation of organic substrates. Oxidation of organic substrates is of industrial and biological significance. A fair number of Schiff base complexes of 3d- transition metal ions and their biological activities are reported in literature. On close survey it was noted that catalytic activity of very few Schiff base complexes were studied and that itself were mainly of salens and the substituted salen complexes. Moreover, the Schiff base complexes encapsulated in the voids of zeolite molecular sieves are few in number when compared with the numbers of simple complexes presented in literature. Interestingly it was noted that most of these zeolite encapsulated Schiff base complexes screened for catalytic activity were also derived from 'salens'. Neither the Schiff base complexes nor the zeolite encapsulated complexes derived from 2-aminobenzothiazole and salicylaldehyde or 4-hydroxy-3-methoxy benzaldehyde have been reported so far. Furthermore, aminobenzothiazole has a biologically very active thiazole ring, containing the heteroatoms sulphur and nitrogen, and the aldehydes chosen for the synthesis of Schiff bases have the activating –OH and –OCH<sub>3</sub> groups. It is presumed that the presence of these atoms and groups may increase the catalytic activity of their complexes. All these factors prompted us to carry out an investigation with the following objectives.

- ❖ To synthesize and characterize Mn(II), Fe(III), Co(II), Ni(II) and Cu(II) complexes of the Schiff bases derived from 2-aminobenzothiosole, salicylaldehyde and vanillin.
- ❖ To immobilize these Schiff base complexes within the supercages of zeolite Y matrix and characterize the encapsulated species.
- ❖ To screen the complexes for the possible use as catalysts for oxidation reactions like the oxidations of H<sub>2</sub>O<sub>2</sub>, benzaldehyde, benzyl alcohol, n-propanol, isopropanol, and cyclohexanol.

\*

## REFERENCES

1. H. Schiff, *Ann.Chim* (Paris) 131, (1864), 118.
2. P.E. Pfeiffer, E.Buchholz and O. Bauer, *J.Prakt.Chem.*, 129, (1931), 163.
3. Holm.R.H, Everett.G.W and Chakravorty.A.,*Prog inorg Chem*,7,(1966),83.
4. Calligaris.M, Nardin.G and RandaccioL., *Coord.Chem.Rev*, 7, (1972), 385.
5. Hobday. M.D, and Smith.T.D., *Coord.Chem.Rev*, 9, (1973), 311.
6. Sheldon.R.A and Kochi. J.K., *Metal catalysed oxidations of organic compounds*, (Academic Press,New York), (1981).
7. Jacobsen.E.N, Zhang. W, Muci.A.R, Ecker.J.R and Deng.L, *J.Amer.Chem.Soc*, 113, (1991), 7063.
8. Goubatsis.S,Perlepes.S.P,and Hadjiliadis.N, *Trans. Met. Chem*,15,(1990),300.
9. R.H.Holm, G.W. Everett Jr. and A.Chakravorty, *Review on metal complexes of Schiff bases and  $\beta$ -ketoamines*, (1965),83.
10. P. Pfeiffer and T.Tsumaki, *Leibigs Ann.Chem.*, 84, (1933), 503,.
11. C.Floriani, F.Calderazzo and L. Randaccio., *J.Chem.Soc.Chem.Comm*, (1973), 384.
12. M. Gerloch, J. Lewis, F,E Mabbs and A.Richards. *J. Chem.Soc.(A)* 1968,112.
13. P.P.Singh and N.B.Singh., *Polyhedron*, Vol. 9, (1990), 4, 557.
14. P.C. Eisman, E.A. Konopka and R.L.Mayer, *Amer.Rev.Tuberc*, 70, (1954), 121,131.
15. J.S. Buck and E.J. Debeer, U.S patent, 2,250,136,*Chem.Abs*,35,(1914), 8212.
14. R.O.Clinton, U.A.Salvador, S.C.Laskowski and C.M.Suter, *J.Amer.Chem.Soc*, 70, (1948), 950.
15. A.Schoberal and G.Wichler, *Angew Chem*, 67,(1955), 417.

16. F.Dogering, *Organic Nitrogen compounds*, Univ.Litho.Printers, Michlgan, USA, 60, (1945), 454.
17. H. Raskova and Z. Voltava, *Chem. Abs*, 44,(1950), 7982.
18. E.M.Hodnett and W.J. Dunn, *J.Med.Chem*, 13,(1970), 768.
19. E.M.Hodnett and P.D. Mooney, *J.Med.Chem*, 13,(1970), 786.
20. Yun Sung Cho, *Chem.Abs*, 79, (1978), 73390.
21. B.Dash , M. Patra and S.Praharaj, *Ind . J. Chem.* 19B, (1980), 894.
22. S.S.Tiwari, M.I. Husain and G. C. Srivastava, *Ind.J.Chem.Soc*, 58, (1981), 214.
23. C.Manzur, C.Bustos, R.Schrebler et.al., *Polyhedron*, Pergamon Press plc, Vol .8, (1989), No.18, p. 2321-2330.
24. Rajib Lal De, Keka Samanta, Chitra Samanta and Alok .K. Mukherjee., *Ind. J. Chem*, 38A, (1998), 1010.
25. Kohutova M, Valent A, Durackova Z. *Chem. Abstract*, Vol.131, (1999), 222506g.
26. Zhang, Xiuying; Xie,Lianying; Zhang,Youjuan; An,Yingge; *Chem. Abstract*, Vol.131, (1999), 222582.
27. Zhou,BaoXue;Jiang,ShuQin;Zhou,Ding;Zhao,YuTing; *China.Chem.Letters*, 10(5),; (1999), 429-432, *Chinese. Chem.Society*.
28. Goswami, Niranjan, Eichhorn, David.M; *Inorg.Chem.*, 38(19), (1999), 4329-4333.
29. Cohan Zahid. H., *Metal based drugs*, Freud Publishing House Ltd, Pakistan., 6(2), (1999), 75-80.
30. Dash.B and Rout. M .K., *J.Ind. Chem.Soc.*, 32, (1955), 663.

31. Sharma.S.C., *Bull.Chem..Soc. (japan)*, 40, (1967), 2422.
32. Patra.M, Mahapatra.S.K, and Dash.B., *J.Ind. Chem.Soc*, 51, (1974), 1031.
33. Farkas.L., *Chem.Abstract*, 84, (1976), 31047.
34. Modi.D, Sabnis.S.S and Deliwala.C.V., *J. mednl.Chem*, 13, (1970), 935.
35. Ujiie. T., *Ann.Rept.Cancer Inst.Kanazawa, Japn*, 1, (1967), 109.
36. Williams. D. R., *Chem.Rev*, 72, (1972), 203.
37. Albert. A., *Aust. J.Sci*, 30, (1967), 1.
38. Metzler.D.E., Ikwa.M, and Snell.E.E., *J.Amer.Chem.Soc*, 76, (1954), 648.
39. B.Dash, M.Patra and S.Praharaj., *Ind. J. Chem*, Vol. 19B, (1980), 894-897.
40. B.Dash, M.Patra and P.K. Mahapatra., *Ind. J. Chem*, 60, (1983), 772-774.
41. B.Dash, Mahapatra. S,K., *J. Inorg. Nucl. Chem*, 37, (1975), 271.
42. Rajendra P.Misra, Bipin B. Mahapatra, and S.Guru., *J. Ind. Chem.Soc.*, 56, (1979), 832.
43. Rajendra P.Misra, Bipin B. Mahapatra, and S.Guru., *J. Ind. Chem.Soc.*, 58, (1981), 808.
44. Herron.N., *Inorg.Chem*, 25, 1986, 4714.
45. D.E.De Vos, E.J.P. Feijen, R.A.Schoonheydt and P.A.Jacobs., *J.Am. Chem. Soc*, 116, (1994), 4746-4752.
46. Laurent Gaillon , Nicolas Sajot, Fethi Bedioui and Jacques Devynck., *J.Electroanal.Chem*, 345, (1993), 157-167.
47. J.H.Lunsford, *Catal.Rev-Sci.Eng.* 12, (1975), 137-162.
48. J.H.Lunsford in *Molecular Sieves-II* American Chemical Society Symposium series, DC, USA (1977), pp.473-492.

49. W.J.Mortier, R.A.Schoonheydt, *Progr.Solid State Chem*, 16, (1985), 1-125.
50. G.A.Ozin, C.Gil, *Chem Rev.* 89, (1989), 1749-1764.
51. G.Schulz-Ekloff and S.Ernst in *Zeolites and Related Molecular Sieves.*, G.Ertel, H.Knozinger and J. Weitkamp(Eds), Wiley-VCH(1997) p.374-387.
52. P.G.Menon., *Chem.Rev*, 94, (1994), 1021.
53. Jiri Cejka and Blanka Wichterlova., *Catalysis Reviews*, 44(3), (2002), 375-421.
54. J.W. Mc Bain, "*The sorption of Gases and Vapours by solids*". Chapter.V, Rutledge and sons, London. 1932.
55. Breck,D.W., *Zeolite Molecular Sieves: Structure ,Chemistry and Use*, John Wiley & sons, New York,1974.
56. D. E . W Vaughan. '*Properties of natural zeolites*' , in "*Natural zeolites, occurrence, properties, use.*" L.B Sand and F . A Mumpton, publishers : Pergamon.
57. John. M. Thomas, Marc Audier and Jacek Klinowski., *J.Chem.Soc. Chem.Comm*, (1981), 1221.
58. M. Bryssee, J.L. Portefaix, M.Vrinat.,*Catal Today*; 10, (1991), 489.
59. Yasuaki Okamoto., *Catal Today*, 39, (1997), 45-59.
60. Purnkala, V.Samant et.al., *Recent Trends in Catalysis*,(1999), Narosa Publishing House, New Delhi.
61. Herron.N., *Inorg.Chem.*, 25, (1986), 4714.
62. F.Bedioui,L.Roue,E.Briot,J.Devynck,K.JBalkus,Jr., *J.Electroanal.Chem.* 373, (1994), 19-29.
63. C.Bowers, P.K.Dutta, *J.Catal*, 122, (1990), 271-279.

64. S.Kowalak,R.C.Weiss,K.J.Balkus.Jr,*J.Chem.Soc.Chem.Commun*, (1991),57-58.
65. B.V. Romanosky, A.G. Gabrielov in *New Developments in Selective Oxidation by Heterogeneous Catalysts* (Eds : P.Ruiz, B.Delmon.), Studies in Surface Science and Catalysis, Elsevier, Amsterdam, Vol.72, (1992), pp 443-452.
66. a).Herron. N., *Inorg .Chem.*(1986), 25, 4714.,(b).*J.Coord. Chem*, 19, (1988), 25-38., (c).*Inclusion Chemistry with Zeolites*, Eds.; Kluwer.Dordrecht,(1995).
67. Herron.N, Stucky.G.D, Tolman .C.A., *Inorg. Chim. Acta*, 100, (1985), 135.
68. Meyer.G, Wohrle.D, Mohl.M, Schulz-Ekloff .G, *Zeolites*, 4, (1984), 30.
69. Sabater.M.J, Corma.A, Domenech.A, Fornes.V, Carcia.H., *Chem. Commun*, (1997), 1285.
70. L.A. Rankel and E. W. Valyocsik,US Patent 4500 503,(1985).
71. a)Wohrle.D, Sobbi.A.K, Franke.O, Schulz-Ekloff.G, *Zeolite*,15, (1995), 540., b)Wohlrab.S, Hoppe.R, Schulz-Ekloff.G, Wohrle.D, *Zeolites*,12,(1992), 862.
72. Anastas.P, Warner.I., *Green Chemistry: Theory and Practice*, Oxford University Press, Oxford,(1998).
73. Paul T. Anastas and Mary M. Kirchoff., *Accounts of Chemical Research*, 35, (2002), 686-694.
74. Borman.S.,Asymetric Catalysis Wins. *Chem. Eng. News*, 79, 2001, (42), 5.
75. Zou.Z, Ye.J Sayama.K, Arakawa.H., Direct splitting of water under visible light irradiation with an oxide semiconductor photocatalyst, *Nature*, 2001, 414, 625-627.
76. J.Smidt, W.Hafner, R.Jira, J.Sedlmeier, R.Ruttinger, and H.Kojer, *Angew. Chem*, 71, (1959), 176.

77. J.Smidt, W.Hafner, R.Jira, J.Sedlmeier and A.Sabel., *Angew. Chem. Int. Ed.*, 1, (1962), 80.
78. J.Smidt., *Chem.Ind.(London)*, (1962), p.54.
79. P.M. Maitlis., “*The organic Chemistry of Palladium.*” Vols. 1 and 2, Academic Press, New York, (1971).
80. E.W. Stern, in “ *Transition Metals in Homogeneous Catalysis*”, (G.N. Schrauzer, ed.) Dekker, New York, (1971), p.93.
81. R. F. Heck., “ *Organotransition Metal Chemistry.*” Academic Press, New York, (1974).
82. B. C. Gates, J.R.Katzer, and G.A. Schuit, “*Chemistry of Catalytic Processes.*” p.129, McGraw – Hill , New York, (1979),
83. Arends . I.W.C.E., Sheldon. R.A., *Appl. Catal. A* 212, (2001), 175.
84. Wende.M, Meier.R, Gladysz.J.A , *J.Am.Chem. Soc.*, 123, (2001), 11490.
85. N. Sridevi and Jaikumar.S., M.Phil Thesis submitted to Cochin University of Science and Technology, Kochi, (2001).
86. Zhong-lin Lu, Ekkehard Lindner and Herman A. Mayer., *Chem. Rev*, 102, (2002), 3543-3578.
87. Guernik.S, Wolfson.A, Herskowitz .M, Greenspoon.N, Geresh.S, *Chem. Commun.* (2001), 2314.
88. Jairton Dupont, Roberto F. de Souza and Paulo A .Z. Suarez., *Chem. Rev*, 102, (2002), 3667-3692.
89. Sellin. M.F , Webb. P.B, Cole- Hamilton.D.J., *J. Chem. Commun*, (2001), 781.

90. Astruc. D, Chardac.F., *Chem. Rev*, 101, (2001), 2991.
91. De Smet.K, Aerts.S, Ceulemans. E, Vankelecom. I.F.J, Jacobs. P.A.,  
*Chem. Commun*, (2001), 597.
92. Crudden. C.M, Allen. D, Mikoluk. M.D, Sun., *J. Chem. Commun*,  
(2001), 1154.
93. Price. P.M, Clark.J.H, Macquarrie. D.J, *J. Chem.Soc, Dalton Trans*, (2000), 101.
94. Sigmund M. Csicsery, *Review on Shape-selective catalysts in zeolites*, Zeolites,  
Vol 4, 1984, 202.
95. Norman Herron., *Chemtech*, (1989,September). 544-548.
96. Choplin.A, Quignard. F, *Coord. Chem.Rev.*, 180, (1998), 1679.
97. Siddal. T. C, Miyara. N., *J.Chem. Soc. Chem. Comm*, (1983), 1185.
98. Samsel.E.G. Srinivasan. K, Kochi., *J,Amer.Chem. Soc*, (1985), 107.
99. Varsha Bansal, Pradeep. K.Sharma and Kalyan .K.Banerji., *Ind.J.Chem*, 39A,  
(2000), 654-659.
100. W. Zhang, J.L.Loebach., *J.Amer. Chem. Soc*, 112, (1990), 2801.
101. N.Kitajima, H. Fukui and Y.Moro- oka., *J. Chem. Soc. Chem. Comm*,  
(1988), 485.
102. M.M. Taqui Khan and A.E. Martell., “*Homogeneous Catalysis by Metal  
complexes*”, Academic Press, New York,(1981).
103. I. Sasaki, D. Pujol and A. Goudemer., *Inorg. Chim.Acta*,(1987), 134.
104. M. Nath, Kamaluddin, J.Cheema., *Ind. J. Chem*, 32A, (1993),108.
105. M.Calvin and A.E . Martell, “*Chemistry of Metal Chelate Compounds*”, p.337,  
Englewood Cliffs, New Jersey.

106. A.Nishinaga, H.Tomita, T.Shimizu and T.Matsuura., *Tetrahedron Lett.* (1980), P.4849, p.4853.
107. D.D.Agarwal, R.P.Bhatnagar, Rajeev Jain and Savitha Srivastava., (1990), *J.Molecular Catalysis*, 59, 385- 395.
108. D.D.Agarwal, Rachana Rastogi, V.K.Gupta and S,Singh., *Ind.J.Chem.* 38A, (1999), 369.
109. D.D.Agarwal, *J.Molecular Catalysis*, 44, (1988), 65.
110. .Mushran.S.P and Agarwal .M.C., *J Sci Ind Res*, 36,(1977),274.
111. Shtamma E.Y, Puermal. A.P. and Scurlatov. Y.J, *Int.J.Chem. Kinet*, 1111,(1979),1979.
112. Ferrai.L and Alonso.A , *Ann Quim*, 79(1983) .
113. Martinez.P , Zuluaga.J, Uribe.D and Van Eldik .R *Inorg.Chim.Acta* , 136(1987),11.
114. Banch B, Martinez . P , Zuluaga . J, Uribe.D , and Van Eldik .R, *Z Phys Chem* 170 (1991),59
115. S. Mayadevi, N.Sridevi and K.K.Mohammed Yusuff., *Ind. J. Chem*, 37A, (1998), 413- 417.
116. Yao,Xiaoquan; Zheng,Zhuo; Pan,Guizhi.,(Dalian Inst.Chem.Physics), The Chinese Academy of Sciences, 20(3), (1999), 233-235.
117. Bennett,Alison Margaret Anne., *Chem. Abstract*, Vol.131, (1999), 259182z.
118. Sharghi,Hashem;Naemi,Hosseini;*Bull.Chem.Soc.Jpn*, 72(7),(1999),1525- 1531.
119. Liang, Fang-Zhen; Du,Ming; Ren,Jian-Cheng and Shen, Han-Xi. *Chem. Abstract* ,Vol.131, (1999), 110388p.

120. H. M. van Dort and H.J. Geursen in “*Metal-Catalyzed oxidations of organic compounds*’, Academic press, New york,(1981).
121. V. M. Kothari and J. J. Tazuma, *J.Catal.*, 41, (1976), 180.
122. T.J.Fullerton and S.P. Ahern., *Tetrahedron Lett*, (1976),p.139.
123. L.H.Vogt, J.G.Wirthand H.L. Finkbeiner., *J.Org. Chem*, 34, (1969), 273.
124. A.Nishinaga., *Chem. Lett.*(1975), p.273.
125. I. Tabushi, T. Nakajima and K.Seto., *Tetrahedron Lett*, 21, (1980), 2565.
126. M.J.Sabater, A.Corma, A.Domenech, V.Fornes, H.Garcia., *Chem.Commun*, (1997), 1285.
127. Norman Herron. *Inorg. Chem.*, 25,(1986), 4714-4717
128. N.Ulagappan and V.Krishnasamy. *Ind.J.Chem*, 35A, (1996), 787-789.
129. Saji P. Varkey and Chandra R Jacob., *Ind.J.Chem*, 38A, (1999), 320-324.
130. Klier.K, Beretta.A, Sun.Qfeelay.O.C and Herman .R.G, *Catalysis Today*, 36 (1997),3.
131. Trissa Joseph, C.S Sajanjikumari, S.S Deshpande and Sarada Gopinathan; *Ind.J.Chem*, 38A, (1999), 792-796.
132. Chandra R Jacob, Saji P. Varkey and Paul Ratnasamy., *Microporous and Mesoporous Materials*, 22, (1998), 465-474.

\*\*\*

# CHAPTER II



## EXPERIMENTAL TECHNIQUES.

### 2.1. Introduction.

Description of materials and general reagents used, preparation of ligands, various analytical and physico-chemical methods employed for the characterization of the metal complexes and zeoliteY encapsulated complexes are provided in this chapter. Procedures regarding the synthesis of metal complexes are presented in the appropriate chapters.

### 2.2. Reagents.

In the present work the following metal salts were used.  $\text{MnCl}_2 \cdot 4\text{H}_2\text{O}$  (E.Merck,GR);  $\text{Fe}(\text{NO}_3)_3 \cdot 9\text{H}_2\text{O}$  (Aldrich);  $\text{CoCl}_2 \cdot 6\text{H}_2\text{O}$  (E.Merck,GR);  $\text{NiCl}_2 \cdot 6\text{H}_2\text{O}$  (BDH, GR);  $\text{CuCl}_2 \cdot 2\text{H}_2\text{O}$  (E.Merck, GR). These metal salts were used for the synthesis of simple complexes as well as for the synthesis of metal exchanged zeoliteY. 2-Aminobenzothiazole (Merck), salicylaldehyde (Merck), vanillin(Merck) were used for the synthesis of ligands. All other reagents or solvents used were of either 99% pure or purified by known laboratory procedures<sup>1</sup>.

ZeoliteY was obtained from Sud Chemie India Ltd, Baroda. The catalytic activities of the prepared samples were monitored with the following substrates. Commercially obtained hydrogen peroxide (Merck, 30% aqueous solution), potassium permanganate (Merck), benzaldehyde (Qualigens), benzyl alcohol (Merck) propan-1-ol

(Merck), propan-2-ol (Merck), cyclohexanol (Merck) and perchloric acid (GR, BDH) were used.

### **2.3. Preparation of Schiff's base Ligands.**

#### **2.3.1. Salicylalidene-2-aminobenzothiazole, (SBT).**

Schiff base ligand derived from 2-aminobenzothiazole and salicylaldehyde was prepared by adopting the general procedure for Schiff bases. 2-Aminobenzothiazole (0.01 mol, 1.5g) in methanol (40mL) was added drop wise, using a dropping funnel, to a solution of salicylaldehyde (0.01 mol; 1.22g,) in methanol (40mL) with magnetic stirring. The bright yellow solution so formed was again stirred for half an hour, then refluxed for half an hour and cooled in a refrigerator. Orange red crystals separated out were collected, recrystallised from benzene and dried over CaCl<sub>2</sub> in a desiccator. Better yield (90%) was obtained by adopting the above procedure. Only 60-65% yield will be obtained if the mixing was carried out without stirring or drop wise addition of the reagents. (Yield: 90%, M:pt . 141°C).

#### **2.3.2. 4-Hydroxy-3-methoxybenzalidene-2-aminobenzothiazole, (VBT).**

The Schiff base ligand derived from 2-aminobenzothiazole and 4-hydroxy-3-methoxybenzaldehyde (vanillin) was prepared by adopting a procedure similar to that of SBT, using a solution of 4-hydroxy-3-methoxybenzaldehyde (1.52g; 0.01 mol) in methanol (25mL) and 2-aminobenzothiazole (1.5g, 0.01mol) in methanol (25mL). It may, however, be noted

that the attempts to obtain pure crystalline material was failed in this case. Hence a method reported<sup>2</sup> for handling oily Schiff bases was adopted here. The bright yellow solution formed was concentrated on a boiling water bath and cooled in a refrigerator. The viscous jelly mass obtained was re-dissolved in 25 mL methanol. This solution was used for the preparation of it's complexes.

## **2.4. Synthesis of zeoliteY supported metal complexes.**

### **2.4.1. Modification of zeoliteY to zeolite NaY.**

Synthetic zeoliteY was first modified as sodium zeoliteY (NaY). For this modification process, sample of dried zeoliteY (5g) was added to NaCl solution (0.1M, 500mL), stirred for 24 hrs at room temperature. Any other cations present in the sample is thus substituted with Na<sup>+</sup> ion. The slurry was filtered, washed several times with distilled water till the filtrate was free from chloride ions. Zeolite NaY was dried in an oven at 120°C for 4hrs. This modified, NaY was kept over calcium chloride for further use.

### **2.4.2. Modification of zeolite NaY to metal exchanged zeoliteY (MY).**

In flexible ligand method, metal ions have to be previously incorporated with in the super cages of zeoliteY framework before the encapsulation of complexes. Zeolite NaY was partially exchanged with the transition metal ions. Metal ion exchange was carried out by the following standard procedure<sup>3</sup>. Zeolite NaY (5g) sample was stirred in

an aqueous solution of the respective metal chlorides (0.01M, 500mL) at 70°C for 4hrs. Ion exchange with Fe<sup>3+</sup> ion was done using a very dilute solution of ferric nitrate (0.0025 M) to prevent dealumination at higher concentrations. The pH of the metal salt solution was adjusted between 4 and 4.5. At pH values lower than 4 aluminium ions are removed from the lattice and the structural framework<sup>4</sup> will collapse. The slurry was filtered and washed several times with distilled water till the filtrate was free from chloride ions. The metal exchanged zeolite was dried at 120°C for 4hrs, and was then dehydrated in muffle furnace at 400°C for 2hrs. Zeolite MY so obtained was kept over calcium chloride.

### **2.4.3. Encapsulation of metal complexes in zeolite Y.**

Flexible ligand method was used for the encapsulation of metal complexes in the voids of zeolite Y matrix. This method is applied, depending on the flexibility of ligands selected for complexation. The ligand diffuses through the pores and channels and get coordinated with the metal ions already introduced into the supercages. The procedure of encapsulation is described in the appropriate chapters.

## **2.5. Analytical methods.**

### **2.5.1. Estimation of metal content in simple complexes.**

Metal content in complexes was estimated by adopting a uniform procedure. The organic part of the complexes was completely eliminated before the estimation of the metals. A known weight of the metal complex (0.002 to 0.007g) was treated with conc:

nitric acid (25mL) and bromine in carbon tetrachloride (20 mL). This mixture was kept aside for 5 hrs. It was then evaporated to dryness on a boiling water bath. The metal ion was converted to its sulphate by fuming several times with small quantities of conc: sulphuric acid (1mL) each time. The resulting metal sulphate was dissolved in water, filtered and was used for the estimation of the metal content in complexes.

Iron and nickel were estimated gravimetrically using the literature procedures<sup>5</sup>. Iron content in the complexes was estimated as ferric oxide. This was done by precipitating the ferric ion in the solution as ferric hydroxide with ammonia solution and then igniting to ferric oxide. Nickel was estimated as nickel dimethylglyoximate complex by the addition of an alcoholic solution of dimethylglyoxime and excess of ammonia solution. Manganese, cobalt and copper contents in the complexes were determined by atomic absorption spectroscopy (AAS).

### **2.5.2. Estimation of Si, Al, Na and transition metal ion content in zeolite Y samples.**

A known weight ( $W_1$ ) of the dried sample of the zeolite was accurately weighed into a beaker. The zeolite framework was destroyed by heating with 40mL conc. sulphuric acid till fumes of  $SO_3$  were evolved, cooled, diluted with water and filtered using ash less filter paper (Whatman. 42). The filtrate was collected in a standard flask marked as filtrate A. The residue in the filter paper was incinerated in a platinum crucible with lid at burning temperature of electric Bunsen ( $\approx 1000^\circ C$ ) for one hour. It was then cooled and weighed ( $W_2$ ). Hydrofluoric acid (10mL, 40%) was added to dissolve the residue and the resulting solution was evaporated on a hot plate to remove

silicon in the form of hydrofluorosilicic acid  $\text{H}_2\text{SiF}_6$ . This was again incinerated at  $1000^\circ\text{C}$ , cooled and weighed ( $W_3$ ). The amount of silica present in the sample can be estimated from the loss in weight as follows:

$$\% \text{ of SiO}_2 = \frac{W_3 - W_2}{W_1} \times 100$$

The residue in the crucible was fused with potassium persulphate till a clear melt was obtained. The melt was dissolved in water and this solution was combined with the filtrate A in the standard flask. The solution was then made up to the known volume. This solution was then analysed for the analysis of aluminium, sodium, and metal contents by atomic absorption spectroscopy (AAS). The unit cell formula of zeolite was calculated from the Si/ Al ratio.

### **2.5.3. C H N analyses.**

Microanalysis for carbon, hydrogen and nitrogen in simple complexes and zeoliteY encapsulated complexes were carried out at Central Drug Research institute, Lucknow.

### **2.5.4. Estimation of Halogen and Sulphur.**

Chlorine content in simple complexes was determined by volumetric estimation using Volhard's method<sup>5</sup>. For sulphur estimation, peroxide fusion of the sample, followed by gravimetric estimation<sup>5</sup> was adopted. The complex was fused with

Na<sub>2</sub>CO<sub>3</sub> and Na<sub>2</sub>O<sub>2</sub> and the resulting sodium sulphate was estimated gravimetrically as barium sulphate.

## 2.6. PHYSICO-CHEMICAL METHODS.

### 2.6.1. Conductance measurements.

Molar conductance of the complexes were determined in nitrobenzene or methanol at 28 ± 2°C using a Elico PR 9500 conductivity bridge with a dip type cell and platinised platinum electrode.

### 2.6.2. Magnetic susceptibility measurements.

Simple Gouy type magnetic balance was used for magnetic susceptibility measurements at room temperature, 28 ± 2°C. The Gouy tube was standardized using Co[Hg(SCN)<sub>4</sub>] as approved by Figgis and Nyholm<sup>6</sup>. The effective magnetic moments were calculated using the equation:

$$\mu_{\text{eff}} = 2.84 (X_m^{\text{Corr}} T)^{1/2} \cdot \text{BM}$$

where T is the absolute temperature and  $X_m^{\text{Corr}}$  is the molar susceptibility corrected for diamagnetism of all other atoms and groups present in the complex using Pascal's constants<sup>7-9</sup>.

### 2.6.3. Surface Area and Pore Volume Analyses.

Surface area and pore volume of the metal exchanged zeolite Y and encapsulated samples were measured on a Micromeritics Gemini 2360 surface area analyzer by multipoint BET method. Surface area measurement is an important factor in assessing the catalyst performance of porous materials. The simultaneous determination of BET<sup>10</sup> surface area and pore volume was monitored by multi-layer adsorption of nitrogen gas at liquid nitrogen temperature and at different relative pressures. Prior to the BET measurements, samples were de-gasified at 125°C for 2hrs to remove any adsorbed gases. The surface area was calculated using the BET equation :

$$1/V_{\text{ads}}(P_0 - P) = 1/V_m C + [C-1]/VC] P/P_0$$

where,

$V_{\text{ads}}$  = volume of gas adsorbed at relative pressure  $P/P_0$ .

$P_0$  = saturated vapour pressure of the adsorbate.

$V_m$  = volume of gas adsorbed for monolayer coverage.

$C$  = BET constant related to the heat of adsorption.

### 2.6.4. X-ray Diffraction studies (XRD).

XRD technique is one of the most widely used techniques in heterogeneous catalysis. Powder X-ray diffraction patterns of zeolite NaY and the zeolite encapsulated complexes were compared and analyzed to know any change in the crystalline structure. The principle of XRD<sup>11</sup> is based on the interaction of X-rays with polycrystalline

material, which acts as a diffraction grating. Incident radiation of fixed wavelength was chosen for the purpose and the diffraction pattern was obtained by observing the intensity of scattered radiation as a function of scattering angle  $2\theta$ . The wave length of incident X-ray beam  $\lambda$ , the angle of diffraction  $\theta$  and the interplanar distance  $d$  are related by Bragg's equation,

$$n \lambda = 2d \sin \theta$$

X-ray diffraction patterns were measured on a Rigaka D-Max C, X-ray diffractometer with a stationary X-ray source, Ni filtered  $\text{CuK}\alpha$  radiation ( $\lambda = 1.5404$ ) and movable detector, which scans the intensity of diffracted radiation with in the range of  $0^\circ$  to  $70^\circ$  as a function of the angle  $2\theta$  between the incident and diffracted beams. This method is effective to know whether the structure of zeoliteY framework is preserved or not after the encapsulation of complexes.

### **2.6.5. Electronic spectra.**

Electronic spectra were taken in solution for the soluble complexes or in solid state for insoluble simple complexes by mull technique following a procedure recommended by Venanzi<sup>12</sup> as described below. Small filter paper strips were impregnated with a paste of the sample in nujol. This was dried and placed over the entrance of the photocell housing. A nujol treated filter paper strip of similar size and shape was used as the blank. The electronic spectra of the complexes were recorded on a Shimadzu UV-Vis 160A spectrophotometer.

### **2.6.6. Diffuse Reflectance UV-Vis Spectra (DRS).**

This is a very effective technique for getting information about d-d transitions and charge transfer transitions in metal complexes encapsulated in solid supports from which, coordination geometries of the encapsulated complexes can be realized. Diffuse reflectance spectra of the zeolite samples were recorded at room temperature within the wavelength range 200 to 850nm, using Ocean Optics, Inc. SD 2000, Fibre optic spectrometer with CCD detector. Zeolite Y is used as the reference. The spectra were computer processed and recorded directly in absorbance mode.

### **2.6.7. FTIR Spectra.**

FTIR spectroscopy is a well-recognized approach for procuring information on the basic characteristics of a molecule namely, identification of various functional groups, the nature of atoms and their chemical linkages. The frequencies and intensities of IR bands can thus provide information about their structure. Infrared spectra of the ligands and the complexes in the region  $400$  to  $4000\text{ cm}^{-1}$  were taken by using KBr pellets on a Shimadzu 8101 FTIR spectrophotometer.

### **2.6.8. EPR spectra.**

The X-band EPR spectra of the copper(II) complexes were taken in chloroform - toluene mixture at liquid nitrogen temperature using varian E-112 X/Q

band spectrophotometer. The EPR of the zeolite encapsulated copper(II) complexes were also recorded. The  $g$  values were determined relative to the standard tetracyanoethylene (TNCE,  $g = 2.0027$ ). From  $g_{||}$  and  $g_{\perp}$  parameters,  $\mu_{\text{eff}}$  values were also determined by using the following equation<sup>13</sup>.

$$\mu_{\text{eff}}^2 = g_{||}^2/4 + g_{\perp}^2/4 + 3kT / \lambda_0 (g - 2).$$

where  $\lambda_0$  ( $= -828 \text{ cm}^{-1}$ ) is the spin orbit coupling constant for the free metal ion.

The density of unpaired electrons at the central atom was computed using the equation<sup>14</sup>

$$\alpha_{\text{Cu}}^2 = (A_{||}/P) + (g_{||} - 2) + 3/7 (g_{\perp} - 2) + 0.04 .$$

where,  $1 - \alpha^2$  is the covalency associated with the bonding of metal ion to the ligand and  $P = 0.036 \text{ cm}^{-1}$ .

### 2.6.9. Thermogravimetric analysis (TG).

In thermogravimetric analysis, the samples to be analysed are subjected to a controlled heating to high temperature at a specified heating rate. The weight loss of the sample on heating is being recorded as a function of temperature. The weight loss was due to the rupture or formation of physical or chemical bonds at elevated temperatures. Thus the technique has widespread application in determining the phase composition, percentage weight loss, stability limits of a complex, drying range, dehydration and decomposition temperature etc.

The TG curves were obtained on a Perkin Elmer 3700 thermal analyzer, at a heating rate of  $10^{\circ}\text{C min}^{-1}$  in an inert atmosphere using a platinum crucible. The mass of the samples used was in the range 5 -10mg.

#### **2.6.10. Scanning electron microscopy (SEM).**

SEM analysis is suitable for obtaining very impressive, in-focus, magnified real-space images from a highly irregular structure (like zeolites). Scanning electron microscopy of a representative zeolite encapsulated complex before and after soxhlet extraction was carried out to analyze the morphology of the samples. The SE micrograph were recorded at Sree Chitra institute of Medical Science and Technology, Thiruvananthapuram.

#### **2.7. Catalytic activity studies.**

The synthesized complexes were screened for catalytic activities for some well-known reactions. Methods used for monitoring the various reactions are described in Chapter VIII. The following instrumental techniques were employed for the catalytic activity studies.

Screening studies of the simple and zeolite encapsulated complexes for the decomposition of  $\text{H}_2\text{O}_2$  was performed with a gas burette at room temperature ( $30 \pm 1^{\circ}\text{C}$ ). Details regarding the instrument are given in Chapter VIII.

The complexes were also screened for the catalytic activity in the oxidations of benzaldehyde, benzyl alcohol, propan-1-ol and propan-2-ol. This was monitored using

a Shimadzu 200 UV-Vis spectrophotometer. Catalytic activity studies involving cyclohexanol was carried out on a Chemito 8510 Gas Chromatograph fitted with a carbowax column and thermal conductivity detector.

\*

## REFERENCES

1. D.D. Perrin, W.L.F. Armarego and D.R.Perrin., *Purification of Laboratory Chemicals*; Pergamon Press, Oxford.(1980).
2. Rajib Lal De, Keka Samanta, Chitra Samanta and Alok K.Mukherjee., (1999), *Ind. J. Chem.* Vol.38A. pp.1010-1014.
3. Norman Herron., *Inorg.Chem.*,25, (1986), 4714.
4. P.G.Menon, 'Molecular sieves in heterogeneous catalysis' in Lectures on Catalysis, 41<sup>st</sup> Ann. Meeting, Ind. Acad. Sci., S.Ramasheshan Ed., (1975).
5. A.I. Vogel., *A Text Book of Qualitative Inorganic Analysis*; Longmans-Green; London. (1978).
6. B.N. Figgis and R.S. Nyholm., *J.Chem.Soc.* (1958) 4190.
7. B.N. Figgis and J.Lewis., *Modern Coordination Chemistry*;Ed, Interscience, New York (1958).
8. P.W. Selwood. *Magnetochemistry*; Interscience, New York (1958).
9. B.N. Figgis and J.Lewis., *Progress in Inorganic Chemistry*; F.A.Cotton, Ed, Interscience, New York (1958).
10. S.Brunauer. P.H, Emmette and E.Teller., *J.Am.Chem.Soc.*,60, (1938), 309.
11. Clive Whiston., "X-ray methods- Analytical Chemistry by Open Learning", John Wiley, New York, (1987), Ch.3.
12. L.N. Venanzi, G.Dyer and J.G.Hartley., *J.Chem.Soc.*(1965), A,1293.
13. B.V.Agarvala., *Inorg. Chim. Acta*, 36, (1979), 209.
14. D.Kivelson and R. Neiman., *J.Chem.Phys.* 35, (1961), 149.

# CHAPTER III



**Mn(II), Fe(III), Co(II), Ni(II) and Cu(II) complexes  
of the Schiff base  
derived from salicylaldehyde and 2-aminobenzothiazole.**

**3.1. Introduction.**

Benzothiazole and thiazole derivatives are well known biologically active compounds<sup>1-5</sup>. Sulphur containing compounds are particularly known for their effectiveness against bacteria and have been found various use in medicine. Thiazole and thiazolidine compounds possess fungicidal and other biological activities. It has been suggested that the presence of azomethine linkage and thiazole moiety are the structural factors that favour the biological activity of these compounds. Further, the biological activity of certain organic compounds has been related to their ability for complex formation with metal ions. Many of the anticancer drugs are also potential ligands. Some of these drugs exhibit increased anticancer activity when administered as metal complexes. The Schiff base complexes of Co, Ni, Cu, and Zn derived from thiazole<sup>6</sup> were tested for their antineoplastic potency against L-1210 lymphoid leukemia<sup>7</sup> and in every case all the animals survived on toxicity day. There are reports about metal complexes of ligands containing electron withdrawing groups exhibiting improved biological activity<sup>8,9</sup>.

Schiff bases formed by the condensation of 2-aminobenzothiazole, 2-amino-6-carboxyethylbenzothiazole or 2-amino-6-methylbenzothiazole with benzaldehyde, N,N-dimethylbenzaldehyde, p-nitrobenzaldehyde, o-nitrobenzaldehyde or o-

chlorobenzaldehyde are reported in literature<sup>10</sup>. Reports of complexes of Schiff bases derived from the derivatives of 2-aminobenzothiazole and substituted salicylaldehyde are also seen in literature. However, complexes of Schiff base derived from 2-aminobenzothiazole and salicylaldehyde has not yet been studied. The role of benzothiazole derivatives and azomethine linkage in certain biological reactions prompted us to synthesize Schiff base containing benzothiazole nucleus and transition metal complexes of this Schiff base. The details regarding the preparation and characterization of complexes of Mn(II), Fe(III), Co(II), Ni(II) and Cu(II) with the Schiff base derived from 2-aminobenzothiazole and salicylaldehyde (SBT) are presented in this chapter.

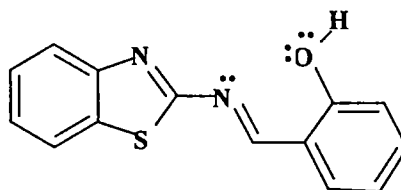


Figure.III.1. Structure of the ligand – SBT

## 3.2 Experimental.

### 3.2.1 Materials.

*The procedure for the preparation and purification of the Schiff base ligand from salicylaldehyde and 2-aminobenzothiazole (SBT) is given in Chapter-II.*

### 3.2.2 Synthesis of SBT complexes.

The complexes of Mn(II), Fe(III), Co(II), Ni(II) and Cu(II) were prepared by the following general procedure.

A solution of metal salt,  $\text{MnCl}_2 \cdot 4\text{H}_2\text{O}$  (1.98g, 0.01mol),  $\text{Fe}(\text{NO}_3)_3 \cdot 9\text{H}_2\text{O}$  (4.04g, 0.01mol),  $\text{CoCl}_2 \cdot 6\text{H}_2\text{O}$  (2.38g, 0.01mol),  $\text{NiCl}_2 \cdot 6\text{H}_2\text{O}$  (2.36g, 0.01mol), or  $\text{CuCl}_2 \cdot 2\text{H}_2\text{O}$  (1.7g, 0.01mol), in methanol (25mL) was added to the solution of SBT (5.08g, 0.02mol) in methanol (40 mL) taken in a round-bottomed flask. This was refluxed for 2 hrs. Solution obtained was concentrated by evaporation and was cooled in refrigerator. The gel formed slowly gets precipitated out when extracted several times with petroleum ether and scratching the mass with a glass rod. It was filtered and dried in vacuum over anhydrous calcium chloride.

(Yield 55-70%).

### **3.2.3. Analytical methods.**

The prepared complexes were characterized by various physico-chemical methods. The details of analytical methods and other characterization technique are given in Chapter II.

## **3.3. Results and Discussion.**

All the complexes are coloured, crystalline and non-hygroscopic and are quite stable to atmospheric oxidation. The complexes are soluble in ethanol, methanol, acetone, and nitrobenzene. The complexes are found to be quite stable for a longer period without undergoing any decomposition.

### **3.3.1 Elemental Analysis.**

Analytical data of the complexes are presented in Table III.1. The data suggest that in the case of all the complexes, except in the case of Mn(II) complex, the ligand

**Table. III.1.**  
Analytical data of SBT Complexes.

| Complex<br>(Colour)  | C (%)<br>found<br>(Calc.) | H (%)<br>Found<br>(Calc.) | N (%)<br>found<br>(Calc.) | S (%)<br>found<br>(Calc.) | Cl (%)<br>Found<br>(Calc.) | M %<br>found<br>(Calc.) |
|--|---------------------------|---------------------------|---------------------------|---------------------------|----------------------------|-------------------------|
| [Mn(SBT) <sub>2</sub> (H <sub>2</sub> O) <sub>2</sub> ]<br>(Bright yellow)                   | 55.97<br>(56.29)          | 3.50<br>(3.69)            | 9.12<br>(9.38)            | 10.96<br>(10.72)          | ---                        | 8.33<br>(9.21)          |
| [Fe(SBT)(NO <sub>3</sub> ) <sub>2</sub> (H <sub>2</sub> O) <sub>2</sub> ]<br>(Reddish brown) | 35.66<br>(35.83)          | 2.42<br>(2.77)            | 11.87<br>(11.94)          | 6.62<br>(6.83)            | ---                        | 11.6<br>(11.91)         |
| [Co(SBT)(Cl) (H <sub>2</sub> O)]<br>(Deep greenish blue)                                     | 45.62<br>(45.98)          | 3.11<br>(3.01)            | 7.78<br>(7.66)            | 8.47<br>(8.76)            | 9.97<br>(9.70)             | 16.57<br>(16.13)        |
| [Ni(SBT) (Cl) (H <sub>2</sub> O)]<br>(Orange)  | 46.39<br>(46.01)          | 3.21<br>(3.01)            | 7.36<br>(7.67)            | 8.47<br>(8.77)            | 9.54<br>(9.71)             | 15.90<br>(16.08)        |
| [Cu(SBT)(Cl)(H <sub>2</sub> O)]<br>(Brown)   | 45.58<br>(45.41)          | 3.20<br>(2.97)            | 7.46<br>(7.57)            | 8.40<br>(8.65)            | 9.62<br>(9.58)             | 16.85<br>(17.18)        |

and the metal ions are in 1:1 mole ratio. In the case of Mn(II) complex this ratio is 1:2. The empirical formulae arrived from the data are [ML(Cl) (H<sub>2</sub>O)] for Co(II), Ni(II) and Cu(II) complexes; [ML<sub>2</sub>(H<sub>2</sub>O)<sub>2</sub>] for Mn(II) complex and [ML(NO<sub>3</sub>)<sub>2</sub>(H<sub>2</sub>O)<sub>2</sub>] for iron(III) complex (where M stands for the corresponding metal ion and L stands for the SBT ligand).

### 3.3.2. Conductance measurements.

The molar conductance of the complexes in 10<sup>-3</sup> M nitrobenzene solutions was measured at 28 ± 2°C. The conductance values are presented in Table.III.2.

**Table. III.2**

Molar conductance and Magnetic moment data.

| Complex   | Yield % | Magnetic moment BM | Molar conductance ohm <sup>-1</sup> cm <sup>2</sup> mol <sup>-1</sup> |
|---|---------|--------------------|---|
| [Mn(SBT) <sub>2</sub> (H <sub>2</sub> O) <sub>2</sub> ]                   | 55      | 5.8                | 4.9   |
| [Fe(SBT)(NO <sub>3</sub> ) <sub>2</sub> (H <sub>2</sub> O) <sub>2</sub> ] | 60      | 5.8                | 2.3   |
| [Co(SBT) (Cl) (H <sub>2</sub> O)]   | 65      | 4.4                | 11.8  |
| [Ni(SBT) (Cl) (H <sub>2</sub> O)]   | 70      | Diamagnetic        | 2.0   |
| [Cu(SBT) (Cl) (H <sub>2</sub> O)]   | 65      | 1.7                | 2.8   |

The molar conductance values<sup>11</sup> are within the range 70-120  $\text{ohm}^{-1}\text{cm}^2 \text{mol}^{-1}$  for 1:1 electrolytes, 120-180 for 1:2 electrolytes. It will be above 180  $\text{ohm}^{-1}\text{cm}^2 \text{mol}^{-1}$  for 1:3 electrolytes. The molar conductance values suggest that all the SBT complexes are non-electrolytes.

### 3.3.3. Magnetic Susceptibility.

The magnetic data provide great deal of information complementary to that available from the electronic spectra. An unpaired electron in a compound has both spin angular momentum and orbital angular momentum. These reinforce with the applied field to get the resultant magnetic susceptibility of the sample. It is necessary to subtract diamagnetic contribution to get the pure paramagnetic susceptibility. Deviation occurs due to the quenching of orbital angular momentum, spin-orbit coupling, TIP etc.

The magnetic moment values of the complexes are measured at room temperature (at  $28 \pm 2^\circ\text{C}$ ) and the values are presented in Table. III.2. The magnetic moment value of MnSBT complex was found to be 5.8 BM, which corresponds to the spin only value of 5.9 BM for  $d^5$  high spin octahedral complex<sup>12</sup>. Since the ground state of high spin Mn(II) ion is  ${}^6A_1$ , orbital contribution will be absent. However, spin-orbit coupling may alter the magnetic moment from spin only value. FeSBT complex exhibits a magnetic moment value of 5.8 BM, which is very near to the spin only value of 5.9 BM. For Fe(III) complexes  $t^3_{2g} e^2_g$  ( $s = 5/2$ ) is the common configuration with  ${}^6A_1$  ground state nearly in all its octahedral complexes except those with the strong ligands.

In such cases, moments will be close to 5.92 BM predicted by the spin only formula. Deviations may arise due to impure materials or due to dimer formation.

CoSBT has a magnetic moment value of 4.4 BM, which is higher than the spin only value of 3.8 BM. This higher value is attributed to the orbital contribution resulting from the ground state term  $^4A_2$  of a tetrahedral complex. Diamagnetic nature of NiSBT complex indicates a square planar structure to the complex. The magnetic moment value of CuSBT is found to be 1.7 BM. Moments of copper complexes are in the range 1.73 – 2.3 BM irrespective of their geometry. The lower value of CuSBT complex suggests a square planar structure to it.

#### 3.3.4. Electronic spectra.

The electronic spectra of the ligand SBT and the complexes in the region 200 to 800 nm are given in Figure. III.2. The spectral data are furnished in Table.III .3. Schiff bases of 2-aminobenzothiazoles show bands in the region of  $40000-36350\text{ cm}^{-1}$  due to  $\pi \rightarrow \pi^*$  transition<sup>10,13</sup>. The Schiff base, SBT, exhibits a band at  $33300\text{ cm}^{-1}$ . This shift of the band to lower frequencies may be due to the extension of conjugation.

The electronic spectrum of ligand SBT shows three absorption bands at  $40000\text{ cm}^{-1}$ ,  $36300\text{ cm}^{-1}$  and  $26300\text{ cm}^{-1}$  respectively owing to intraligand transitions. Intensity as well as width of these peaks was found to be decreased in the spectra of complexes. Further, shift in the positions of some of these region of absorption in the spectra of complexes can be taken as a positive evidence of complex formation. Such shift in absorption bands on complex formation was reported by the earlier workers<sup>10</sup> as due to the extended conjugation of bonds.

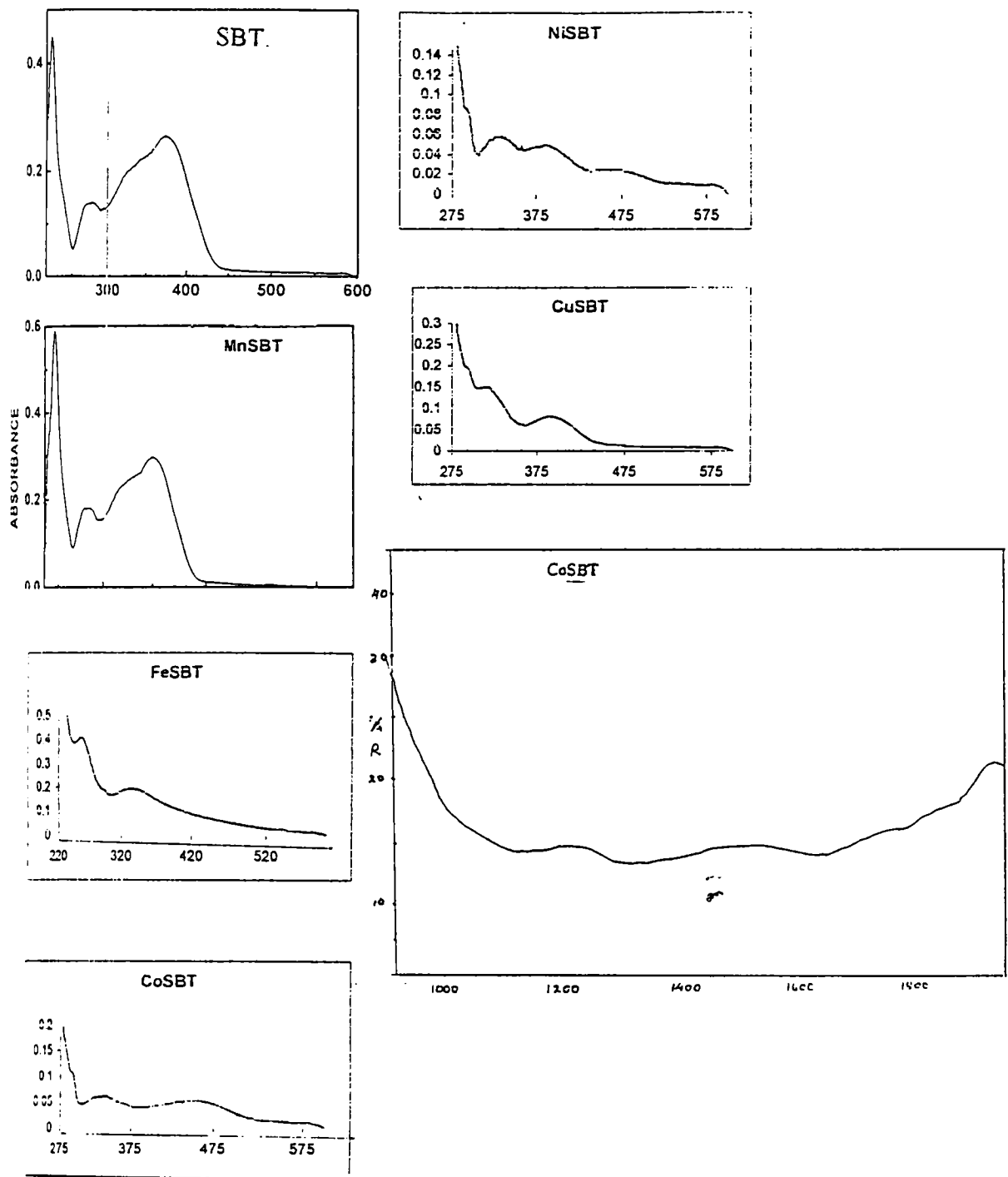


Figure.III.2. Electronic Spectra of ligand SBT and MSBT complexes.

**Table. III.3**  
Electronic spectral data.

| Complex   | Abs. Max<br>(cm <sup>-1</sup> ) | Tentative<br>assignments                                      |
|---|---------------------------------|---|
| [Mn(SBT) <sub>2</sub> (H <sub>2</sub> O) <sub>2</sub> ]                   | 40000                           | Intra-ligand transition                                       |
|   | 35700                           | Charge transfer transition                                    |
|   | 26670                           | d-d transition  |
| [Fe(SBT)(NO <sub>3</sub> ) <sub>2</sub> (H <sub>2</sub> O) <sub>2</sub> ] | 40000                           | Intra-ligand transition                                       |
|   | 35700                           | Charge transfer transition                                    |
|   | 30300                           | d-d transition  |
| [Co(SBT) (Cl) (H <sub>2</sub> O)]   | 40000                           | Intra-ligand transition                                       |
|   | 35000                           | Charge transfer transition                                    |
|   | 22000                           | <sup>4</sup> A <sub>2</sub> → <sup>4</sup> T <sub>1</sub> (P) |
|   | 10200                           | <sup>4</sup> A <sub>2</sub> → <sup>4</sup> T <sub>1</sub> (F) |
|   | 6684                            | <sup>4</sup> A <sub>2</sub> → <sup>4</sup> T <sub>2</sub> (F) |
| [Ni(SBT)(Cl)(H <sub>2</sub> O)]   | 40000                           | Intra-ligand transition                                       |
|   | 35000                           | Charge transfer transition                                    |
|   | 21000                           | <sup>1</sup> A <sub>1g</sub> → <sup>1</sup> B <sub>1g</sub>   |
| [Cu(SBT)(Cl)(H <sub>2</sub> O)]   | 40000                           | Intra-ligand transition                                       |
|   | 34500                           | Charge transfer transition                                    |
|   | 33000                           | ”   |
|   | 22300                           | d-d transition  |

The electronic spectrum of MnSBT complex seems obscured in the lower regions, which might be due to the high intensity of  $\pi \rightarrow \pi^*$  transitions in the region  $40000\text{cm}^{-1}$  to  $25000\text{cm}^{-1}$ . For the high spin Mn(II) complexes, the ground state is  ${}^6A_1$  in a weak field so that all excited states of  $d^5$  ion have different spin multiplicity and hence transitions to them are spin forbidden. Therefore absorption bands due to d-d transitions are extremely weak, even though a number of transitions were expected between the region  $15000\text{ cm}^{-1}$  to  $30000\text{ cm}^{-1}$ . High spin d-d transitions in this case are difficult to assign. As in the case of Mn(II) complexes, FeSBT also has the ground state term  ${}^6A_1$  and has no other sextuplet state in the excited states. Hence all the transitions are spin forbidden. Therefore the absorption bands due to d-d transitions are extremely weak and difficult to assign. As the charge transfer absorption occurs at lower energy region due to the high positive charge of Fe(III), most of the very weak intensity d-d bands<sup>14</sup> will be obscured.

CoSBT shows two bands around  $40000\text{ cm}^{-1}$  and  $35000\text{ cm}^{-1}$  (as in the case of all the other complexes), which can be assigned to the intraligand and charge transfer transitions. Three other weak bands of low energy were observed for this Co(II) complex suggesting a tetrahedral structure. The ground state of tetrahedral  $d^7$  system is  ${}^4A_2$ . The bands at  $22000\text{ cm}^{-1}$ ,  $10200\text{ cm}^{-1}$  and  $6680\text{ cm}^{-1}$  can be assigned to  ${}^4A_2 \rightarrow {}^4T_1(P)$ ,  ${}^4A_2 \rightarrow {}^4T_2(F)$  and  $A_2 \rightarrow {}^4T_1(F)$  transitions respectively. Tetrahedral complexes for Co(II) are in fact more in number than those for other metal ions, since octahedral site preference energy is smaller for Co(II) ion compared to other metal ions. The deep greenish - blue colour of the complex is also indicative of tetrahedral geometry.

Nickel(II) complex of SBT shows a band at  $21000\text{ cm}^{-1}$  in the electronic spectrum of the complex that can be assigned to  ${}^1A_{1g} \rightarrow {}^1B_{1g}$  transition<sup>15</sup> corresponding to the square planar structure of the complex. Other bands observed at  $40000\text{ cm}^{-1}$ ,  $35000\text{ cm}^{-1}$  are assigned to the intra-ligand and charge transfer transitions. In the case of electronic spectrum of CuSBT complex, the bands around  $40000\text{ cm}^{-1}$  and  $34500\text{ cm}^{-1}$  are assigned to the intraligand and charge transfer transition bands. The broad band of low intensity observed at  $22300\text{ cm}^{-1}$  may be assigned to d-d transition band. The magnetic moment of 1.79BM supports square planar geometry to the complex. The brown colour of the complex may also be due to the tailing of the CT transitions into the blue end of the visible spectrum<sup>16</sup>.

### 3.3.5. FTIR Spectra.

The characteristic infrared frequencies of the Schiff base ligand SBT and the complexes along with their assignments are given in Table. III .4 and the spectra of the ligand SBT and that of the complexes are presented in Figure.III.3. and Figure.III.4 respectively.

Ligand SBT possesses azomethine nitrogen, oxygen atom of phenolic group, sulphur and nitrogen atom of thiazole ring. All these sites can be used for coordination with the metal ions. IR spectra of 2-aminobenzothiazole (ABT) shows two bands at  $3393\text{ cm}^{-1}$  and  $3279\text{ cm}^{-1}$  due to the stretching frequencies of free  $-\text{NH}_2$  group<sup>17</sup>. Disappearance of these bands in the spectra of ligand-SBT and the appearance of a new band at  $1667\text{ cm}^{-1}$  (due to the stretching frequency of  $-\text{C}=\text{N}$  group) clearly indicates that the primary amino group has involved in the formation of azomethine group of the Schiff base ligand. The spectrum of SBT ligand exhibits another band at  $1613\text{ cm}^{-1}$ , which can

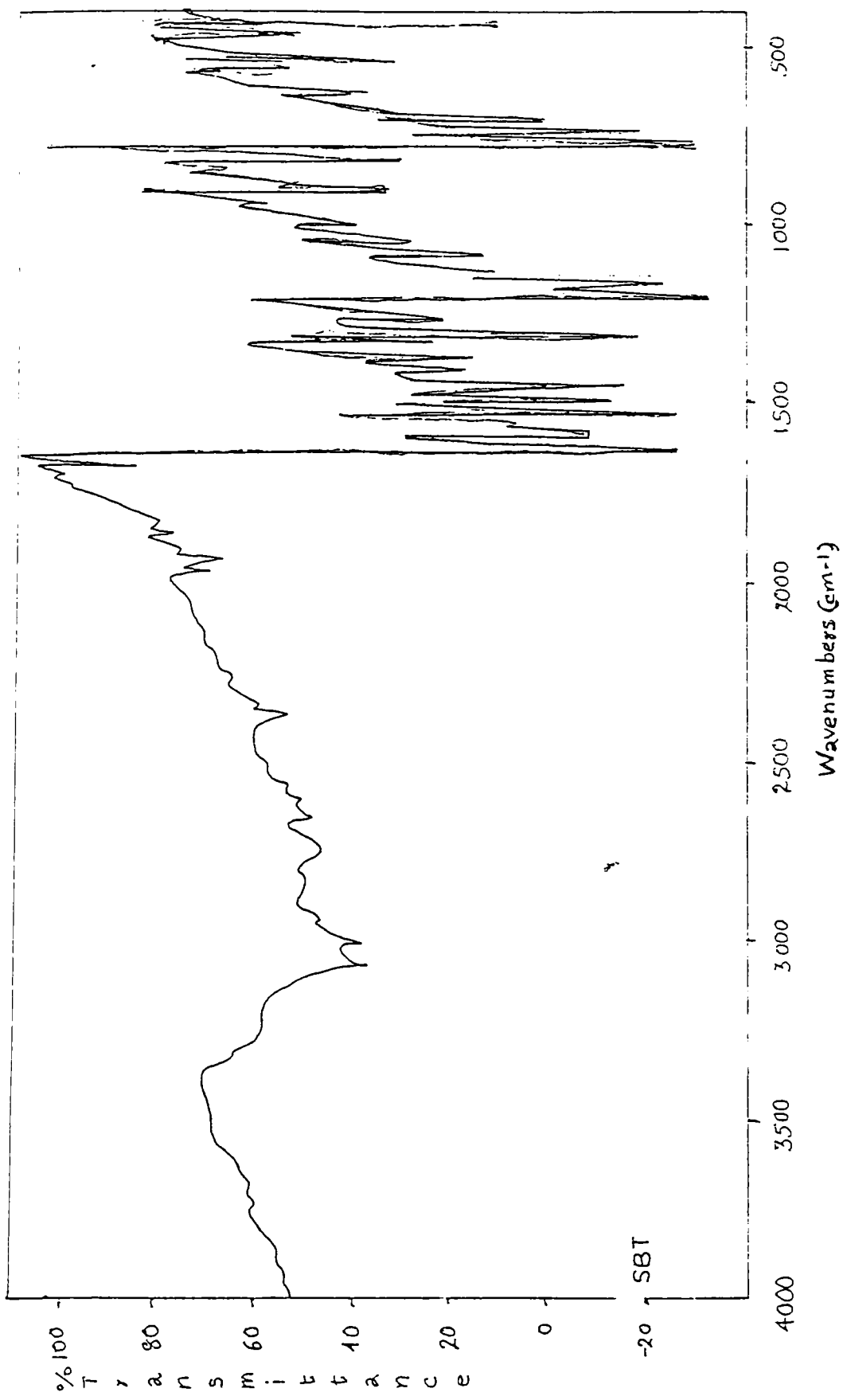


Figure.III.3. FTIR spectra of ligand SBT.

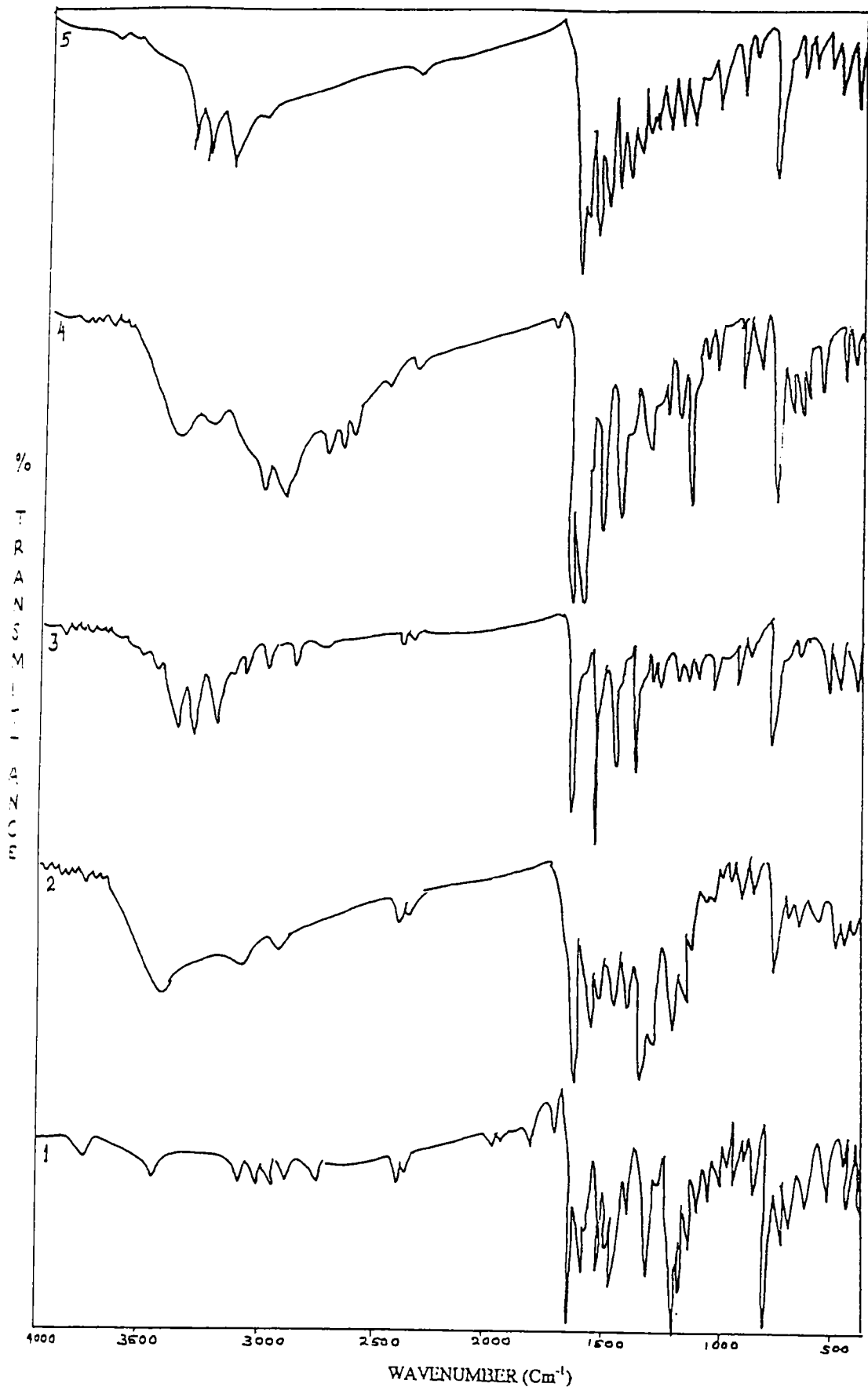


Figure.III.4. FTIR spectra of MSBT complexes.  
1).MnSBT 2). FeSBT 3).CoSBT  
4).NiSBT 5). CuSBT.

**Table. III. 4.**  
 Infra-red absorption frequencies (cm<sup>-1</sup>)

| SBT   | MnSBT | FeSBT  | CoSBT  | NiSBT | CuSBT  | Tentative assignments of the more relevant bands |
|-------|-------|--------|--------|-------|--------|--|
| (1)   | (2)   | (3)    | (4)    | (5)   | (6)    | (7)  |
| -     | 3436w | 3409s  | 3350s  | 3403s | 3370s  | VOH <sub>antisym</sub> str. H <sub>2</sub> O     |
| -     | 3287  | -      | 3290s  | 3283s | 3297s  | VOH <sub>sym</sub> str. (H <sub>2</sub> O)       |
| -     | -     | -      | 3177s  | 3091w | 3184s  |  |
| 3063w | 3051w | -      | 3051w  | 3058w | -      | VOH <sub>(phenolic)</sub>                        |
| 1667m | 1659w | 1640sh | 1619s  | 1646s | 1625sh | VC=N   |
| -     | -     | 1619s  | -      | -     | -      |  |
| 1613s | 1613s | 1613s  | 1613sh | 1619s | 1613s  | VC=N(ring)                                       |
| 1452m | 1448w | 1452sh | 1448m  | 1453m | 1454m  | VC-S(ring)                                       |
| -     | -     | 1434m  | -      | -     | -      | VNO <sub>3</sub> (monodentate)                   |
| -     | -     | 1321s  | -      | -     | -      | VNO <sub>3</sub> (onodentate)                    |
| 1290s | 1288s | 1288s  | 1288s  | 1288s | 1288s  |  |
| 1182s | 1182s | 1184s  | 1182s  | 1182s | 1186s  | VC-S(ring)                                       |
| 1148m | 1146m | 1150m  | 1144m  | 1142m | 1150m  |  |
| 1067m | 1078w | 1089w  | 1089w  | 1072w | 1080sh | VC-O(Phenolic)                                   |
| -     | 1030m | 1030m  | 1023m  | 1023m | 1030w  |  |
| -     | -     | 1023w  | -      | -     | -      | VNO <sub>3</sub> (monodentate)                   |
| 840m  | 844sh | 844w   | 837w   | 845w  | 850w   |  |
| 757s  | 756m  | 758m   | 754m   | 758m  | 751m   |  |
| -     | 724m  | 711sh  | 711w   | 714m  | 714sh  | ν <sub>H<sub>2</sub>O</sub>                      |
| 683m  | 680w  | 678w   | 671w   | 674w  | 675w   |  |
| 552m  | 558w  | 558w   | 553sh  | 555sh | 539sh  |  |
| -     | 525w  | 528w   | 512w   | 525sh |        | ν <sub>H<sub>2</sub>O</sub>                      |
| -     | -     | -      | 486m   | 492m  | 492m   | ν <sub>M-Cl</sub>                                |
| 434s  | 432s  | 430m   | 433s   | 433m  | 426w   |  |

be assigned to  $\nu_{C=N}$  of the thiazole ring. But this band is seen in 2-aminothiazole at  $1647\text{cm}^{-1}$ . The red shift of this band to  $1613\text{cm}^{-1}$  may be due to the extended conjugation through Schiff base formation. The bands around  $1452\text{cm}^{-1}$  and  $1182\text{cm}^{-1}$  are characteristic<sup>18</sup> of the  $\nu_{C-S}$  of thiazole ring. These bands remain at the same position in the spectra of Schiff base as well as in the case of its complexes revealing that sulphur atom of thiazole ring is not taking part in coordinate bond formation with the metal ions. A broad band near  $3500\text{-}2700\text{cm}^{-1}$  in all the complexes indicates<sup>19</sup> the presence of coordinated water molecules.

The band at  $\sim 720\text{ cm}^{-1}$  due to rocking ( $\rho r\text{H}_2\text{O}$ ) and another band near  $\sim 520\text{ cm}^{-1}$  due to twisting ( $\rho t\text{ H}_2\text{O}$ ) modes of coordinated water molecule are also seen in the spectra. Azomethine group  $\nu_{C=N}$  appear as a strong band at  $1667\text{cm}^{-1}$  in the spectra of ligand. This band shifted (by  $\sim 10\text{-}40\text{ cm}^{-1}$ ) towards lower frequencies in the spectra of all the complexes, which clearly suggests that complexation has taken place through the nitrogen atom of azomethine group<sup>20-22</sup>. The participation of phenolic oxygen in coordination to the metal ion is supported by an upward shift<sup>9,23</sup> in  $\nu_{C-O}(\text{phenolic})$  at  $1067\text{cm}^{-1}$  of the ligand to the extent of  $\sim 12\text{-}22\text{ cm}^{-1}$  in all the complexes.

Three bands in the finger print region at  $1434\text{cm}^{-1}$ ,  $1321\text{cm}^{-1}$  and  $1023\text{cm}^{-1}$  correspond to uni dentate nitrate<sup>19,24-26</sup> group in FeSBT complex. The separation between two highest frequency bands is  $113\text{ cm}^{-1}$ , which confirms that the nitrate group in this complex is uni dentate in nature. Furthermore, these bands are absent in the spectrum of ligand. New medium bands at  $\sim 490\text{ cm}^{-1}$  in CoSBT, NiSBT and CuSBT might be due to  $\nu_{M-Cl}$  in these complexes<sup>27</sup>. This band was not seen neither in IR- spectra of the ligand nor in MnSBT or FeSBT complexes.

In the light of foregoing discussion it can be concluded that the ligand SBT is coordinated to the metal ion through the nitrogen atom of the azomethine group and phenolic –OH group. Coordinated water molecule is also present in all the complexes.

### 3.3.6. EPR Spectra.

The EPR spectrum obtained for the CuSBT complex at liquid nitrogen temperature (LNT) in methanol medium, is presented in Figure.III.5. In the spectrum at LNT, four peaks of small intensity originating from  $g_{\parallel}$  component have been identified. The,  $g_{\parallel}$ ,  $g_{\perp}$ ,  $A_{\parallel}$ , bonding parameter ( $\alpha^2$ ),  $\mu_{\text{eff}}$  of the CuSBT complex are computed and presented in Table.III.5.

**Table. III.5**  
EPR spectral data of the CuSBT complex

| EPR parameter                   | CuSBT                                  |
|---------------------------------|--|
| $g_{\parallel}$                 | 2.2                                    |
| $g_{\perp}$                     | 2.03                                   |
| $A_{\parallel}$                 | $136.95 \times 10^{-4} \text{cm}^{-1}$ |
| $g_{\parallel} / A_{\parallel}$ | 160.6 cm                               |
| $g_{\text{av}}$                 | 2.16                                   |
| $\alpha^2$                      | 0.63                                   |
| $\mu_{\text{eff}}$              | 1.82                                   |

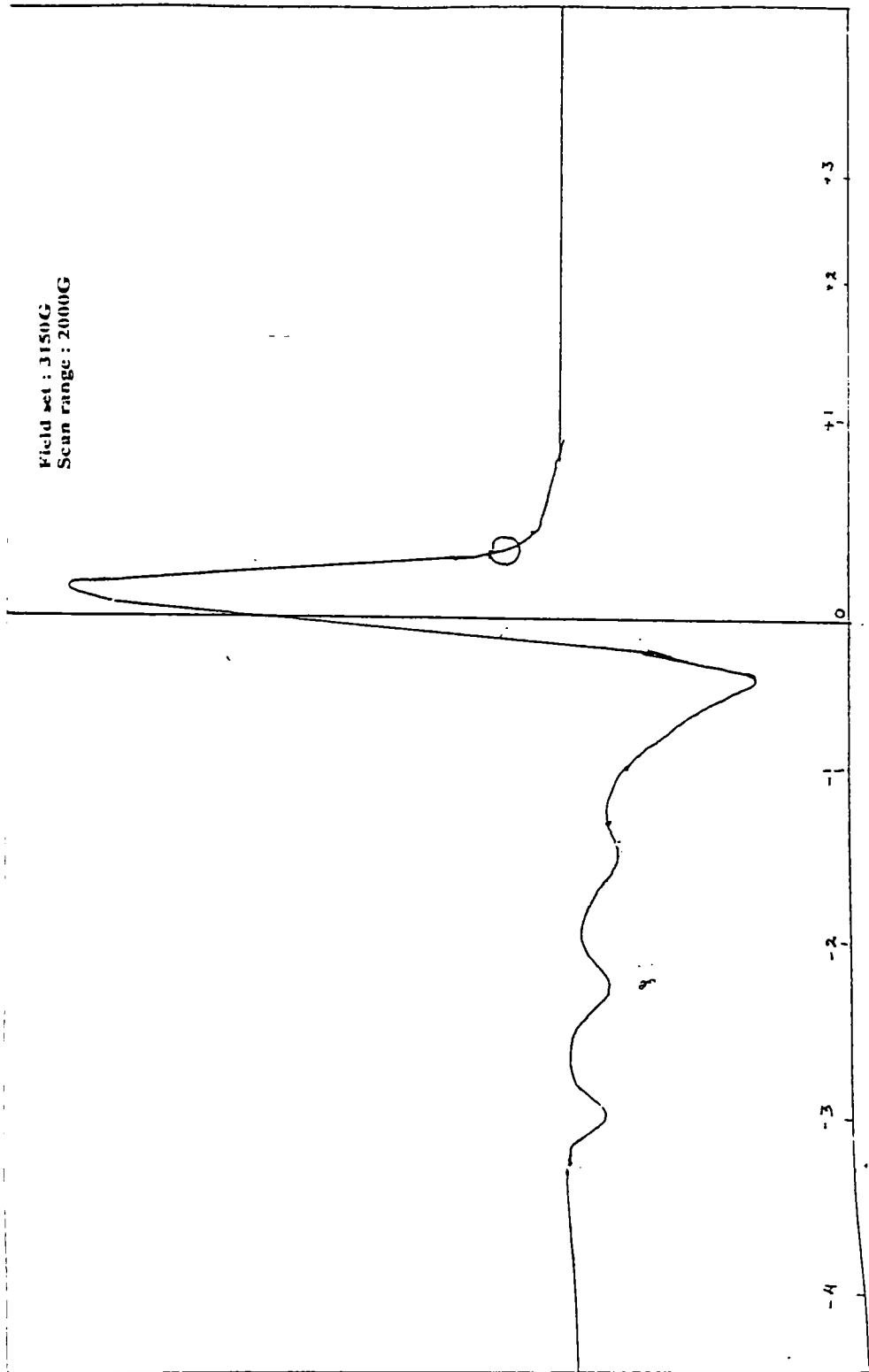


Figure III.5. EPR spectra of CuSBT complex.

The  $g_{\parallel}$  and  $g_{\perp}$ , are computed from the spectrum using diphenyl picrylhydrazyl (DPPH) free radical as field marker as per the procedure given by Kneubuhl<sup>28</sup>. The  $g_{\parallel}$  value will be less than 2.3 for covalent character of metal ligand bond and will be greater than 2.3 for ionic character<sup>29</sup>. Applying this criterion, the  $g_{\parallel}$  value of 2.2 indicates the covalent nature of the complex. The bonding parameter ( $\alpha^2$ ) for the complex is 0.63, which also can be attributed to covalent nature of the complex. This value will be in the range 0.62-0.7 for complexes with covalent nature<sup>30</sup>. The trend  $g_{\parallel} > g_{\perp} > g_e$  (2.0033) observed for the complex suggests that the unpaired electron is localized in  $dx^2-y^2$  orbital of the copper(II) ion. The extend of tetragonal distortion,  $f = g_{\parallel} / A_{\parallel}$  for the complex lie within the range of 130-160  $\text{cm}^{-1}$  suggested for a distorted tetrahedral geometry.

### 3.3.7. Thermo gravimetric analysis.

The TG analysis of NiSBT complex was carried out and the data so obtained is given in Table III.6.

**Table. III.6.**  
Thermal analysis data of NiSBT complex

| Complex                         | Temperature range, °C | % weight loss |
|---------------------------------|-----------------------|---------------|
| [Ni(SBT)(Cl)(H <sub>2</sub> O)] | 29-110                | 5.6           |
|                                 | 110-293               | 20.0          |
|                                 | 293-586               | 60.5          |
|                                 | 586-800               | 4.5           |

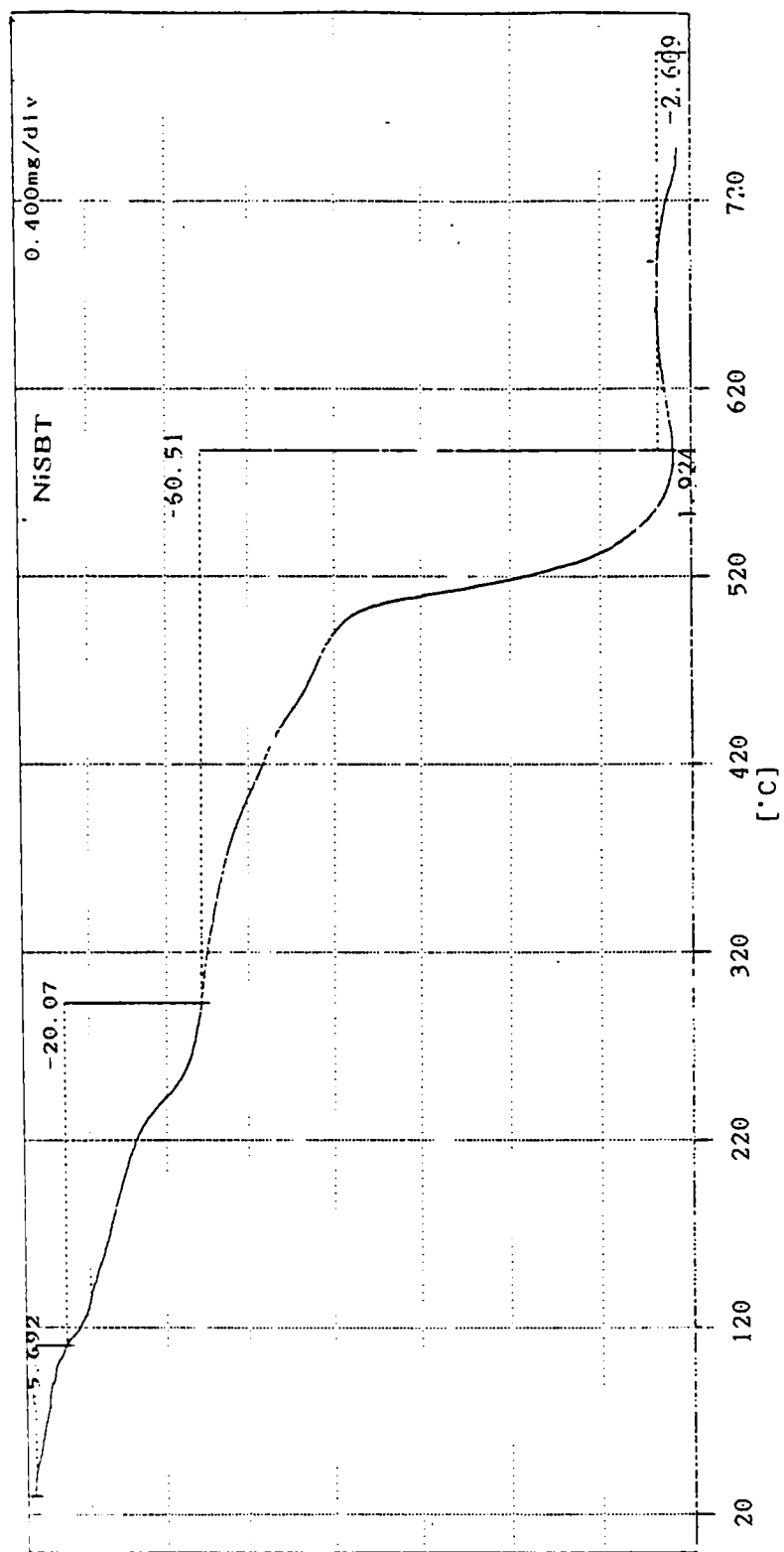
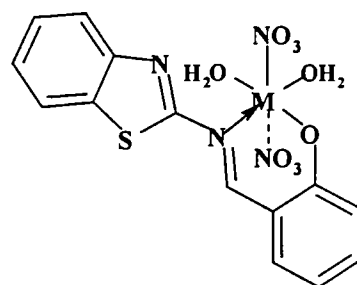
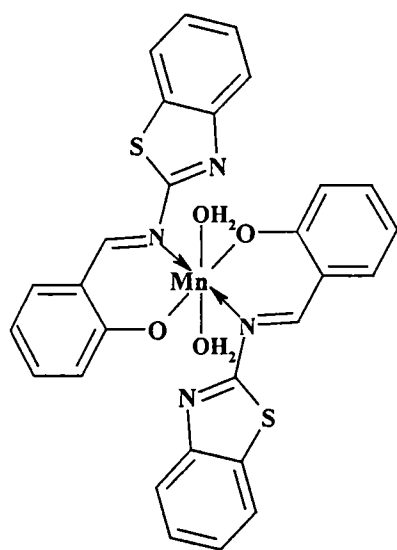


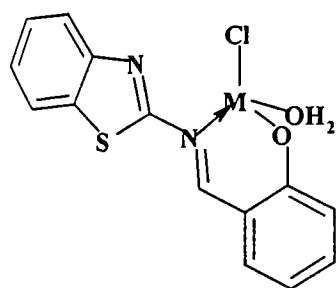
Figure.III.6. TG curve of NiSBT complex.

The decomposition pattern of the complex is given in Figure. III.6. Three main stages of decomposition of the complex were observed. The initial part of the curve shows mass loss due to the loss of the adsorbed moisture. The first stage of decomposition begins near 100 °C. A weight loss of 5.6% at this stage coincides with the expulsion of one molecule of coordinated water. The second stage begins at 120 °C and has a shoulder at 220 °C. The weight loss at this region corresponds to the removal of coordinated hydroxyl group and the -Cl atom. The very prominent effect is observed in the range 400 - 580 °C with a hump at 480 °C. The 60.5% mass loss data recommend the removal of Schiff base SBT from the complex. The product at the end of this stage is the metal oxide. TG analysis thus compromise with the proposed structure of the complex arrived at from the other characterization techniques.

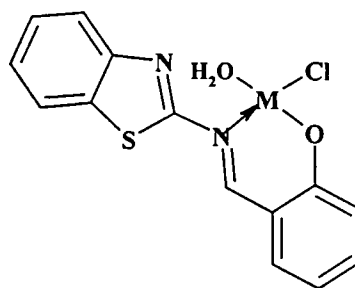
From the above studies, the following tentative structures are assigned for the complexes (Figure.III.7)



M = Fe



M = Co



M = Ni or Cu

Figure.III.7. Probable structures of the complexes.

## REFERENCES.

1. Dash . B. and Rout. M.K., *J.Indian Chem Society.* 32 (1955), 182.
2. Sharma. S.C., *Bull Chem Soc. (Japan)* , 40, (1967), 2422.
3. Farkas. L, Ger.Offen., *Chem Abstr* ; 84, (1976) 31047
4. Alaimo. R.J,US. Pat. 4, 012,409 ( Cl 260-305,CO7D 419/00) ; 15<sup>th</sup> Mar 1977.  
*Chem Abstr* 87, (1977) , 5952.
5. Patra M; Mahapatra S. K and Dash B., *J Ind. Chem Soc.* 51, (1974) 1031.
6. Dash.B,and Mahapatra.S.K., *J.Inorg.Nucl.Chem*, 37, (1975), 271.
7. Geran.R.J, Greenberg.N.H, Macdonald.M.M, Schumacher.A.M, Abbot.B.J.,  
*Cancer Chemother,Rep*,(1972),[DHEW PublicationNo.(NH)73-22],3.
8. Saegusa.Y,Harada.S and Nakamura.S., *J.Het.Chem*, 27, (1990), 739.
9. K.Hussain Reddy and Y.Lingappa., *Ind.J.Chem*, 33A, (1994), 919.
10. A.K.D.Mazumdar, N.K.Saha, K.D. Banerji., *J. Ind.Chem,Soc.*, LVI,  
(1979), 999.
11. W.J.Geary, *Coord.Chem.Rev.*, 7, (1971), 81.
12. A.B.P.Lever,*Inorganic Electronic Spectroscopy*”, Elsevier, New York (1968).
13. R.A. Mathes and James T. Gregory., *J.Amer.Chem.Soc*, 74, (1952), 3867.
14. R.S.Drago., *Physical Methods in Chemistry*, Saunders, Philadelphia.(1969).
15. D.M.L.Goodgame,M.GoodgameandF.A.Cotton.,*J.Am.Chem.Soc.*, 83,  
(1961), 4161.
16. F.A.Cotton and G.Wilkinson., “Advanced Inorganic Chemistry”, 2<sup>nd</sup> Edn, Wiley  
Eastern University Edition, New Delhi,(1972).

17. Rajendra.P.Misra,Bipin.B.MahapatraandS.Guru.,*J.Ind.Chem.Soc*, (1981),LVIII,p.808.
18. H.Singh, L.D.S.Yadav and J.P. Chaudhary.,*J.Ind.Chem.Soc*,(1983), LX, p.768-771.
19. Kazuo Nakamoto., *Infrared and Raman Spectra of inorganic coordination compounds*,Part-B,5<sup>th</sup> Edn, Wiley Interscience,NewYork.(1990).
20. Kovacie.J.E., *Spectrochim Acta*,. (1967) 23A, 183., Dey.K, Konar.D, Biswas .A.K and Ray.S.B., *J.Chem.Soc.Dalton Trans*, (1982),911.
21. K.K.M.Yusuff and R.Sreekala., *Synth. React. Inorg. Met-rg. Chem.* 21, (1991), 553.
22. Kamalendu Dey, Kartik Kumar Nandi.,*Ind.J.Chem*, 33A, (1994), 908.
23. Srivastava S.K,Pandya K.Pand Nigam .H.L., *Ind.J.Chem*, 12, (1974), 530.
24. B.M. Gatehouse, S.E.Livinstone and R.S.Nyholm., *J.Chem.Soc*,(1957),4222., *J.Inorg.Nucl.Chem.* 8, (1958), 75.
25. N.F.Curtis and Y.M. Curtis., *Inorg. Chem*, 4, (1958), 804.
26. E.J.Duff, M.N.Aughes and K.J.Rutt.,*J. Chem.Soc, A*, (1969), 2126.
27. R.J.H. Clark and C.S. Williams., *Inorg. Chem*, 4, (1965), 350.
28. F.K.Kneubuhl., *J. Chem. Phys.*, 33, (1960), 1074.
29. Kivelson.D and Nieman.R., 35, (1961), 149.
30. Bew M.J, Hathaway B.J, and Faraday R.J., *J. Chem. Soc. Dalton trans*, (1972), 1229.

\*

# CHAPTER IV



**Mn(II), Fe(III),Co(II),Ni(II)and Cu(II) Complexes  
of the Schiff base  
derived from vanillin and 2-aminobenzothiazole.**

**4.1. Introduction.**

Schiff bases are well known to have pronounced biological activities<sup>1,2</sup>. Their complexes have been suggested as models for enzymes such as galactose oxidase<sup>3</sup>. Schiff bases and their metal complexes derived from thiazole amines have been reported<sup>4,5</sup>. Schiff base derived from 4-substituted and 4,5-disubstituted-2-amino thiazoles and vanillin were synthesized and were screened for their fungicidal activity<sup>6</sup>. Fe(II), Mn(II), Fe(III), Co(II), Ni(II) and Cu(II) complexes of a Schiff base derived from vanillin and hydrazine have been prepared and characterized<sup>7</sup>. Complexes of Uranyl nitrate with ten Schiff bases obtained by the condensation of vanillin (4-hydroxy-3-methoxybenzaldehyde) and veratraldehyde (3,4-dimethoxybenzaldehyde) with benzhydrazide, salicyloylhydrazide, anthranilic acid, 2-aminophenol and 4-amonoantipyrine were reported<sup>8</sup>. A search through the literature has revealed that complexes of Schiff base derived from 2-aminobenzothiazole and vanillin(VBT) have not yet been studied.

Herein, we report the synthesis and characterization of a new series of Mn(II), Fe(III), Co(II), Ni(II) and Cu(II) complexes of the Schiff base derived from 2-aminobenzothiazole and vanillin (VBT).

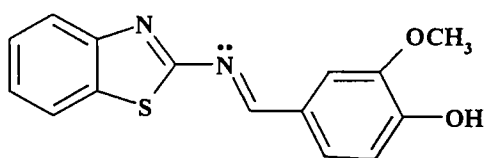


Figure. IV.1. Structure of the ligand-VBT

## 4.2 Experimental.

### 4.2.1 Materials.

The procedure for the preparation of Schiff base derived from 2-aminobenzothiazole and vanillin (4-hydroxy-3-methoxybenzaldehyde) (VBT) is given in Chapter-II.

### 4.2.2. Synthesis of the Complexes.

The complexes of Mn(II), Fe(III), Co(II), Ni(II) and Cu(II) were prepared by the following procedure. The viscous yellow jelly mass of the ligand-VBT was prepared afresh (see chapter II) using 2-aminobenzothiazole (1.5g, 0.01 mol) and vanillin (1.52g, 0.01 mol), dissolved in methanol and mixed with the corresponding metal salt solutions, {MnCl<sub>2</sub>.4H<sub>2</sub>O (1.98g, 0.01mol), Fe(NO<sub>3</sub>)<sub>3</sub>.9H<sub>2</sub>O (4.04g, 0.01mol), CoCl<sub>2</sub>. 6H<sub>2</sub>O (2.38g, 0.01mol), NiCl<sub>2</sub>.6H<sub>2</sub>O (2.36g, 0.01mol), or CuCl<sub>2</sub>.2H<sub>2</sub>O (1.7g, 0.01mol) in methanol (25mL)}. This solution was taken in a round-bottomed flask and refluxed for 2 hrs, concentrated by evaporation on water bath, was cooled in a refrigerator. The gel obtained was washed several times with small quantities of n-hexane and scratching the gel in the flask with a glass rod gave the solid complexes. CoVBT was finally extracted with dichloromethane to

get the solid complex. The prepared complexes were dried in vacuum over anhydrous calcium chloride. (Yield 60-70%).

### 4.2.3. Analytical methods.

The details of analytical methods and other characterization technique are given in Chapter II.

## 4.3 Results and Discussion.

All the complexes are coloured, crystalline and non-hygroscopic and are quite stable to atmospheric oxidation. The complexes are soluble in ethanol, methanol, benzene, acetone and moderately soluble in nitrobenzene. The complexes are found to be stable for a longer period without undergoing any decomposition.

### 4.3.1. Elemental Analysis.

Analytical data of the complexes are presented in Table IV.1. The results of elemental analysis reveal that 1:1 mole ratio exist between ligand and the metal ions in the complexes except in the case of Mn(II) complex. The complexes have the empirical formulae,  $[ML_2Cl_2]$  for the Mn(II) complex,  $[ML(H_2O)_2]Cl_2$  for the Co(II) complex,  $[MLCl_2].H_2O$  for the Cu(II) and Ni(II) complexes and  $[ML(NO_3)_2(OH)(H_2O)]$  for iron(III) complex (where L=VBT and M=the corresponding metal ion).

**Table. IV. 1**  
Analytical data of VBT complexes.

| Complex<br>(colour)  | C%               | H (%)           | N (%)            | S (%)           | Cl (%)           | M (%)            |
|--|------------------|-----------------|------------------|-----------------|------------------|------------------|
|  | Found<br>(Calc)  | found<br>(Calc) | found<br>(Calc)  | found<br>(Calc) | found<br>(Calc)  | found<br>(Calc)  |
| [Mn(VBT) <sub>2</sub> Cl <sub>2</sub> ]<br>(Brown)                                 | 51.68<br>(51.89) | 3.18<br>(3.46)  | 8.38<br>(8.07)   | 9.54<br>(9.22)  | 10.13<br>(10.22) | 7.75<br>(7.92)   |
| [Fe(VBT)(NO <sub>3</sub> ) <sub>2</sub> (OH)(H <sub>2</sub> O)]<br>(Reddish Brown) | 36.43<br>(36.08) | 3.24<br>(3.01)  | 11.09<br>(11.23) | 6.75<br>(6.41)  | -                | 11.58<br>(11.20) |
| [Co(VBT)(H <sub>2</sub> O) <sub>2</sub> ]Cl <sub>2</sub><br>(Greenish blue)        | 40.32<br>(40.02) | 3.37<br>(3.56)  | 6.28<br>(6.22)   | 6.92<br>(7.11)  | 15.48<br>(15.76) | 13.34<br>(13.10) |
| [Ni(VBT)Cl <sub>2</sub> ]. H <sub>2</sub> O<br>(Yellowish Brown)                   | 41.44<br>(41.70) | 3.32<br>(3.24)  | 6.39<br>(6.49)   | 7.15<br>(7.41)  | 16.18<br>(16.43) | 13.80<br>(13.60) |
| [Cu(VBT)Cl <sub>2</sub> ]. H <sub>2</sub> O<br>(Brown)                             | 41.35<br>(41.24) | 3.52<br>(3.21)  | 6.68<br>(6.42)   | 7.42<br>(7.33)  | 16.54<br>(16.24) | 14.51<br>(14.56) |

#### 4.3.2. Conductance measurements.

The molar conductances of the complexes were measured in 10<sup>-3</sup>M solutions in methanol at 28±2°C. The conductance values obtained are presented in Table.IV.2. The molar conductance values suggest that the VBT complexes of Mn(II), Fe(III), Ni(II) and Cu(II) complexes are non-electrolytes<sup>9</sup> and Co(II) is 1:2 electrolyte in methanol. The conductance values of 43.7 and 24.5 ohm<sup>-1</sup>cm<sup>2</sup>mol<sup>-1</sup>

for the Ni(II) and Cu(II) complexes might be due to the slight dissociation of the complex in methanol solution.

**Table. IV.2.**

Molar conductance and Magnetic moment data

| Complex   | Yield % | Magnetic moment (BM) | Molar Conductance ( $\text{Ohm}^{-1}\text{cm}^2\text{mol}^{-1}$ ) |
|---|---------|----------------------|---|
| $[\text{Mn}(\text{VBT})_2 \text{Cl}_2]$                                 | 70      | 5.8                  | 2.9   |
| $[\text{Fe}(\text{VBT})(\text{NO}_3)_2(\text{OH})(\text{H}_2\text{O})]$ | 75      | 5.8                  | 8.9   |
| $[\text{Co}(\text{VBT})(\text{H}_2\text{O})_2]\text{Cl}_2$              | 60      | 4.42                 | 142.4   |
| $[\text{Ni}(\text{VBT}) \text{Cl}_2] \cdot \text{H}_2\text{O}$          | 70      | Diamagnetic          | 43.7  |
| $[\text{Cu}(\text{VBT}) \text{Cl}_2] \cdot \text{H}_2\text{O}$          | 65      | 1.7                  | 24.5  |

#### 4.3.3. Magnetic susceptibility.

The magnetic moment values of the complexes are measured at room temperature,  $28 \pm 2^\circ\text{C}$ . The values are presented in Table.IV.2. MnVBT complex exhibits a magnetic moment of 5.8 BM, which is very near to the spin only value of 5.9BM for high spin octahedral complex<sup>10</sup>. FeVBT complex has a  $\mu_{\text{eff}}$  value of 5.8 BM which is expected for high spin octahedral complex<sup>11</sup>. Magnetic moment value around 4.42 BM indicates a tetrahedral structure<sup>12</sup> for Co(II) complex. VBT complex of Ni(II) was found to be diamagnetic. This recommends a square planar

structure to the complex. Cu(II)VBT complex shows a magnetic moment of 1.7 BM indicating a square planar structure to the complex.

#### 4.3.4. Electronic spectra.

The electronic spectra of the complexes are given in Figure.IV.2. The spectral data are presented in Table.IV.3. Electronic spectral bands are observed around  $40000\text{cm}^{-1}$ ,  $35000\text{cm}^{-1}$  and at  $32000\text{cm}^{-1}$  in all the complexes. These bands are not included in the figure or table and may be assigned to intra ligand transitions and charge transfer transitions respectively. However, low intensity bands characteristics of d-d transitions are also observed for these complexes.

Due to the spin forbidden transitions in Mn(II) complex; all the bands observed are extremely weak. Two weak bands at  $25000\text{cm}^{-1}$  and at  $17000\text{cm}^{-1}$  may be assigned to d-d transitions. As in the case of Mn(II) complex, all the bands of the iron(III) complex are very weak in intensity suggesting octahedral structure. A band observed at  $16500\text{cm}^{-1}$  of CoVBT complex can be assigned to the  ${}^4\text{A}_2 \rightarrow {}^4\text{T}_1(\text{P})$  transition due to the tetrahedral structure possessed by the complex. Two other transitions at the lower frequency regions,  $10500\text{cm}^{-1}$  and  $6800\text{cm}^{-1}$  also suggests the tetrahedral geometry. Only one transition is identified in the NiVBT complex due to d-d transition. This band is probably due to  ${}^1\text{B}_{1g} \leftarrow {}^1\text{A}_{1g}$  transition expected for a diamagnetic square planar complex. Other bands are obscured, that may be due to the tailing of CT transitions into the low energy region. It is difficult to distinguish between square planar and tetrahedral structure for Cu(II) complex. The band obtained at  $22000\text{cm}^{-1}$  in the electronic spectra of the CuVBT complex can be assigned to the d-d transition in square planar geometry.

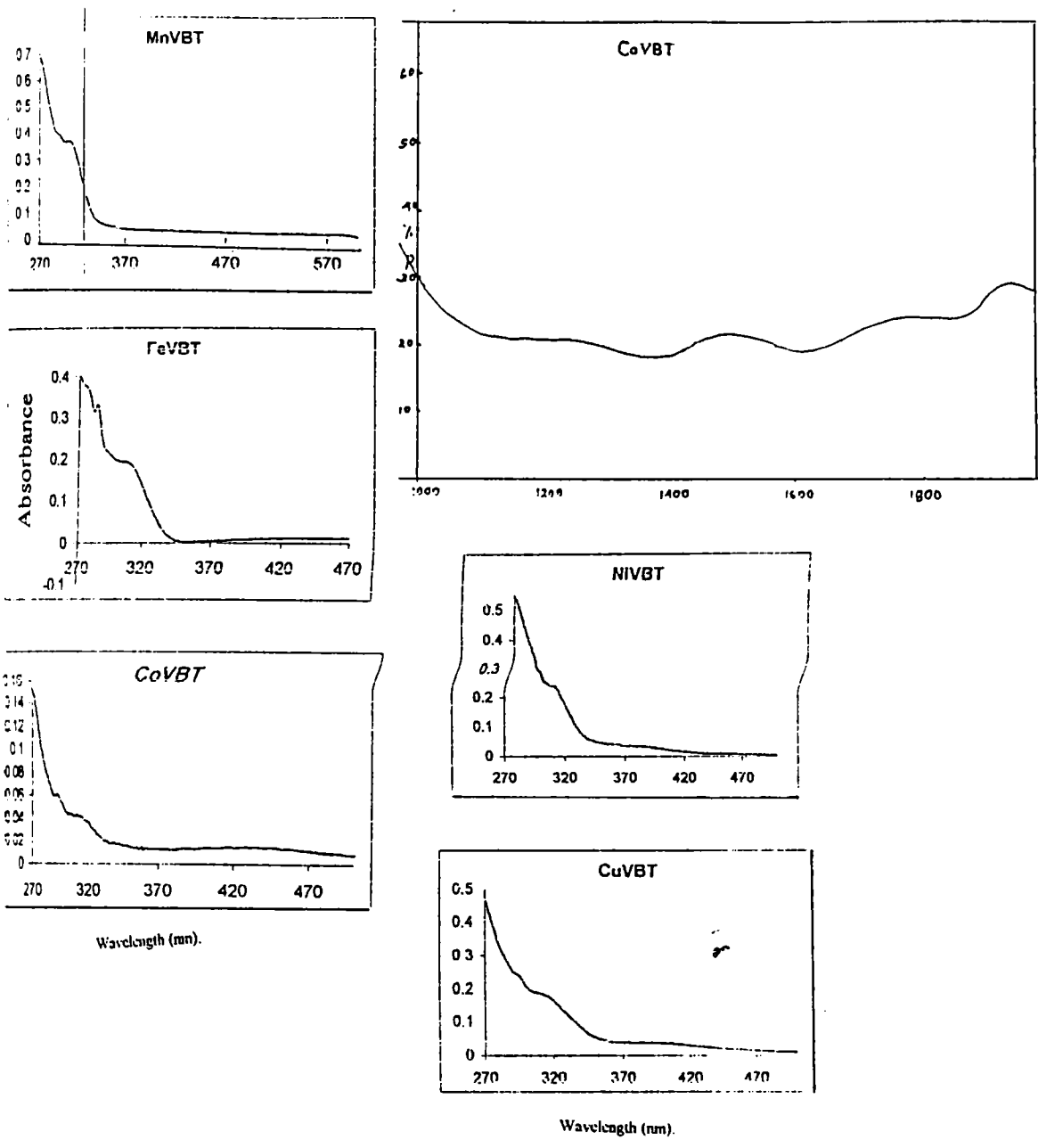


Figure.IV.2. Electronic Spectra of MVBT complexes.

**Table. IV.3**

Electronic spectral data of VBT complexes.

| Complex   | Abs. Max<br>( $\text{cm}^{-1}$ ) | Tentative<br>assignments                                      |
|---|----------------------------------|---|
| [Mn(VBT) <sub>2</sub> Cl <sub>2</sub> ]                         | 25000                            | d-d transition  |
|   | 17000                            | "   |
| [Fe(VBT)(NO <sub>3</sub> ) <sub>2</sub> (OH)(H <sub>2</sub> O)] | 24900                            | d-d transition  |
|   | 18500                            | d-d "   |
| [Co(VBT)(H <sub>2</sub> O) <sub>2</sub> ]Cl <sub>2</sub>        | 33200                            | C-T transition  |
|   | 29850                            | "   |
|   | 22900                            | "   |
|   | 16500                            | <sup>4</sup> T <sub>1</sub> (P) ← <sup>4</sup> A <sub>2</sub> |
|   | 8350                             | <sup>4</sup> T <sub>1</sub> (F) ← <sup>4</sup> A <sub>2</sub> |
|   | 6650                             | <sup>4</sup> T <sub>2</sub> (F) ← <sup>4</sup> A <sub>2</sub> |
| [Ni(VBT)Cl <sub>2</sub> ]. H <sub>2</sub> O                     | 31700                            | C-T transition  |
|   | 26300                            | "   |
|   | 21200                            | <sup>1</sup> B <sub>1g</sub> ← <sup>1</sup> A <sub>1g</sub>   |
| [Cu(VBT)Cl <sub>2</sub> ]. H <sub>2</sub> O                     | 33200                            | C-T transition  |
|   | 31700                            | "   |
|   | 22000                            | d-d transition  |

#### 4.3.5. FTIR spectra.

The Infrared spectra of the metal complexes were recorded and the important bands along with their tentative assignments are given in Table IV.4. and the spectra of complexes are shown in Figure.IV.3..

Getting the VBT ligand in solid form was difficult and hence an IR spectrum of ligand was not recorded. The group frequencies of the VBT complexes were arrived at by comparing the spectra with that of the ligand SBT and 2-aminobenzothiazole.

A band near  $3500\text{-}3300\text{cm}^{-1}$  in the spectra of all the complexes indicates the presence of water molecules. The IR spectrum of the ligand SBT exhibits a medium band at  $1667\text{cm}^{-1}$  assignable to azomethine stretching mode. This band was shifted  $\sim 15\text{-}30\text{ cm}^{-1}$  to the lower frequency side in the spectra of all the VBT complexes suggesting that the nitrogen atom of the azomethine group is coordinated to the metal ion.

The bands around  $1452\text{ cm}^{-1}$  and  $1182\text{ cm}^{-1}$  in spectrum of 2-aminobenzothiazole are due to the  $\nu_{\text{C-S}}$  of thiazole ring. These bands are red shifted to about  $20\text{-}40\text{cm}^{-1}$  in all the complexes, suggesting coordination of the sulfur atom of the thiazole ring. Gatehouse et al<sup>13</sup> noted that monodentate  $\text{NO}_3$  group exhibits three NO stretching bands near  $1434\text{cm}^{-1}$ ,  $1321\text{cm}^{-1}$  and  $1025\text{cm}^{-1}$ . Three bands at  $1460\text{cm}^{-1}$ ,  $1341\text{cm}^{-1}$  and  $1023\text{cm}^{-1}$  in the spectrum of iron(III) complex can be attributed to monodentate  $\text{NO}_3$  group on the complex. The separation between the two highest frequency bands is  $119\text{cm}^{-1}$  which again confirms the monodentate nature of  $\text{NO}_3$  group in the complex<sup>14</sup>.

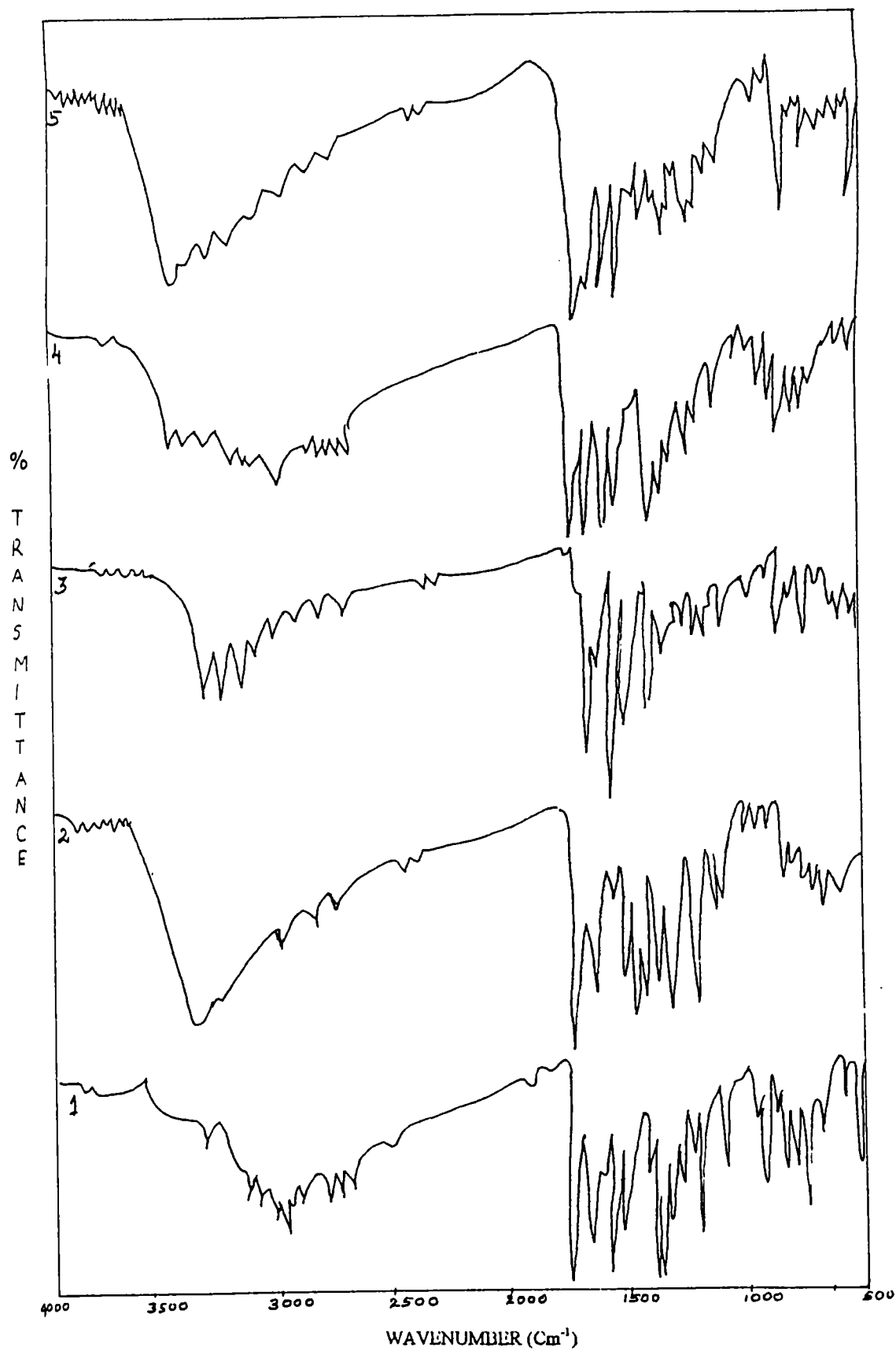


Figure.IV.3. FTIR Spectrum of (1) MnVBT (2) FeVBT (3) CoVBT (4) NiVBT (5) CuVBT.

**Table. IV. 4**  
 Infra-red absorption frequencies (cm<sup>-1</sup>)

| MnVBT | FeVBT | CoVBT | NiVBT | CuVBT | Tentative assignments of the more relevant bands |
|-------|-------|-------|-------|-------|--|
| (1)   | (2)   | (3)   | (4)   | (5)   | (6)  |
| -     | 3700b | 3350s | 3423w | 3376s | VOantisymstrH <sub>2</sub> O                     |
| -     | 3100b |       | 3363w | -     |  |
| 3297w | -     | 3277s | 3283w | 3277w | VOH (hydroxyl).                                  |
| 3058m |       | 3177s | 3104w | 3177w | VCH <sub>3</sub> (methylether)                   |
| 2945m | 2965w | 2959w | 2939m | 2925w |  |
| 2746m | 2932w | 2853w | 2740w | 2853w |  |
| 2707m | 2813w | 2727w | 2707w | 2720w |  |
| 2647m | -     | -     | 2647w | -     |  |
| 1653s | 1656s | 1636s | 1646s | 1639s | VC=N   |
| 1586s | 1586s | 1593m | 1580s | 1586w | VC=N(ring)                                       |
|       | 1460s |       |       |       | VNO <sub>3</sub> monodentate                     |
| 1427w | 1420s | 1434s | 1424s | 1444s | VC-S   |
| 1375m | 1381s | 1378s | 1368s | 1377m |  |
| -     | 1341m | -     | -     | -     | NO <sub>3</sub> monodentate                      |
| 1155s | 1149s | 1155m | 1155m | 1142s | VC-S   |
| 1069s | 1062m | 1069m | 1069m | 1066w | VC-O (Phenolic)                                  |
| 1029s | 1030s | 1029m | 1025m | 1026m | VC-O (Methoxl)                                   |
| -     | 1023  | -     | -     | -     | VNO <sub>3</sub> monodentate                     |
| 870m  | 877m  | 817w  | 890w  | 864w  |  |
| -     | 718w  | 718m  | 744s  | 718w  | ρ <sub>r</sub> (H <sub>2</sub> O)                |
| 492m  | -     | 486m  | 492m  | 486w  | VM-Cl  |
| 426m  | -     | 419m  | 433m  | 419m  |  |

The phenolic oxygen of the SBT ligand absorbs at  $1069\text{cm}^{-1}$ . This band is seen at the same position in the spectra of all the VBT complexes. Similarly the peak due to oxygen atom of the methylether at  $1030\text{cm}^{-1}$  does not undergo any shift by complex formation. Thus both these groups are not involved in coordination with the metal ions in complexes. Presence of medium bands at  $\sim 490\text{ cm}^{-1}$  in complexes except in Fe(III) complex are identified as  $\nu_{\text{M-Cl}}$  in these complexes.

Therefore it can be concluded that ligand VBT coordinates to the metal through the nitrogen atom of the azomethine linkage and also through sulphur atom of thiazole ring.

#### 4.3.6. EPR spectra.

The EPR spectrum of Cu(II)VBT complex in methanol at liquid nitrogen temperature was recorded and presented in Figure.IV.4. The EPR parameters calculated from the spectrum are given in Table.IV.5. The  $g$  values are calculated relative to tetracyanoethylene (TCNE,  $g = 2.0023$ .)

Nitrogen hyperfine splitting can be clearly seen in the spectrum taken at LNT, which indicate that the nitrogen atom of the azomethine group was involved in the bonding between the metal atom and the Schiff base. The  $\mu_{\text{eff}}$  value calculated for the complex from the spectrum was in close agreement with that measured experimentally by Gouy method. The magnetic susceptibility of 1.72 BM once again points towards the possibility of a square planar structure to the CuVBT complex. The  $g_{\parallel}$  value is a measure of covalent character<sup>15</sup> of the complex. If  $g_{\parallel} > 2.3$ , the bond will be ionic. For CuVBT,  $g_{\parallel} = 2.31$ , indicate significant ionic character.

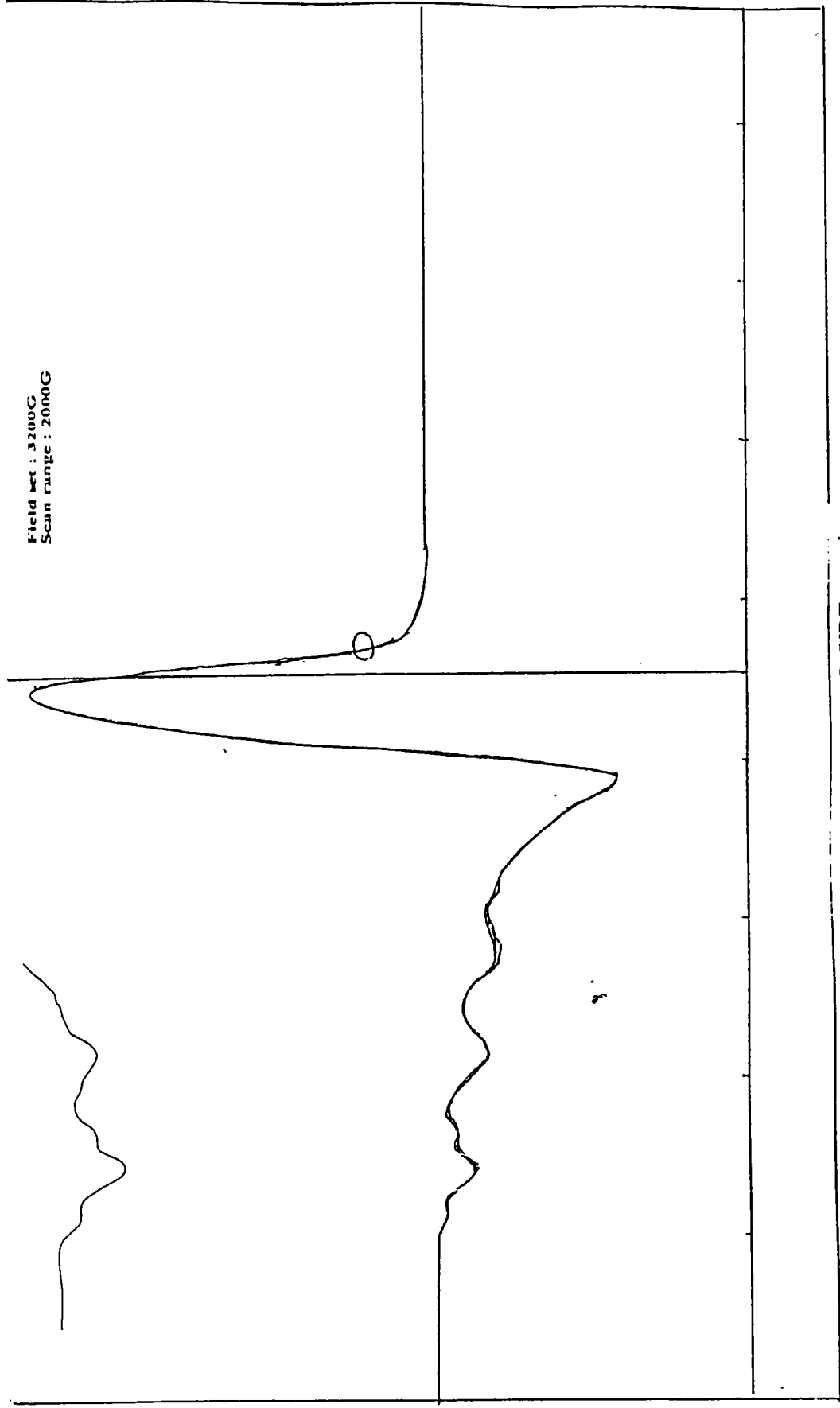


Figure. IV. 4 – EPR Spectra of CuVBT complex.

The extent of tetragonal distortion  $f = g_{\parallel} / A_{\parallel} = 164.93 \text{ cm}$  was in agreement with a square planar structure to the complex. In plane  $\sigma$  bonding parameter  $\alpha^2$  was usually in the range 0.75 – 0.9. If  $\alpha^2 = 1$  the bond will be purely ionic, and bonding will be covalent if the value is 0.5. CuVBT complex has the inplane parameter  $\alpha^2 = 0.75$ , which shows that the bond between the metal ion and the Schiff base VBT is not purely covalent.

**Table. IV. 5**

EPR spectral data of the CuVBT complex.

| EPR parameter                   | CuVBT                                   |
|---------------------------------|---|
| $g_{\parallel}$                 | 2.31                                    |
| $g_{\perp}$                     | 2.03                                    |
| $A_{\parallel}$                 | $140.06 \times 10^{-4} \text{ cm}^{-1}$ |
| $g_{\parallel} / A_{\parallel}$ | 164.93 cm                               |
| $g_{\text{av}}$                 | 2.12                                    |
| $\alpha^2$                      | 0.75                                    |
| $\mu_{\text{eff}}$              | 1.72 BM                                 |

#### 4.3.7. Thermogravimetric analysis.

The thermal analysis of NiVBT complex was carried out and the data so obtained is given in Table IV.6. The TG curve is shown in Figure.IV.5.

**Table. IV.6.**  
Thermal analysis data of NiVBT complex.

| Complex | Temperature range °C | % weight loss |
|---------|----------------------|---------------|
| NiVBT   | 27-110               | 4.20          |
|         | 110-472              | 28.20         |
|         | 472-800              | 56.70         |

Stage-I decomposition of the complex shows a weight loss corresponding to one molecule of water in the temperature range 27-110 °C, which might be due to the removal of adsorbed moisture. The second stage of decomposition starts at 110 °C and extends to 472 °C and might be due to the removal of the part of the ligand. The rest of ligand is removed at the last stage of decomposition in the range 472-800 °C with peak position at 480 °C. The final product may be the metal oxide. Based on the above studies, the following tentative structures are assigned for the VBT complexes.

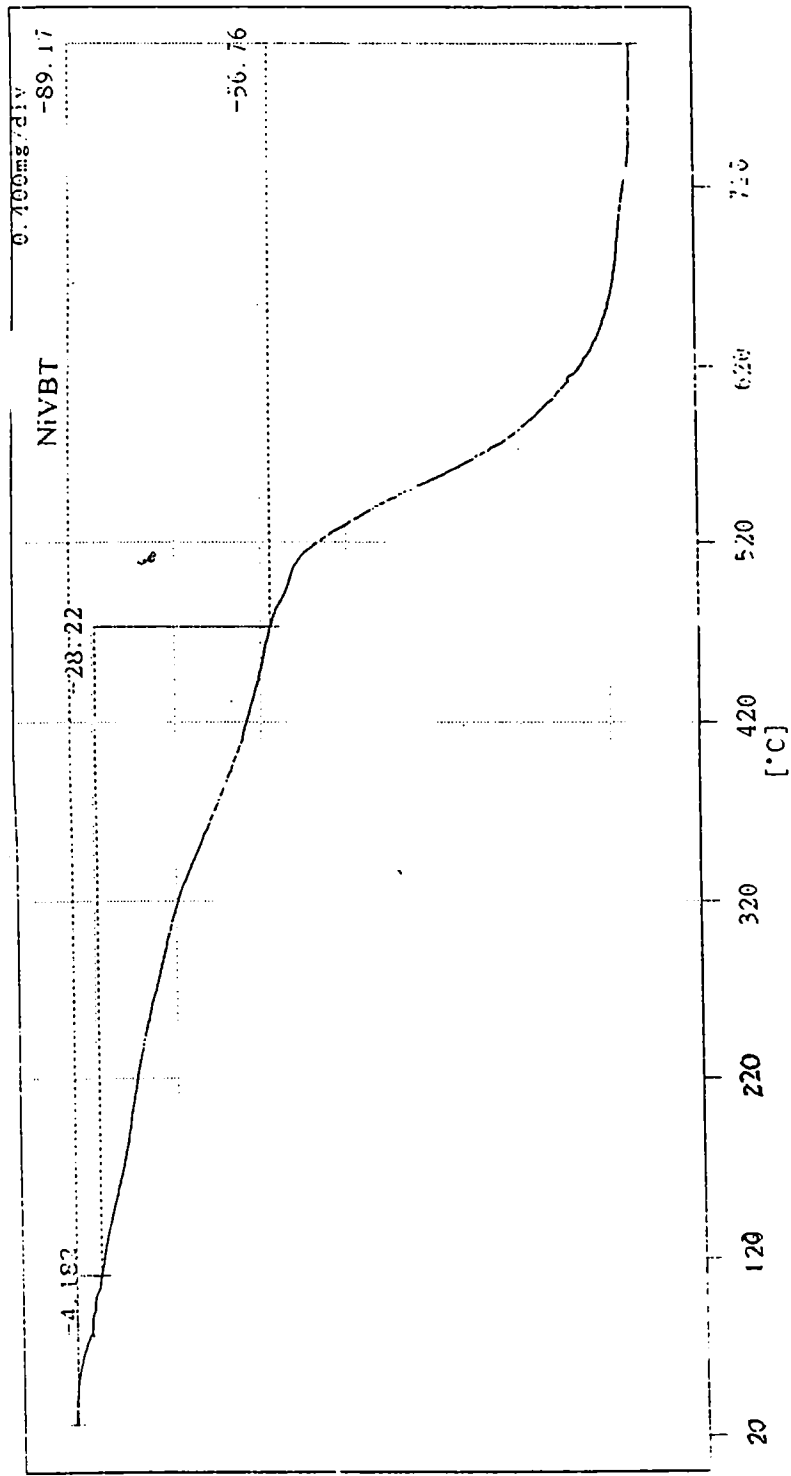


Figure.IV.5. TG curve of NiVBT complex.

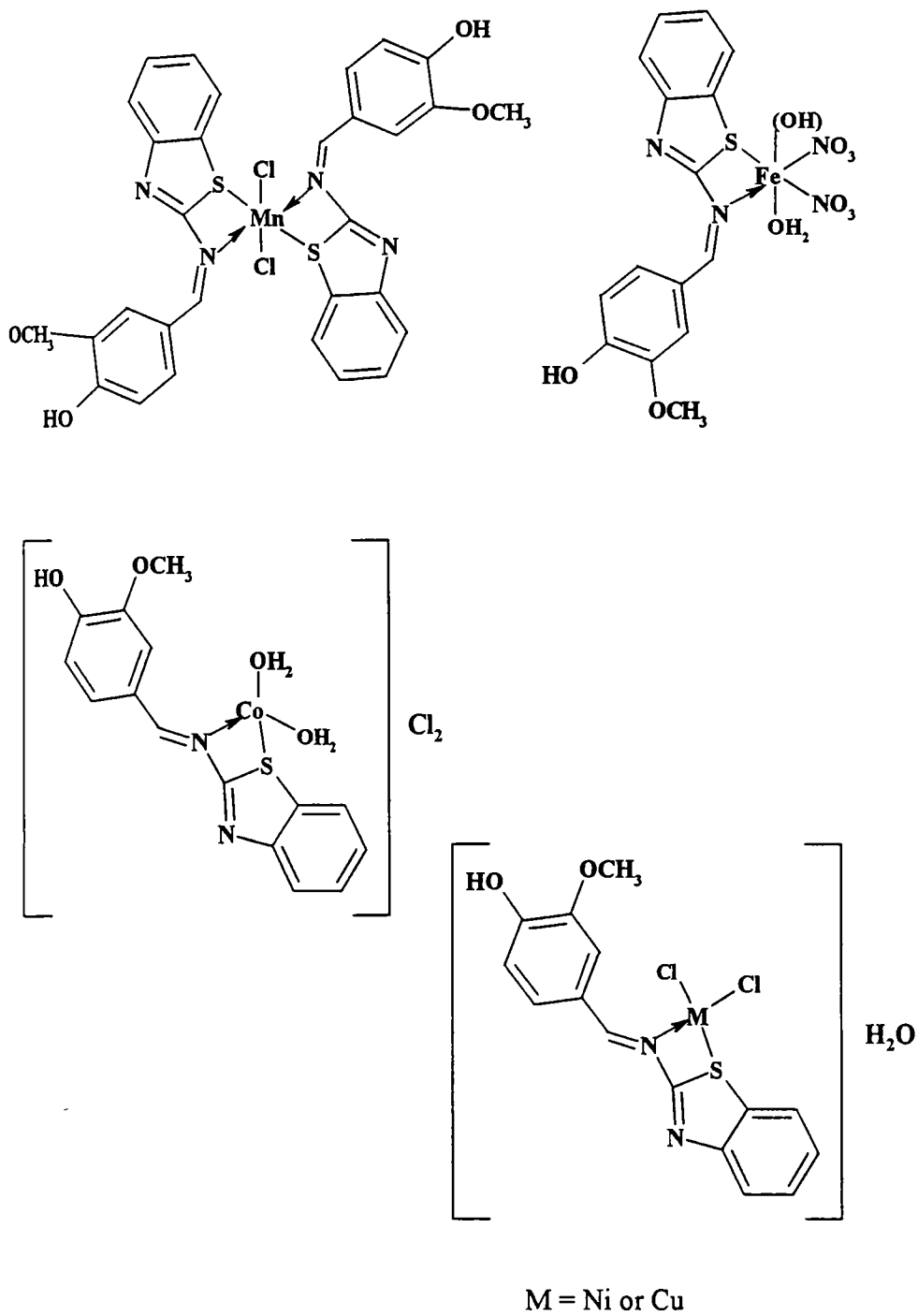


Figure. IV.6. Probable structures of VBT complexes.

## REFERENCES.

1. E.M.Hodnett and P.D.Mooney., *J.Med.Chem*, 13, (1970), 780.
2. H.J.Billmann and R.L.Schmidgall., *J.Pharm.Sci*, 59, (1970), 1191.
3. R.S.Giordano and R.D.Beneman., *J.Amer.Chem.Soc*, 96, (1974), 1017,1098.
4. B.Dash, M.Patra and S.Praharaj., *Ind.J.Chem.*,19B,(1980), 894.
5. B.Dash and S.K. Mahapatra., *J.Inorg.Nuclear.Chem*, 37, (1975), 271.
6. B.Dash, M.Patra and P.K. Mahapatra., *J.Ind.Chem.Soc*, LX, (1983), 772.
7. Purushotham B. Chakrawarti and Pramila Khanna., *J.Ind.Chem.Soc*, LXI, (1984), 112.
8. G.Sobhana Devi and P.Indrasenan., *Ind.J.Chem*, 27A, (1988), 809-811.
9. Geary W. J., *Coord Chem Rev.*,7, (1971), 81.
10. R.L.Dutta, A.Syamal, '*Elements of Magnetochemistry*' (2<sup>nd</sup> Edn), East West press, New Delhi.
11. R.L. Martin and A.H.White, *Inorg.Chem.*, 6, (1967), 712.
12. M.Goodgame and F.A. Cotton , *J.Am.Chem. Soc*, 84, (1962), 1543.
13. B.M. Gatehouse, S.E. Livinstone and R.S. Nyholm ., *J.Chem.Soc*, (1957), 4222; *J. Inorg. Nucl. Chem*, 8 , (1958), 75.
14. N.F. Curtis and Y.M. Curtis., *Iorg. Chem*, 4, (1965), 804.
15. U.Sakaguchi and A.W.Addison., *J.Chem. Soc, Dalton Trans*, (1979), 600.

•

# CHAPTER V



**ZeoliteY encapsulated Mn(II), Fe(III), Co(II), Ni(II) and Cu(II)  
complexes of the Schiff base derived  
from salicylaldehyde and 2-aminobenzothiazole (SBT).**

**5.1. Introduction.**

More recently there has been a significant incentive to develop new catalytic systems. There was some success in the design and synthesis of catalysts, which are active for organic substrate conversions. Furthermore, improving the design is aimed at catalyst recovery and product selectivity. Transition metal complexes are reported to be very effective homogeneous catalysts for many reactions. ZeoliteY encapsulation of these complexes almost fulfills the above said characters of a catalyst. ZeoliteY encapsulated Schiff base complexes derived from salicylaldehyde are reported as viable catalysts for a number of organic reactions<sup>1-7</sup>.

In this chapter studies on synthesis and characterization of zeoliteY encapsulated complexes of Mn(II), Fe(III), Co(II), Ni(II) and Cu(II) ions with the Schiff base derived from salicylaldehyde and 2-aminobenzothiazole (SBT) are presented. Applications of these complexes as catalysts were studied and the results of these studies are discussed in chapter VIII.

**5.2 . EXPERIMENTAL.**

**5.2.1 Materials.**

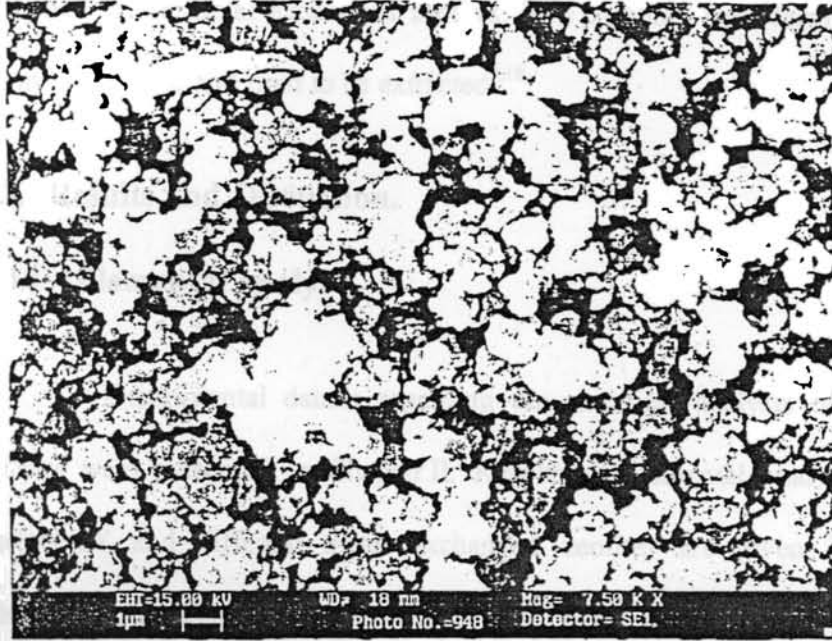
The procedure for the preparation of metal exchanged zeolite Y is

described in chapter II. Flexible ligand method was used for synthesis of the complex within the super cages of metal exchanged zeolite Y matrix.

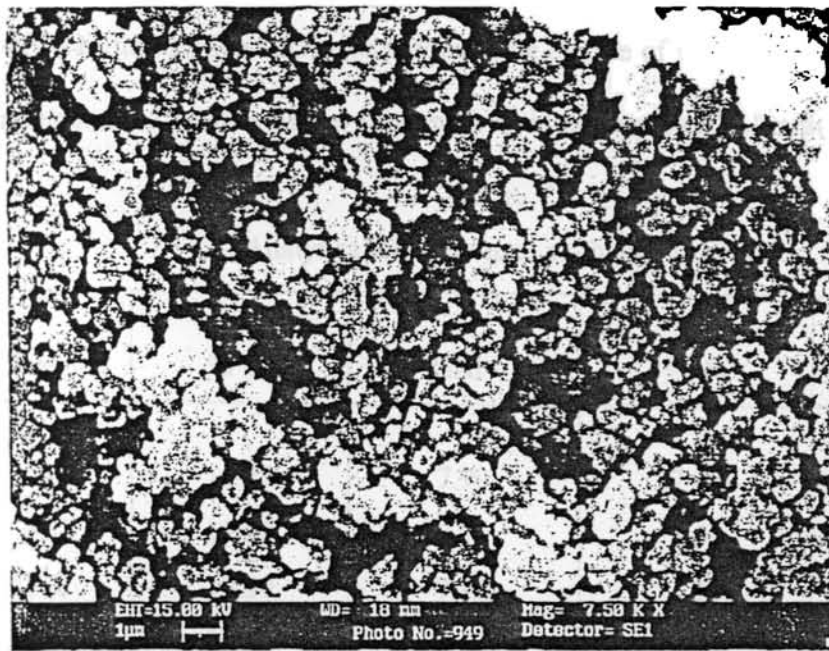
### **5.2.2. Synthesis of zeolite Y encapsulated SBT complexes.**

Flexible ligand method<sup>8</sup> was used to entrap the complex in the super cages of metal exchanged zeolite Y matrix. In this method, encapsulation can be carried out either by sealed heating of the mixture of solid ligand and the metal exchanged zeolite Y or by refluxing the mixture in suitable solvent of the ligand for several hours.

Recrystallised ligand, SBT (1.2 g) and 2g of the metal exchanged zeolite Y are mixed thoroughly in a mortar. This was then ampouled in a test tube and heated for two hours at 115°C in a muffle furnace. The purification procedure involves the removal of surface adhering uncomplexed ligands by soxhlet extraction of the above sample with methanol and then with dichloromethane for 4-5 days till the colour of the solvent becomes clear. Uncomplexed metal ions remaining in the zeolite cavities were removed by stirring with NaCl solution (0.01M) for 24 hrs. The complex was filtered and the chloride ions were removed by washing with hot distilled water till no precipitate was obtained with AgNO<sub>3</sub>. This sample was then dehydrated at 120°C for 2hrs and stored in vacuum over anhydrous calcium chloride. These complexes herein onwards are designated as YMSBT, where M represents the corresponding metal atom. Scanning electron microscopy (SEM) of the sample, YCoSBT before and after soxhlet extraction was taken (Figure.V.1) to know whether any surface species are present. The SEM reveals that the impurities formed on the surface were removed by soxhlet



Before Soxhlet extraction



After Soxhlet extraction

Figure.V.1. SEM of YCoSBT

extraction. These purified encapsulated complexes have different colours, when compared to the metal exchanged zeolites. The complex once formed within the cavity is too large and rigid to be extracted<sup>9,10</sup>.

### 5.3. Results and Discussion.

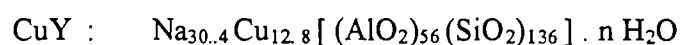
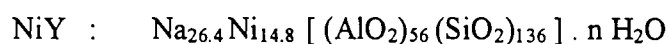
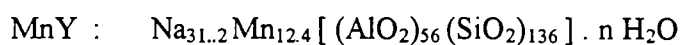
#### 5.3.1. Elemental analysis.

Experimental details regarding the chemical analysis of the various samples were presented in Chapter.II. Results of elemental analysis of parent zeolite-NaY and different metal exchanged zeolites are given in Table.V.I. The analytical data shows that the Si /Al ratio was 2.43 for NaY, which corresponds to the idealized unit cell formula<sup>11</sup>  $\text{Na}_{56}[\text{AlO}_2]_{56}(\text{SiO}_2)_{136} \cdot n\text{H}_2\text{O}$  for the parent zeolite-NaY. The Si /Al ratio remains the same in all the metal exchanged zeolites indicating that no damage has taken place to the zeolite framework after the ion exchange process. The degree of ion exchange in various metal exchanged zeolites was in agreement with that reported in literature<sup>(12,13)</sup>.

**Table. V.1.**  
Analytical data of metal exchanged zeolites.

| Sample | % Si  | %Al  | %Na  | % Metal |
|--------|-------|------|------|---------|
| NaY    | 19.42 | 7.99 | 7.48 |         |
| MnY    | 19.38 | 7.95 | 3.50 | 3.23    |
| FeY    | 19.20 | 7.89 | 4.73 | 2.56    |
| CoY    | 19.29 | 7.94 | 3.34 | 3.58    |
| NiY    | 19.24 | 7.87 | 3.42 | 3.86    |
| CuY    | 19.21 | 7.90 | 3.70 | 3.15    |

From the above data following unit cell formulae have been calculated for the metal exchanged zeolites.



Results of elemental analysis of zeoliteY encapsulated complexes are presented in Table.V.2. The microanalyses of C, H, N and S indicate that the metal ligand mole ratio was found to be 2:1 in the case of Mn(II) and Fe(III) complexes, while it is 1:1 around Co(II), Ni(II) and Cu(II) ions.

**Table.V.2.**

Analytical data of zeoliteY encapsulated SBT complexes.

| Sample | Elemental Analysis. |      |      |         |      |      |      |      |
|--------|---------------------|------|------|---------|------|------|------|------|
|        | % Si                | % Al | % Na | % Metal | % C  | % H  | % N  | % S  |
| YMnSBT | 19.38               | 7.76 | 6.25 | 1.64    | 5.65 | 2.43 | 0.60 | 0.82 |
| YFeSBT | 19.65               | 7.87 | 6.94 | 1.09    | 5.23 | 2.50 | 0.65 | 0.87 |
| YCoSBT | 19.37               | 7.83 | 6.39 | 1.48    | 2.17 | 2.26 | 0.22 | 0.43 |
| YNiSBT | 19.41               | 7.76 | 6.07 | 1.39    | 2.34 | 2.31 | 0.29 | 0.47 |
| YCuSBT | 19.23               | 7.69 | 6.20 | 1.64    | 2.14 | 2.2  | 0.38 | 0.57 |

The metal content of the encapsulated complexes were less compared to the corresponding metal exchanged zeolites, which suggests that uncomplexed metal ions were re-exchanged with Na<sup>+</sup> ions.

### 5.3.2. Surface area and pore volume analysis.

Surface area and pore volume analyses of the samples using BET multiple point measurement in a Micromeritics Gemini 2360 Surface area analyzer, are presented in Table.V.3. The loss in surface area and pore volume of metal exchanged zeolites on encapsulating the complexes is shown diagrammatically in Figure.V.2 and V.3 respectively.

**Table. V.3**  
Surface Area and Pore volume of  
zeoliteY encapsulated SBT complexes

| Sample | MY                                   |                    | YMSBT                                |                    |
|--------|--------------------------------------|--------------------|--------------------------------------|--------------------|
|        | BET surface area (m <sup>2</sup> /g) | Pore volume (cc/g) | BET surface area (m <sup>2</sup> /g) | Pore volume (cc/g) |
| NaY    | 523                                  | 0.3045             | -                                    | -                  |
| YMnSBT | 496                                  | 0.2964             | 367                                  | 0.2568             |
| YFeSBT | 510                                  | 0.3013             | 386                                  | 0.2632             |
| YCoSBT | 490                                  | 0.2986             | 373                                  | 0.2502             |
| YNiSBT | 489                                  | 0.2934             | 365                                  | 0.2468             |
| YCuSBT | 497                                  | 0.2959             | 378                                  | 0.2541             |

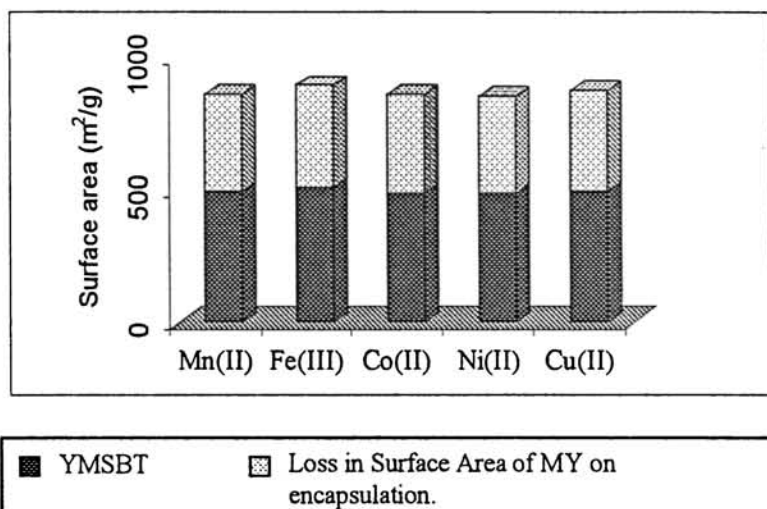


Figure. V.2. Decrease in surface area of the metal exchanged zeolites on encapsulation of SBT complexes

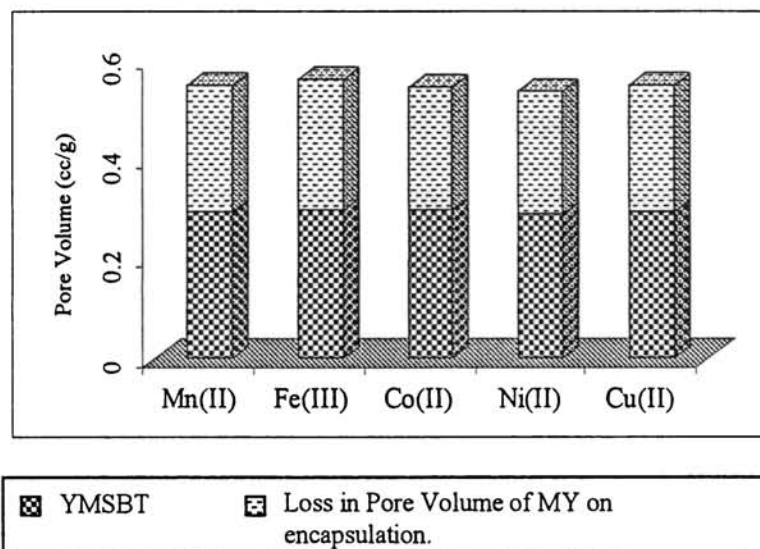


Figure. V.3. Decrease in pore volume of the metal exchanged zeolites on encapsulation of SBT complexes

A decrease in surface area and pore volume of the encapsulated complexes was reported<sup>8,14,15</sup> as the manifestation of encapsulation of the complexes. The surface area of the zeoliteY encapsulated complexes (YMSBT) was compared with that of the sodium exchanged zeoliteY (NaY) and the corresponding metal exchanged zeoliteY (MY) to ensure the encapsulation of the complexes. On the basis of nitrogen adsorption, the surface area and pore volume of NaY are 523m<sup>2</sup>/g-zeolite and 0.3045cm<sup>3</sup>/g-zeolite respectively. For YMnSBT the corresponding values were 367m<sup>2</sup>/g and 0.2568cm<sup>3</sup>/g. The observed decrease of 156 m<sup>2</sup>/g and 0.047cm<sup>3</sup>/g indicate that the metal complex was accommodated in the host cage. The data for the other complexes also indicate their encapsulation inside the super cages of the zeolite framework.

A more stonger evidence regarding encapsulation would have been obtained, if the volume occupied by the metal complex were estimated. Such a study was carried out by Yasuaki Okamoto<sup>16</sup> to compare the volume occupied by the metal complex species and the metal complex in NaY and get the evidence for encapsulation. For lack of facility the volume analysis was not carried out.

### **5.3.3. X-ray diffraction studies.**

The XRD patterns for the zeoliteNaY is presented in Figure.V.4 and that of zeoliteY encapsulated (YMSBT) complexes are given in Figure.V.5. A comparison of the patterns indicates no destruction of the structure of the host zeolite upon the introduction of the complexes. No changes in the diffraction pattern suggest that the crystallinity of the zeolite host has been retained even after encapsulation. However, the intensities of few diffraction peaks decreased while

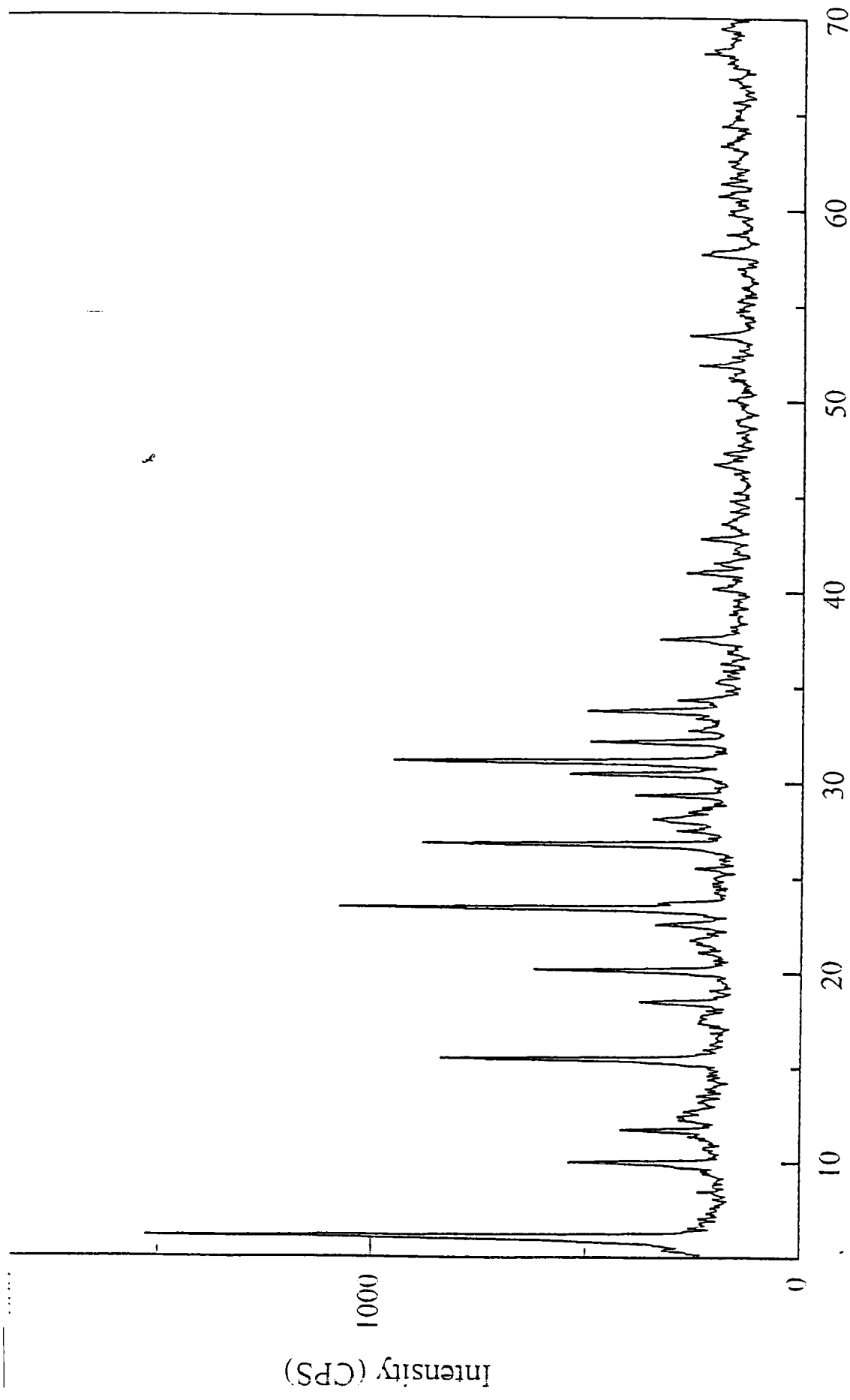


Figure V.4. XRD pattern of parent NaY

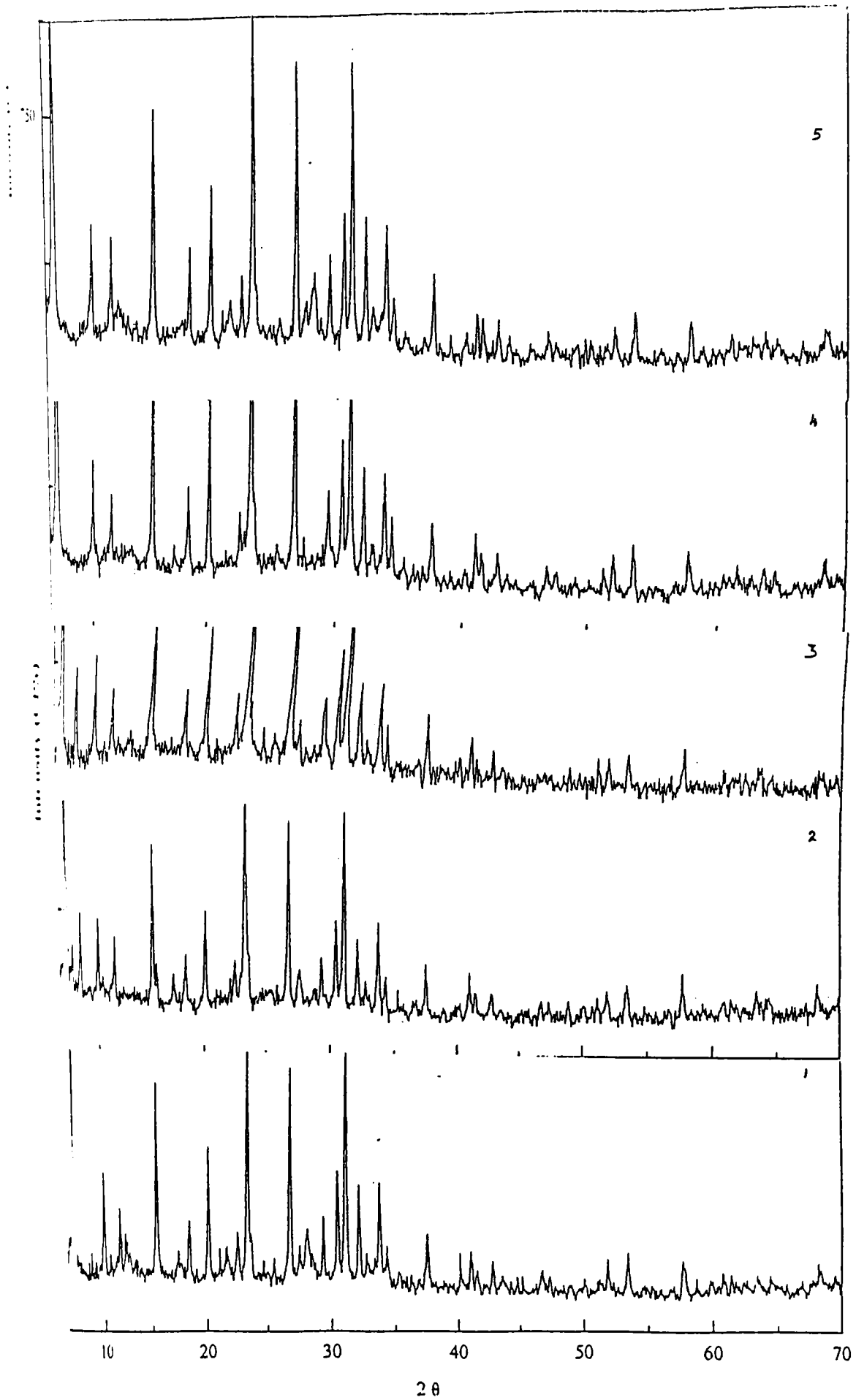


Figure.V.5. XRD patterns of 1).YMnSBT 2). YFeSBT  
3).YCoSBT 4).YNiSBT 5). YCuSBT.

the intensities of certain others increased on accommodation of the complexes, which might be due to the presence of exchanged metal ions on the framework. This variation in intensities shows that the metal complexes were entrapped inside the zeolite pores itself<sup>16</sup>. Decrease in intensity of the XRD pattern on encapsulation was reported by other workers<sup>16,17</sup> also.

#### 5.3.4. Magnetic susceptibility.

Gouy method, Faraday method and NMR methods are widely used for determining magnetic susceptibilities of coordination compounds. Faraday magnetic balance is generally applied for the magnetic measurements of zeolite encapsulated samples since the samples are highly sensitive to moisture<sup>18</sup>. But for the present investigation, due to the lack of such a facility, magnetic susceptibility measurements were carried out on a Guoy balance.

Magnetic measurements at the room temperature,  $29 \pm 2^\circ\text{C}$  of the metal exchanged zeolites and zeoliteY encapsulated complexes were carried out on a Gouy balance. The diamagnetic contribution of the parent zeolite NaY at room temperature was measured and calculated using the unit cell formula determined from analytical data. The paramagnetic contribution of the encapsulated complex, being in a low loading level, is extremely small, and hence determination of the diamagnetic contribution is vital for obtaining accurate values of the paramagnetic susceptibility. The diamagnetic correction due to the ligand part was also being taken into account. Thus only a qualitative measurement of the magnetic behavior was possible in the case of zeoliteY encapsulated complexes. The magnetic moment  $\mu_{\text{eff}}$  of the encapsulated complexes so obtained are presented in Table V.4.

YMnSBT complex exhibits a magnetic moment of 5.8 BM that is close to the spin only value for a  $d^5$  ion irrespective of the geometry being octahedral, tetrahedral or lower symmetry. Similar is the case with Fe(III) complex for which the  $\mu_{\text{eff}}$  value is 5.6 BM. For the simple complexes the structure of these complexes are assigned as octahedral.

Co(II) complex in zeoliteY super cages has a magnetic moment of about 4.9 BM which is in agreement with that reported for the simple complex having a tetrahedral geometry. The value of the moment was larger than the spin only value for a high spin  $d^7$  ion, which may be due to large orbital contribution expected for this electronic arrangement.

**Table.V. 4**  
Magnetic moment data of the  
zeoliteY encapsulated SBT complexes.

| Complex | Magnetic moment<br>$\mu_{\text{eff}}$ (BM) |
|---------|--|
| YMnSBT  | 5.8  |
| YFeSBT  | 5.6  |
| YCoSBT  | 4.9  |
| YNiSBT  | diamagnetic                                |
| YCuSBT  | 1.9  |

Dehydrated metal exchanged CoY exhibits  $\mu_{\text{eff}}$  values in the range 4- 4.6 BM which has been attributed to tetrahedral Co(II) species.  $\text{Co}^{2+}$  species exist as octahedral

aquo complexes in the large cavities, however on dehydration migrates to the sodalite units and attains a tetrahedral geometry<sup>18,19</sup>. The complex, YNiSBT was found to be diamagnetic within the supercages indicates that this complex acquired square planar geometry. Simple Cu(II) complexes generally have magnetic moments in the range 1.73 to 2.3BM irrespective of whether the structure is octahedral or tetrahedral<sup>20</sup>. The low magnetic moment value for CuSBT complex around 1.9BM. suggests a square planar geometry to this complex.

### 5.3.5. Diffuse Reflectance Spectra.

The zeoliteY encapsulated complexes were characterized by comparing the diffuse reflectance spectra of the ligand and that of the simple complexes. Diffuse reflectance spectra of the zeoliteY encapsulated SBT complexes are shown in Figure.V.6. The spectral data and their tentative assignments are given in Table.V.5. For all the samples, considerable weakening of the bands below 15000  $\text{cm}^{-1}$  and intense ligand transitions beyond 25000  $\text{cm}^{-1}$  and the stronger bands near 35000  $\text{cm}^{-1}$  may very well be observed. Absorption band above 33200 $\text{cm}^{-1}$  for YMnSBT and YFeSBT are due to LMCT transitions. Additional weak band with a maximum at 14250  $\text{cm}^{-1}$  is due to the d-d transition. Octahedral geometry can be assigned to YMnSBT and YFeSBT complexes. The band maxima in these cases were not significantly altered from that of the respective simple complexes.

The diffuse reflectance spectra of YCo(II)SBT complex comprise of ligand to metal charge transfer transitions, in which an electron is excited from ligand to metal orbital. This band can be seen near 22000  $\text{cm}^{-1}$ .

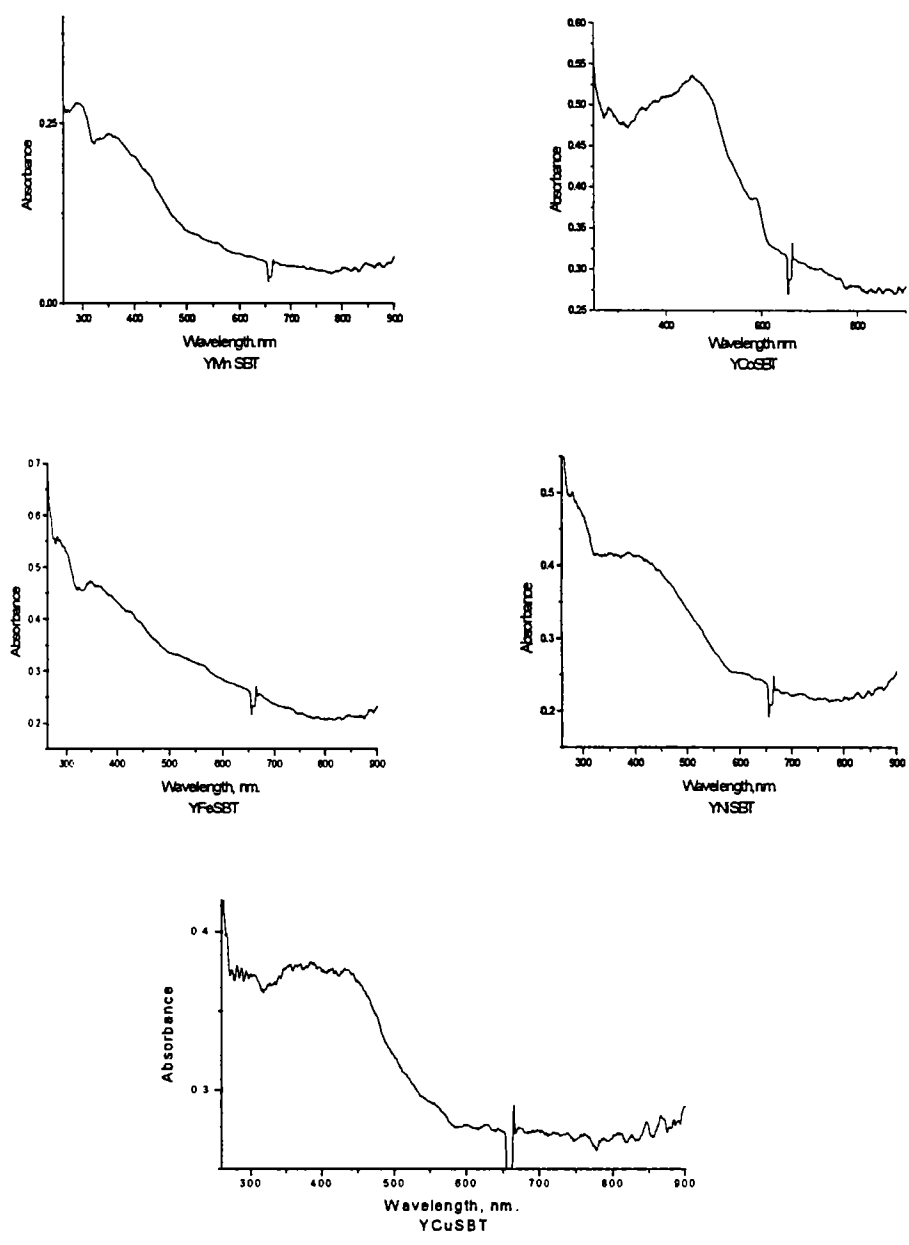


Figure. V.6. Diffuse reflectance spectra of YMSBT complexes.

**Table.V.5**  
Electronic spectral data of  
zeoliteY encapsulated SBT complexes.

| Complex | Abs. Max<br>(cm <sup>-1</sup> ) | Tentative<br>Assignments                           |
|---------|---------------------------------|--|
| YMnSBT  | 33200<br>26600<br>14250         | Charge transfer<br>”<br>d-d transition             |
| Y FeSBT | 35700<br>25000<br>16100         | Charge transfer<br>”<br>d-d transition             |
| YCoSBT  | 22200<br>12150                  | Charge transfer<br>$^4A_2 \rightarrow ^4T_1(P)$    |
| YNiSBT  | 23800<br>16660                  | Charge transfer<br>$^1A_{1g} \rightarrow ^1B_{1g}$ |
| YCuSBT  | 25000<br>16600                  | Charge transfer<br>d-d transition                  |

For neat CoSBT complex this band occurs near  $35000\text{ cm}^{-1}$ . Three other bands observed in simple complex of SBT were also found red shifted in this zeolite encapsulated complex. There is a band at  $12150\text{ cm}^{-1}$ . The data indicate that the tetrahedral geometry of the simple complex is preserved in the case of the CoSBT complex encapsulated inside the zeolite Y.

The absorption maxima for YNiSBT and its diamagnetic nature point towards a square planar structure of the molecule within the super cavities of the aluminosilicate framework. The transition observed at  $16660\text{ cm}^{-1}$  for this species correspond to  ${}^1A_{1g} \rightarrow {}^1B_{1g}$  transition. Most of the copper complexes have a band<sup>21</sup> around  $20000\text{ cm}^{-1}$ . The band at  $16600\text{ cm}^{-1}$  in YCuSBT complex was indicative of a square planar nature, which is in agreement with the magnetic moment value of 1.9BM. The electronic spectral analysis compared with the magnetic moment measurements indicate that the chemical stoichiometry and structural integrity of the SBT Schiff base complexes were almost preserved to a large extent on encapsulation of these complexes in the super cavities of zeolite Y.

### 5.3.6. FTIR- Spectra.

Infrared spectroscopy can give information on whether the ligand molecules have coordinated to the metal cations present inside the zeolite cavities, since characteristic bands due to the coordination sites shifts on chelation. According to group frequency concept, IR absorption band of a group occurs at about the same frequency irrespective of the molecule to which it belongs. The zeolite bands are seen to encompass the bands due to encapsulated complexes. Hence the IR bands of all the encapsulated complexes were weak due to their low

concentration in the zeolite cages. The FTIR spectra of the metal exchanged zeolites are shown in Figure.V.7 and the encapsulated SBT complexes are shown in Figure.V.8. Comparison of IR spectral bands of metal exchanged zeolite MY, ligand SBT and encapsulated metal complexes is presented in TableV.6. IR spectral bands of zeolites can be attributed to the internal versus external vibrations<sup>22</sup> of  $\text{SiO}_4$  and  $\text{AlO}_4$  tetrahedra designated as  $\text{TO}_4$ .

Comparison of the infrared spectra of simple complexes and metal exchanged zeoliteY with that of the encapsulated ones confirms the formation of the complex inside the pores. The characteristic spectral bands obtained for them are presented in Table.V.6. The encapsulated SBT complexes show significant shift in the azomethine group frequency  $\nu_{\text{C=N}}$  at  $1667\text{cm}^{-1}$  of the ligand showing the involvement of the azomethine group.

Another coordination site utilized by the ligand to coordinate with the metal ion is oxygen atom of the phenolic group at the ortho position of the azomethine group in the ligand. This was indicated by the red shift of  $\sim 40\text{cm}^{-1}$  in phenolic stretching frequency<sup>22</sup>  $\nu_{\text{C-O}}$  at  $1067\text{cm}^{-1}$  of the ligand in the encapsulated complexes. Broad and strong absorption band at  $3460\text{cm}^{-1}$ , and at around  $570\text{cm}^{-1}$  can be assigned to vibrations due to lattice water present in zeolite cavities and framework<sup>23</sup>. Band at  $3060\text{cm}^{-1}$  in the IR spectra of the ligand SBT was due to the  $\nu_{\text{C-H}}$  of aromatic ring. This band was found merged with the lattice water vibrations of zeolite cavities. Bands at  $1385\text{cm}^{-1}$  and  $757\text{cm}^{-1}$  are assigned to various aromatic ring vibrations.

**Table. V.6**  
 Infra Red spectral data (cm<sup>-1</sup>) of  
 zeoliteY encapsulated SBT complexes.

| MY   | SBT  | YMnSBT | YFeSBT | YCoSBT | YNiSBT | YCuSBT |
|------|------|--------|--------|--------|--------|--------|
| 3461 | -    | 3461   | 3454   | 3450   | 3461   | 3462   |
| 1640 | 1667 | 1647   | 1647   | 1633   | 1647   | 1640   |
| -    | 1573 | -      | -      | 1580   | -      | 1573   |
| -    | 1512 | 1539   | 1539   | 1527   | 1546   | 1534   |
| -    | 1452 | 1452   | 1458   | 1453   | 1458   | 1450   |
| -    | 1385 | -      | -      | 1388   | -      | 1381   |
| -    | 1325 | -      | -      | 1335   | -      | 1328   |
| -    | 1182 | -      | -      | 1182   | -      | -      |
| -    | 1067 | 1013   | 1020   | -      | -      | -      |
| 987  | 906  | -      | -      | 997    | 993    | 990    |
| 764  | 757  | 757    | 757    | 758    | 757    | 758    |
| -    | 683  | 685    | -      | 692    | 690    | 685    |
| 569  | 552  | 575    | 575    | 572    | 569    | 572    |
| 461  | -    | 461    | 467    | 466    | 467    | 466    |

### 5.3.7. EPR Spectra.

EPR parameters calculated from the spectrum are presented in Table.V.7.

The spectrum is given in Figure.V.9. Covalent environment of the metal ion was

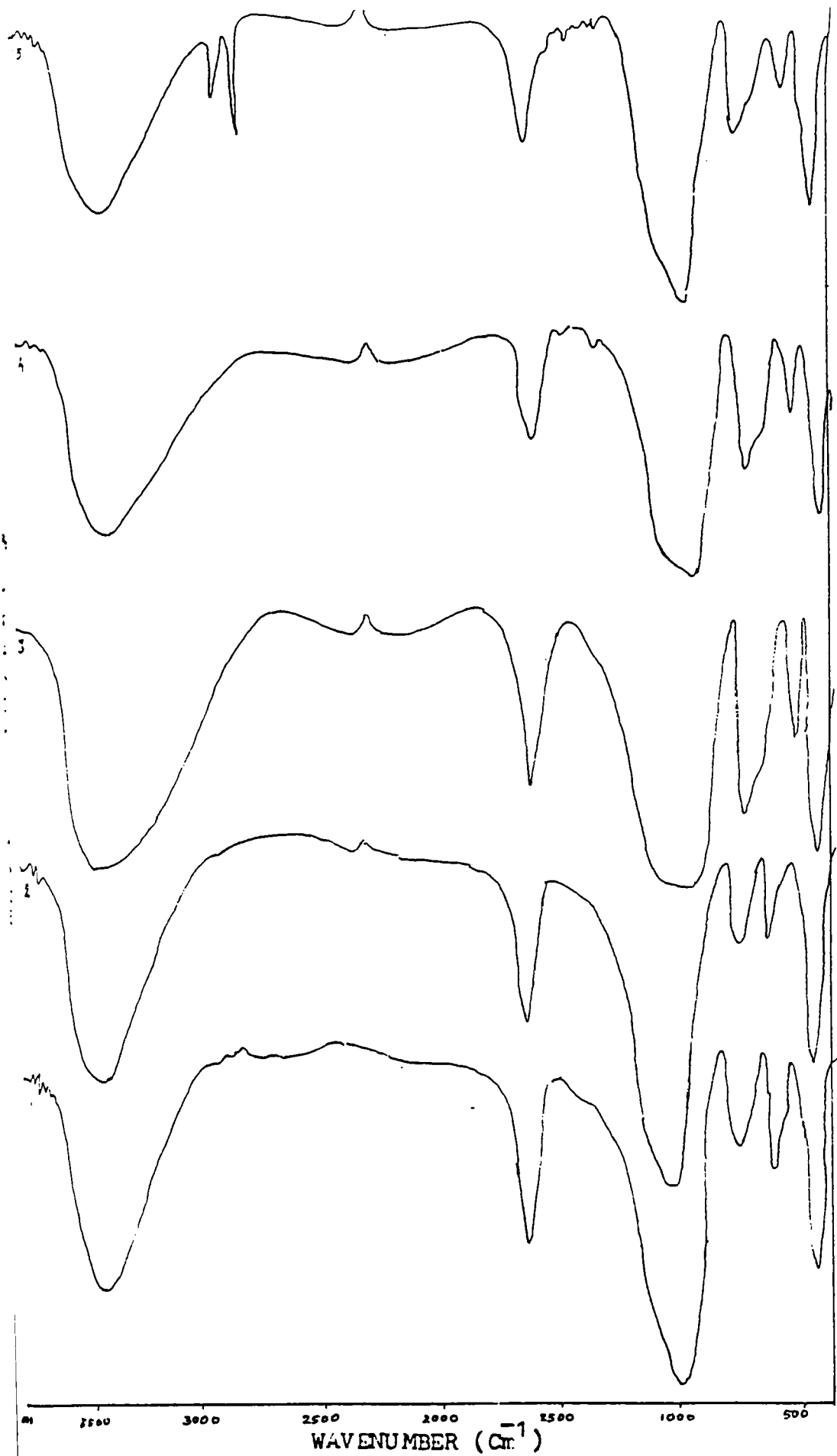


Fig. V.7. FTIR-Spectra of (i) MnY (ii) FeY (iii) CoY (iv) NiY (v) CuY.

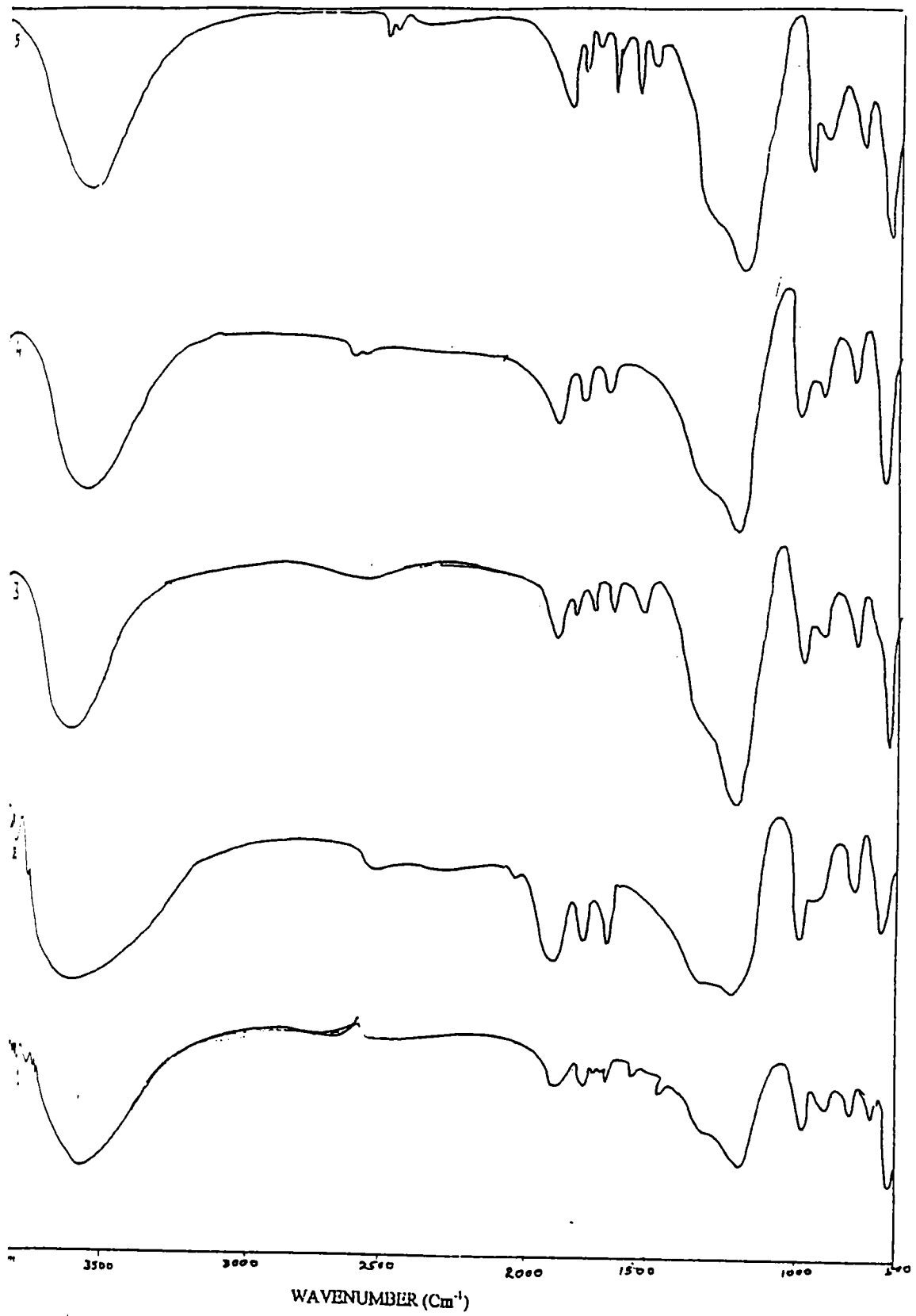


Figure V.8. FTIR Spectrum of (1) YMnSBT (2) YFeSBT (3) YCoSBT (4) YNiSBT (5) YCuSBT.

indicated by the  $g_{\parallel}$  value of 2.26. The in-plane  $\sigma$  bonding parameter  $\alpha^2 = 0.8$  signifies the covalent character of the metal- ligand bond. Since  $g_{\parallel} > g_{\perp} > 2.0023$ , it can be assumed that molecule may have a square planar geometry. The  $g_{\parallel} / A_{\parallel}$  ratio of 186.5cm points towards the distorted tetrahedral structure.  $\mu_{\text{eff}}$  value 1.93 BM obtained from the EPR spectral data calculation is very close to the value obtained by Gouy method. The value suggests a square planar structure to the complex.

**Table.V. 7**  
EPR spectral data of zeoliteY  
encapsulated CuSBT complex.

| EPR parameter                   | YCuSBT                                 |
|---------------------------------|--|
| $g_{\parallel}$                 | 2.28                                   |
| $g_{\perp}$                     | 2.06                                   |
| $A_{\parallel}$                 | $126.61 \times 10^{-4} \text{cm}^{-1}$ |
| $G_{\parallel} / A_{\parallel}$ | 186.5cm                                |
| $g_{\text{av}}$                 | 2.17                                   |
| $\alpha^2$                      | 0.80                                   |
| $\mu_{\text{eff}}$              | 1.93 BM                                |

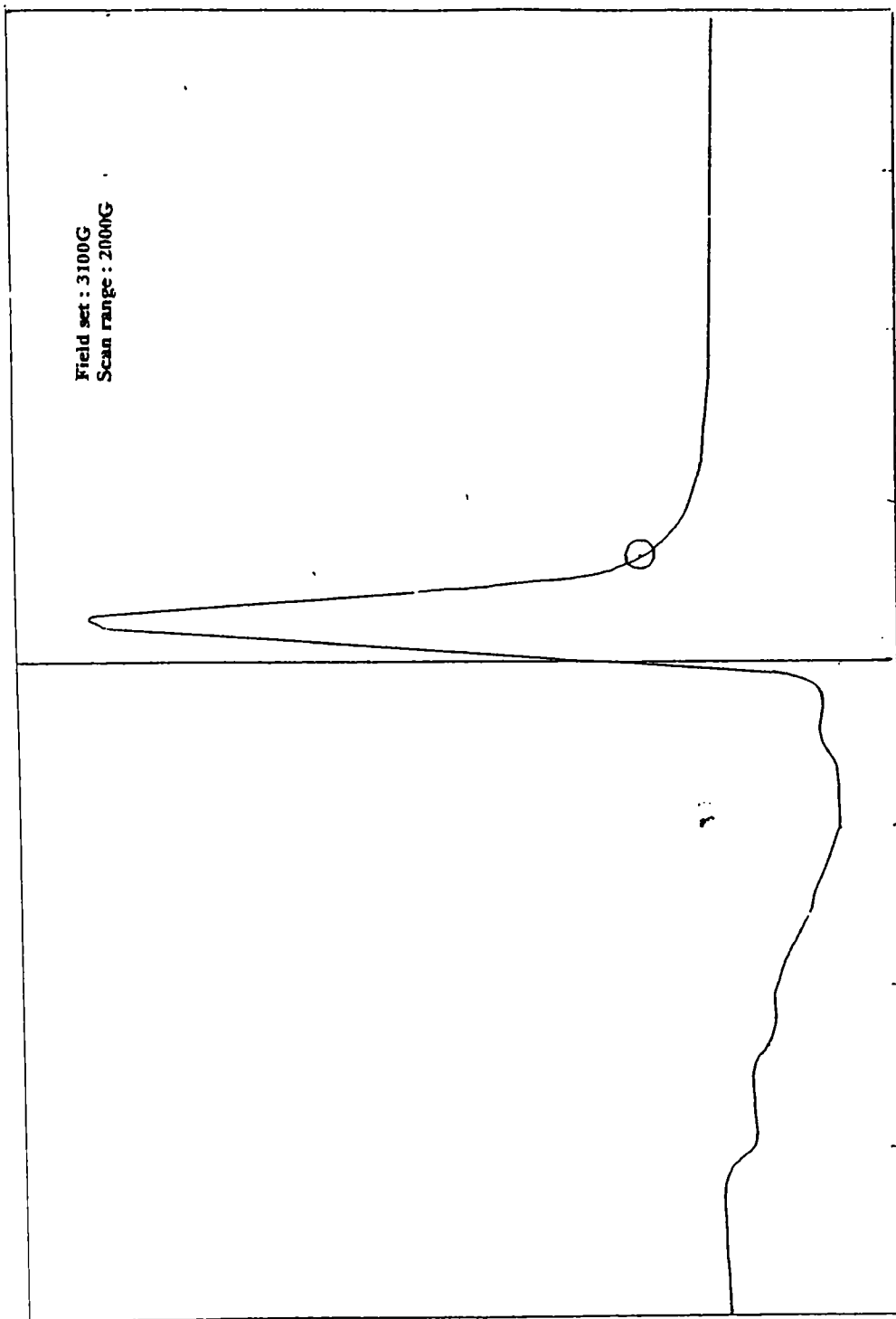


Figure V.9. EPR spectra of YCuSBT complex.

### 5.3.8. Thermogravimetric analysis.

Thermogravimetric analysis of zeolite encapsulated complexes, YMnSBT, YFeSBT and YCoSBT were carried out from room temperature to 1000°C at a heating rate of 10°C per minute to determine the thermal stability of these systems. TG analysis data are presented in Table.V.8. and the patterns are given in Figure.V.10.

**Table. V.8**  
TG data of zeoliteY encapsulated SBT complexes.

| Sample | Temperature range | % Mass loss |
|--------|-------------------|-------------|
| YmnSBT | 27-110            | 7.60        |
|        | 110-312           | 10.00       |
|        | 312-1000          | 17.25       |
| YfeSBT | 27-110            | 7.70        |
|        | 110-292           | 10.30       |
|        | 292-1000          | 19.20       |
| YcoSBT | 27-110            | 5.60        |
|        | 110-310           | 10.60       |
|        | 310-800           | 10.20       |

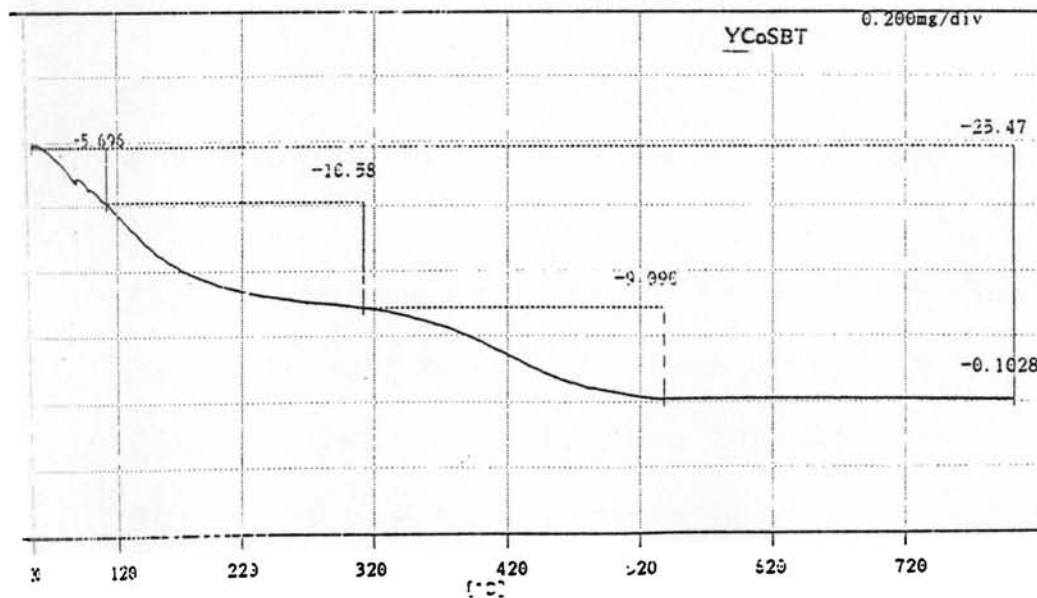
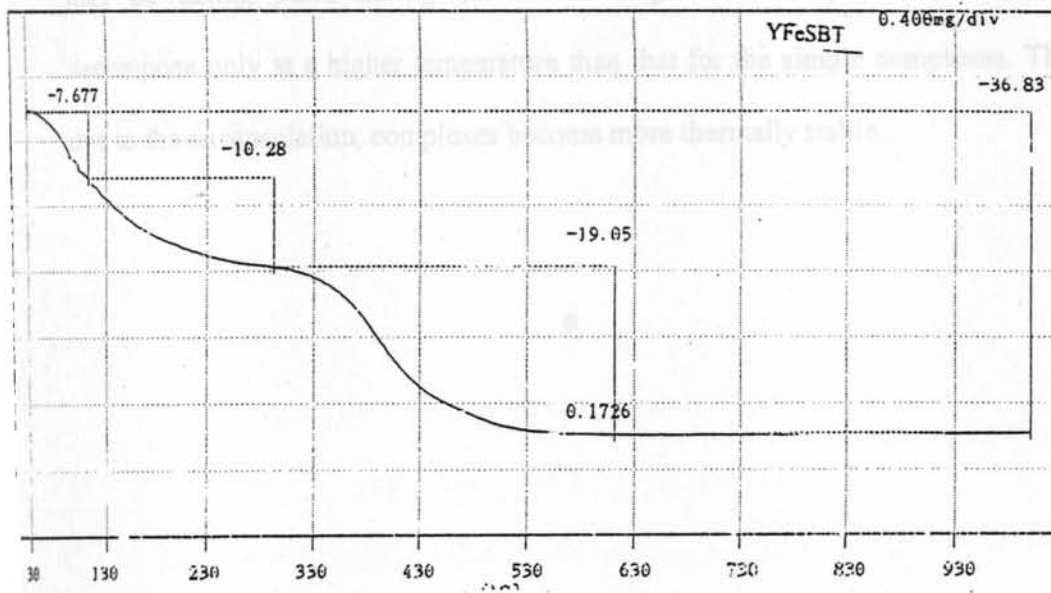
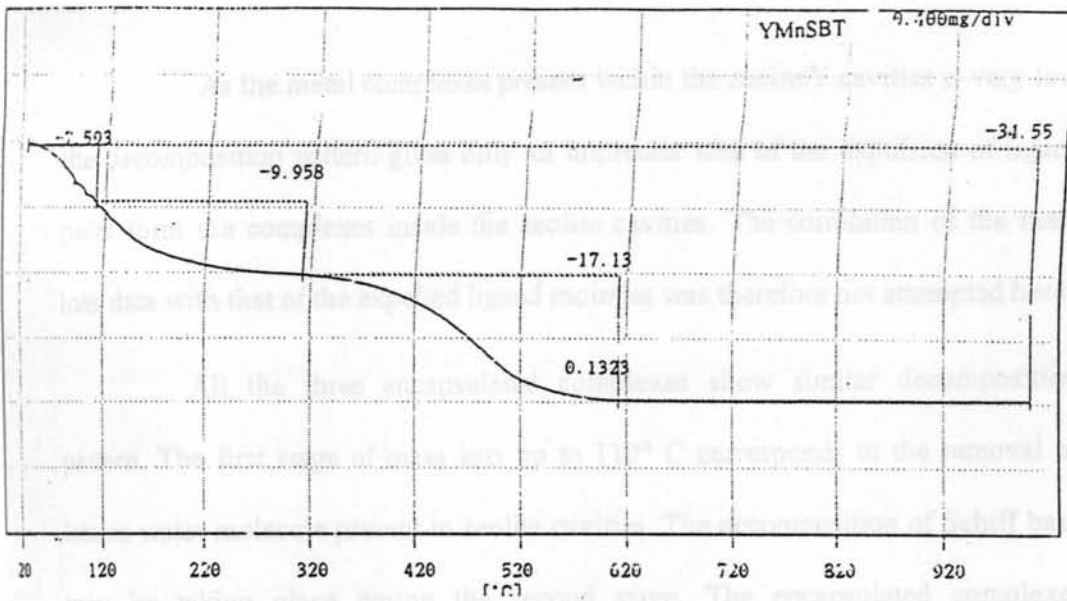


Figure.V.10. TG curves of YMSBT complexes.

G8498

As the metal complexes present within the zeoliteY cavities is very low, the decomposition pattern gives only an imprecise idea of the expulsion of ligand parts from the complexes inside the zeolite cavities. The correlation of the mass loss data with that of the expelled ligand moieties was therefore not attempted here.

All the three encapsulated complexes show similar decomposition pattern. The first stage of mass loss up to 110° C corresponds to the removal of lattice water molecule present in zeolite cavities. The decomposition of Schiff base may be taking place during the second stage. The encapsulated complexes decompose only at a higher temperature than that for the simple complexes. Thus due to the encapsulation, complexes become more thermally stable.

\*

## REFERENCES.

1. Saji P Varkey and Chandra R Jacob; *Ind. J. Chem.* 1999,38A,320.
2. Trissa Joseph, C.S. Sajanikumari, S.S.Deshpande and Sarada Gopinathan; *Ind.J.Chem.* 1999, 38A, 792.
3. Stainslaw Kowalak, Ralph.C. Weiss and Kenneth J. Balkus,Jr., *J. Chem. Soc. Chem. Commun*, (1991), 57.
4. T.Kimura, A.Fukuoka, M.Ichikawa., *Catal. Lett*, (1990), 4, 279, -286.
5. Norman Herron., *New. J. Chem*, (1989), 13,761-766.
6. Norman Herron., *J. Coord. Chem*, (1988), 19, 25.
7. G.Herici-Olive and S.Olive., *J.Mol. Catal*, (1975-76), 1, 121.
8. K.J. Balkus Jr. and A.G.Gabrielo., *J.Inclusion Phenom. Recogn. Chem*, (1995), 21,159.
9. Romanovsky.B.V., *Proc.In.Syn.Zeolites Catal*, (1985), 215. Meyer.G, Wohrle.D, Mohl.M, Schulz-Ekloff.G., *Zeolites*, (1984), 4, 80.
10. Norman Herron., *Inog.Chem*, (1986), 25, 4714-4717.
11. C.Tollman and Norman Herron., *Symposium on Hydrocar. Oxidation*, 194<sup>th</sup> National Meeting of American Chemical Society,New Orleans, LA, Aug. 30-Sept.4, 1987.
12. N.Herron, G.D.Stucky and C.A.Tolmann., *J.Chem.Soc, Chem. Commun.* (1986), 1521.
13. E.Paez-Mozo, N.Gabriunas, F.Lucaaaioni, D.D. Acosta, P.Patrono, A.La Ginestra, P.Ruiz and B. Delmon., *J.Phys. Chem*, (1993), 97, 12819.
14. P.M.Edgardo, G.Nyole, L.Fabio, D.D.Acosta , P.Pasquale, L.G.Aldo, R.Patricio and D. Bernard., *J. Phys. Chem*,(1993).

15. S.P. Varkey and C.R.Jacob., *Ind .J. Chem*,(1998) ,37A, 407.
16. Yasuaki Okamoto., *Catalysis Today*, Elsevier, (1997), 39, 45-59.
17. V.V. Balasubramanian, I. Sudarsan Kumar, V.Umamaheswary, A.Pandurangan, S.Kutti Rani, M.Palanichamy and V.Murugesan., *Recent trends in Catalysis*, (1999), Narosa Publishing House,New Delhi.
18. S.K. Tiwary and S. Vasudevan., *Inorg. Chem*, (1998), 37, 5239-5246.
19. Rani Abraham, Ph.D Thesis submitted to Cochin University of Science and Technology, Kochi-22.,(1999).
20. A. Earnshaw., "*Intrduction to Magnetochemistry*", Academic Press, New York,(1968).
21. A.B.P.Lever, *Inorganic Electronic Spectroscopy*, Elsevier, Amsterdam, (1968).
22. R.M.Silverstein, G.C. Bassler., *Spectroscopic Identification of Organic Compounds*, John Wiely, USA,(1967).
23. R.S. Drago., *A textbook of Physical methods in Chemistry*,Reinhold Publishing House, New York. (1965).

\*

# CHAPTER VI



**Zeolite Y encapsulated Mn(II), Fe(III), Co(II), Ni(II) and Cu(II)  
complexes of the Schiff base  
derived from vanillin and 2-aminobenzothiazole (VBT).**

**6.1. Introduction.**

Incorporation of transition metal complexes in the supercages of zeolites offers number of advantages over their counterparts in homogeneous solution. Zeolite encapsulated complexes have also been suggested as model compounds for enzyme mimicking<sup>1-3</sup> in which zeolite framework behave as the protein mantle of the enzyme and the entrapped metal complex mimics the active sites of the enzyme<sup>1</sup>. In addition to the difference in activity, interesting selectivity changes are also observed upon immobilization of the complexes in the microporous matrix.

An attempt has been made to encapsulate the Mn(II), Fe(III), Co(II), Ni(II) and Cu(II) complexes of the Schiff base derived from 4-hydroxy-3-methoxybenzaldehyde(vanillin) and 2-aminobenzothiazole in the super cages of zeoliteY. These encapsulations have been carried out with a view to develop new solid heterogeneous catalysts. In this chapter, the results of our studies on the synthesis and characterization of zeoliteY encapsulated complexes of Mn(II), Fe(III), Co(II), Ni(II) and Cu(II) of Schiff base derived from vanillin and 2-aminobenzothiazole (VBT) are presented. Further it is considered worthwhile to study the effect of the electron donating groups such as -OH and -OCH<sub>3</sub> on catalytic activity of these complexes in the cavities of zeoliteY. The resultsof these catalytic activity studies are presented in chapter VIII. It is known that electron withdrawing substituents like -Cl, -Br or -NO<sub>2</sub> on the salen ligand enhanced the

low temperature oxidation of phenol, styrene and p-xylene and the rates of decomposition of  $\text{H}_2\text{O}_2$  than their non-substituted analogues<sup>4,5</sup>.

## **6.2 Experimental.**

### **6.2.1 Materials.**

Details of synthesis of the Schiff base ligand VBT are presented in chapter II. The procedure for the modification of commercially available zeoliteY to NaY and metal exchanged zeolites is given in chapter.II.

### **6.2.2. Synthesis of zeoliteY encapsulated VBT complexes.**

The metal exchanged zeoliteY (5g, dried at  $400^\circ\text{C}$ ) was refluxed with the ligand VBT solution (25mL) in a round bottomed flask on a water bath for 10-15 hrs and filtered. To ensure encapsulation of the complex, this was then ampouled in a test tube and heated to  $115^\circ\text{C}$  in a muffle furnace. Change in colour of the metal exchanged zeoliteY is an indication of the encapsulation of the complex. The encapsulated complex so formed was then purified by soxhlet extraction, first with methanol and then with dichloromethane to remove the uncomplexed ligand on the zeolite surface and cavities. This soxhlet extraction was continued for 4-5 days till the colour of the solvent becomes clear. The uncomplexed metal ion was then re-exchanged with  $\text{Na}^+$  ion by stirring with NaCl solution (0.01M) for 24hrs. The encapsulated complex was then freed from chloride ions by washing several times with hot distilled water. Finally it was dried and dehydrated at  $120^\circ\text{C}$  for 4hrs and stored in vacuum over anhydrous calcium chloride.

### 6.3. Results and Discussion.

#### 6.3.1. Elemental analysis.

The methods used for the elemental analysis are described in chapter II. The results of the elemental analysis are presented in Table.VI.1. The Si /Al ratio was found to be in the range 2.4 to 2.46, so the possibility of dealumination can be discarded. The percentages of C in the encapsulated complexes suggest that only a small amount of metal complexes are present in cavities.

**Table. VI.1**  
Analytical data of zeolite Y encapsulated VBT complexes

| Sample | Elemental Analysis |      |      |         |      |      |      |      |
|--------|--------------------|------|------|---------|------|------|------|------|
|        | % Si               | % Al | % Na | % Metal | % C  | % H  | % N  | % S  |
| YMnVBT | 19.40              | 7.82 | 6.72 | 2.03    | 5.44 | 2.38 | 0.38 | 0.51 |
| YFeVBT | 19.47              | 7.93 | 6.58 | 1.32    | 5.12 | 2.22 | 0.35 | 0.54 |
| YCoVBT | 19.32              | 7.87 | 6.19 | 1.87    | 2.38 | 2.43 | 0.21 | 0.28 |
| YNiVBT | 19.35              | 7.94 | 6.55 | 1.24    | 2.94 | 1.45 | 0.23 | 0.36 |
| YCuVBT | 19.41              | 7.83 | 6.61 | 1.90    | 2.39 | 2.47 | 0.29 | 0.32 |

The data given in Table.VI.1 indicate a ligand to metal mole ratio of 2:1 for the encapsulated YMnVBT and YFeVBT complexes, and 1:1 for YCoVBT, YNiVBT and YCuVBT complexes. Therefore two molecules of ligand might be coordinated in the case of Mn(II) and Fe(III) complexes and one molecule might

be coordinated in the case of Co(II), Ni(II) and Cu(II) complexes encapsulated in zeoliteY.

### 6.3.2. Surface area and pore volume analysis.

BET method was used to measure the surface area and pore volume of the metal exchanged zeolites and the encapsulated complexes at liquid nitrogen temperature and the values obtained are given in Table.VI.2. The surface area of the encapsulated complexes is considerably lower than that of NaY and the metal exchanged substrates. The complexes probably play the role of pore-filling agents in the zeolite matrix, which is a positive indication of encapsulation of the complexes<sup>6,7</sup>

**Table. VI.2**  
Surface Area and Pore volume of  
zeoliteY encapsulated VBT complexes

| Sample | MY                                   |                    | YMVBT                                |                    |
|--------|--------------------------------------|--------------------|--------------------------------------|--------------------|
|        | BET surface area (m <sup>2</sup> /g) | Pore volume (cc/g) | BET surface area (m <sup>2</sup> /g) | Pore volume (cc/g) |
| NaY    | 523                                  | 0.3045             | -                                    | -                  |
| YMnVBT | 496                                  | 0.2964             | 334                                  | 0.2393             |
| YFeVBT | 510                                  | 0.3013             | 359                                  | 0.2398             |
| YCoVBT | 490                                  | 0.2986             | 345                                  | 0.2318             |
| YNiVBT | 489                                  | 0.2934             | 340                                  | 0.2371             |
| YCuVBT | 497                                  | 0.2959             | 366                                  | 0.2113             |

The loss in surface area and pore volume of metal exchanged zeolites on encapsulation of VBT complexes is shown diagrammatically in Figure.VI.1 and VI.2. respectively.

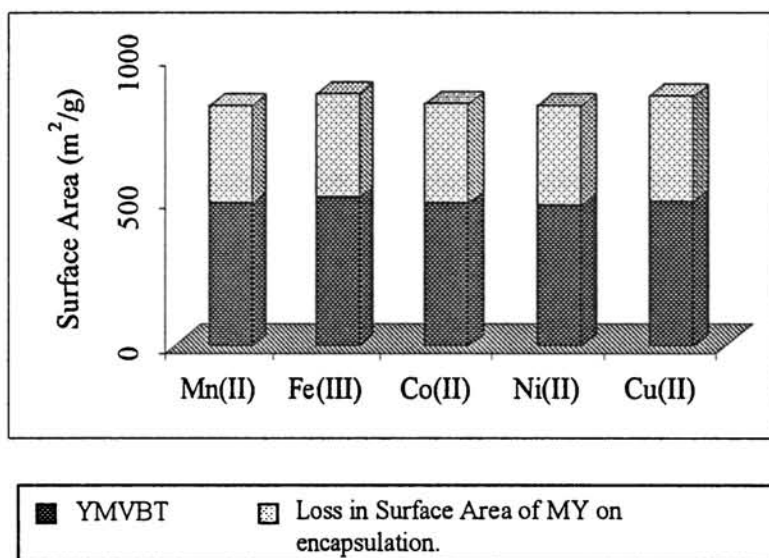


Figure.VI.1. Decrease in surface area of metal exchanged zeolites on encapsulation of complexes.

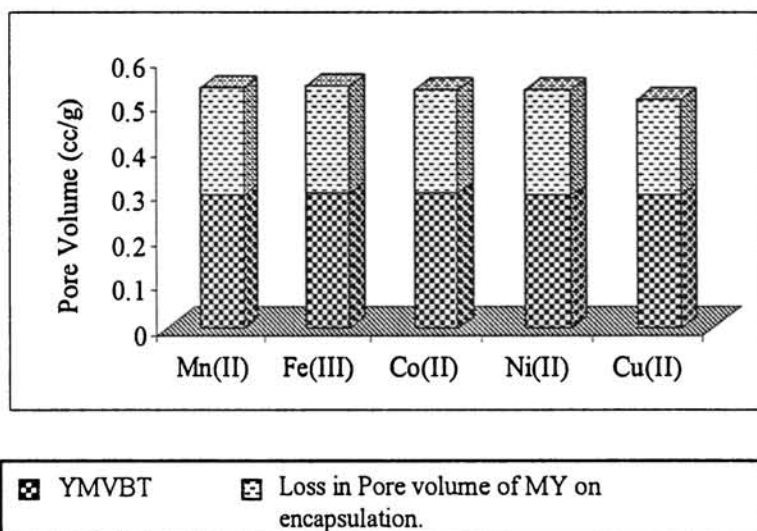


Figure.VI.2. Decrease in pore volume of metal exchanged zeolites on encapsulation of complexes.

### 6.3.3. X-ray diffraction studies.

The XRD patterns of the VBT complexes synthesized in the supercages of zeolite Y are given in Figure VI.3. Comparison of these patterns with that of the parent zeolite NaY shows that, no change in the peak position has taken place by encapsulation process. This ensures that crystallinity of zeolite framework has been preserved after the encapsulation. In the XRD pattern the relative intensities of some peaks showed significant changes after complex formation. The intensity of some of the peaks in NaY was increased while that of some others gets decreased in encapsulated complexes. Such changes indicate complex formation in the supercages<sup>8</sup>. However the complexes bound to external surface do not contribute towards the intensity change<sup>9</sup>.

### 6.3.4. Magnetic susceptibility.

The Gouy method was applied at room temperature for measuring the magnetic susceptibility of the metal exchanged zeolites and the zeolite encapsulated complexes.  $\chi_m$  values were calculated using approximate molecular weight of the encapsulated complex. The diamagnetic contribution of the parent zeolite NaY at room temperature was calculated using the unit cell formula determined from analytical data and was subtracted along with the diamagnetic correction due to the ligand from the  $\chi_m$  values calculated for encapsulated complexes. The magnetic moment values are presented in Table.VI.3. The magnetic moment values indicate that the zeolite Y encapsulated complexes have almost the same geometry as that of the simple complexes.

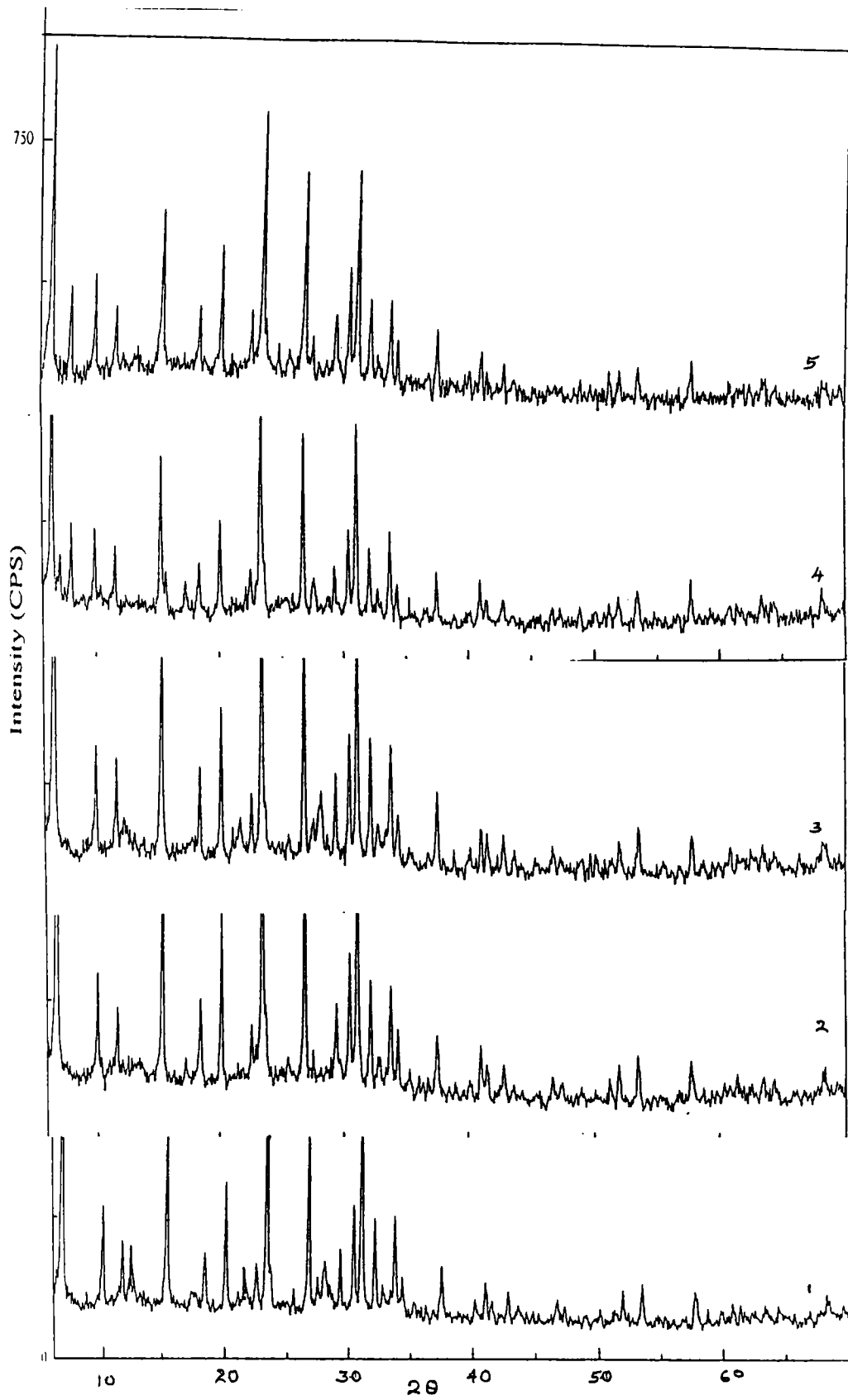


Figure. VI.3. XRD Patterns of 1). YMnVBT 2). YFeVBT  
3). YCoVBT 4). YNiVBT 5). YCuVBT

**Table. VI.3**

Magnetic moment data of the zeoliteY encapsulated VBT complexes.

| Complex | Magnetic moment<br>$\mu_{\text{eff}}$ (BM) |
|---------|--|
| YMnVBT  | 5.8  |
| YFeVBT  | 5.7  |
| YCoVBT  | 4.8  |
| YNiVBT  | diamagnetic                                |
| YCuVBT  | 1.7  |

Magnetic susceptibility of the zeolite encapsulated MnVBT complex is 5.8 BM. This is very close to spin only value for a high spin octahedral complex. Octahedral Mn(II) complexes were reported<sup>10</sup> to have magnetic moments in the range 5.6 – 6.0 BM. For Fe(III) complex the magnetic moment value was found to be 5.7 B.M. This lies on the verge of the range 5.7 to 6.0 BM expected for high spin octahedral complex<sup>11</sup>. YCoVBT exhibits magnetic moment value of 4.8 BM indicating tetrahedral structure for the complex. The diamagnetic nature of YNiVBT complex suggests a square planar structure for the encapsulated complex. The copper VBT complex exhibits a room temperature moment of 1.7 BM. indicating a square planar structure to the encapsulated complex.

### 6.3.5. Diffuse Reflectance Spectra.

Electronic spectra of the zeolite Y encapsulated complexes were recorded in diffuse reflectance mode. Representative spectra are given in Figure VI.4. The absorption maxima for the encapsulated complexes and tentative assignments of the bands are given in Table VI.4. Some low intensity bands were observed in all the samples below  $10000\text{ cm}^{-1}$  regardless of the nature of the metal ion or other species present in the matrix. These bands are attributed<sup>13</sup> to the overtones and combinations of the stretching and bending vibrations of water molecules. The bands observed for the YMnVBT complex are very weak when compared to the UV-Vis spectra obtained for the corresponding simple complex of VBT. This may be due to low concentration of metal ions in the zeolite cavities. However low intensity bands observed in the region  $13000\text{ cm}^{-1}$  to  $20000\text{ cm}^{-1}$  were assignable to forbidden d-d transitions.

The electronic spectral bands and the magnetic moment of 5.8 BM suggest octahedral geometry to YMnVBT complex. Mn(II) salen complexes are reported<sup>14</sup> to have an octahedral geometry for the complex in the cages of Yzeolite. As in the case of Mn(II) complex, the low intensity bands observed for YFeVBT could be assigned to the forbidden d-d transitions<sup>15</sup>. The data indicates octahedral structure to the Fe(III) complex in the zeolite voids.

The diffuse reflectance spectrum of Co(II) complex in zeolite super cages exhibit one d-d transition. The  $d^7$  system in a tetrahedral environment gives three transitions corresponding to  ${}^4T_1(P) \leftarrow {}^4A_2(F)$ ,  ${}^4T_1(F) \leftarrow {}^4A_2(F)$ ,  ${}^4T_2(F) \leftarrow {}^4A_2(F)$  transitions. Generally  ${}^4T_2(F) \leftarrow {}^4A_2(F)$  appears<sup>15</sup> in the near IR region  $8000\text{-}5000\text{ cm}^{-1}$ . But in YCoVBT system these regions were masked by the

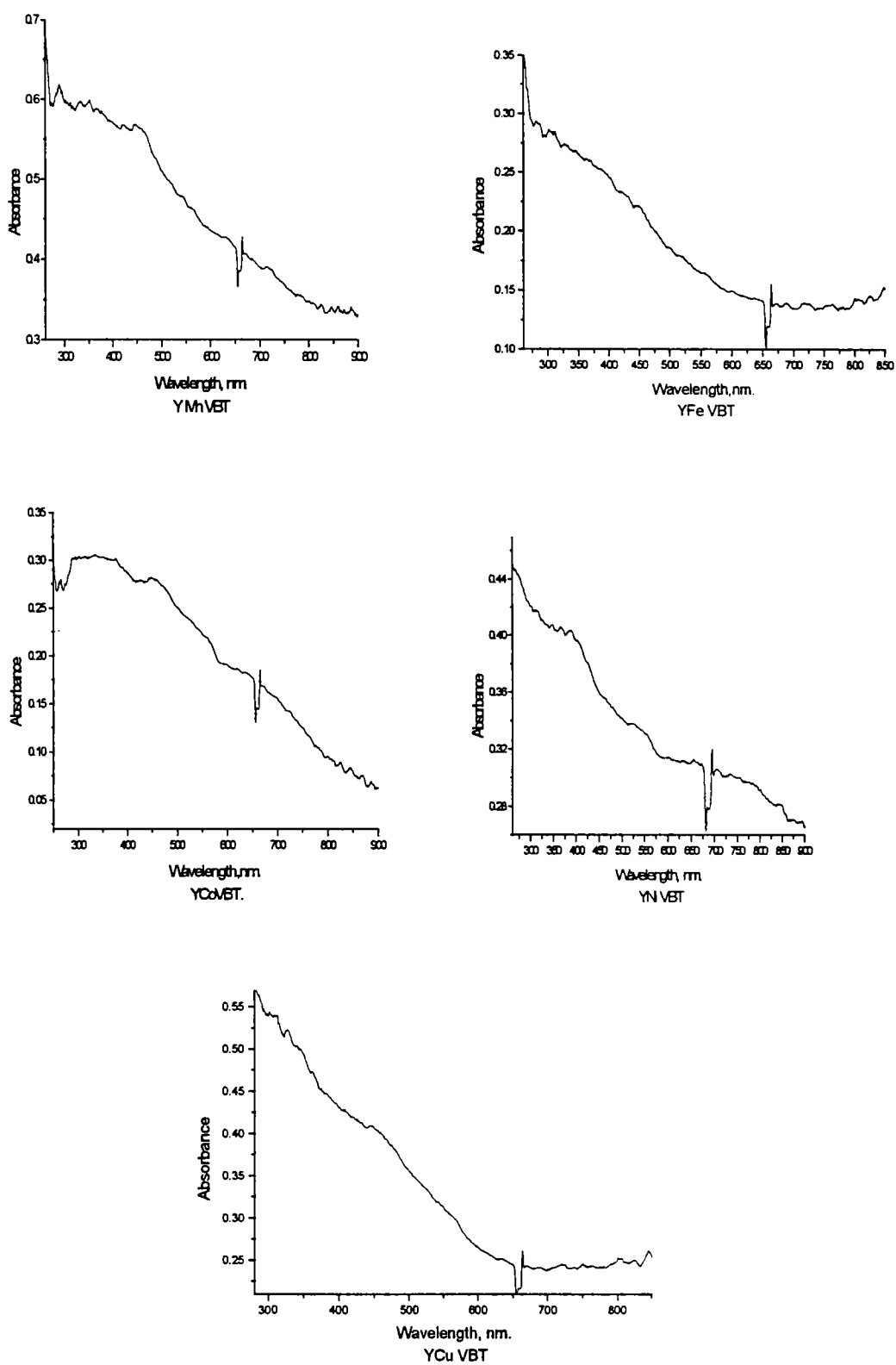


Figure. VI.4. Diffuse reflectance spectra of YMVBT complexes.

**Table.VI.4**  
Electronic spectral data of  
zeoliteY encapsulated VBT complexes

| Complex | Abs. Max<br>(cm <sup>-1</sup> ) | Tentative<br>Assignments                                      |
|---------|---------------------------------|---|
| YMnVBT  | 28500                           | Charge transfer   |
|         | 19230                           | d-d transition  |
|         | 16600                           | "   |
|         | 14200                           | "   |
|         | 13000                           | "   |
| YFeVBT  | 35700                           | Charge transfer   |
|         | 28240                           | "   |
|         | 18600                           | d-d transition  |
|         | 17000                           | "   |
|         | 13300                           | "   |
| YCoVBT  | 28570                           | Charge transfer   |
|         | 13800                           | <sup>4</sup> A <sub>2</sub> → <sup>4</sup> T <sub>1</sub> (P) |
| YNiVBT  | 31250                           | Charge transfer   |
|         | 18180                           | <sup>1</sup> A <sub>1g</sub> → <sup>1</sup> B <sub>1g</sub>   |
| YCuVBT  | 28500                           | Charge transfer   |
|         | 16500                           | d-d transition  |

zeolite framework transitions. Magnetic moment value also suggests a tetrahedral structure to CoVBT complex in zeolite cavities.

The d-d transitions observed for Ni(II) complex was in agreement with that for a square planar geometric environment around the metal ion. Band observed at  $16500\text{ cm}^{-1}$  points to a square planar geometry for the YCuVBT complex. The magnetic susceptibility of 1.7 BM also suits to the square planar structure.

### 6.3.6. FTIR- Spectra.

The FTIR profiles of the encapsulated complexes are given in Figure VI.5 and the spectral data are presented in Table VI.5. The encapsulated have almost all frequencies due to the presence of ligand molecule coordinated to the metal ion. This was generally considered as a physico-chemical evidence for the encapsulation<sup>16</sup> of metal complexes.

The  $\nu_{\text{C=N}}$  stretching band observed at  $1667\text{cm}^{-1}$  in the Schiff base ligand was characteristic of azomethine linkage<sup>17</sup>. This band is seen at a lower energy (by  $10\text{-}20\text{ cm}^{-1}$ ) in the infrared spectra of the encapsulated complexes indicating the coordination of nitrogen atom of the Schiff base. The  $\nu_{\text{C-S}}$  vibration of the thiazole ring appears at  $1452\text{ cm}^{-1}$  and  $1182\text{ cm}^{-1}$  in the IR spectra of free 2-aminobenzothiazole molecule. On encapsulation these bands were found missing, which might have been shifted to  $\sim 1390\text{cm}^{-1}$  and thus got masked by the zeolite framework vibrations. Thus the ligand VBT might be binding to metal ion through nitrogen atom of the azomethine group and also through the sulphur atom of the thiazole ring.

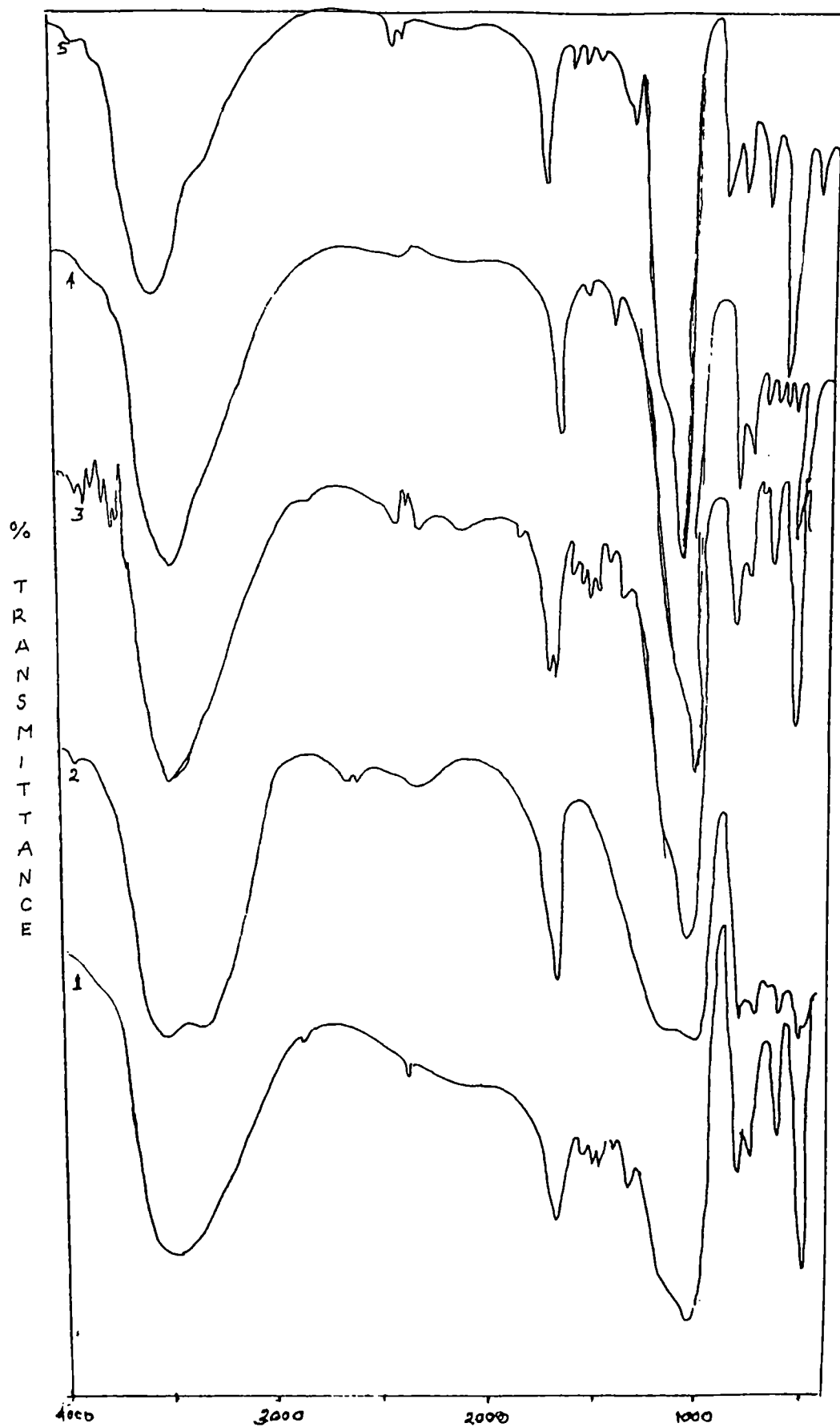


Figure. VI.5. FTIR spectra of 1). YMnVBT 2). YFeVBT  
3). YCoVBT 4). YNiVBT 5). YCuVBT

**Table. VI. 5**  
 Infra Red spectral data ( $\text{cm}^{-1}$ ) of  
 zeoliteY encapsulated VBT complexes.

| MY   | YMnVBT | YFeVBT | YCoVBT | YNiVBT | YCuVBT |
|------|--------|--------|--------|--------|--------|
| 3461 | 3474   | 3542   | 3488   | 3462   | 3456   |
| 1640 | 1654   | 1650   | 1647   | 1659   | 1653   |
| -    | 1506   | 1560   | 1553   | 1553   | 1558   |
| -    | 1330   | 1355   | 1398   | 1390   | 1381   |
| -    | 1000   | 1025   | 1007   | 1030   | 1018   |
| 987  | 975    | 973    | 993    | 990    | 996    |
| 764  | 764    | 760    | 757    | 764    | 758    |
| -    | 697    | 690    | 697    | 691    | 685    |
| 569  | 575    | 582    | 569    | 559    | 565    |
| 461  | 461    | 461    | 467    | 466    | 459    |

The broad band at  $\sim 3450\text{cm}^{-1}$  due to  $-\text{O}-\text{H}$  stretching of water in zeolite lattice was seen in all the metal exchanged zeolites and zeolite encapsulated complexes. This band seems to mask the aromatic ring stretching modes  $\nu$  ( $=\text{C}-\text{H}$ ) expected at  $3080\text{cm}^{-1}$  and  $3010\text{cm}^{-1}$ .

### 6.3.7. EPR spectra.

The EPR spectra of zeolite encapsulated CuVBT complexes recorded at LNT is presented in Figure.VI.6.

**Table. VI.6**  
EPR spectral data of  
zeoliteY encapsulated CuVBT complex.

| EPR parameter                   | YCuVBT                                 |
|---------------------------------|--|
| $g_{\parallel}$                 | 2.23                                   |
| $g_{\perp}$                     | 2.06                                   |
| $A_{\parallel}$                 | $157.18 \times 10^{-4} \text{cm}^{-1}$ |
| $g_{\parallel} / A_{\parallel}$ | 146.32cm                               |
| $g_{av}$                        | 2.15                                   |
| $\alpha^2$                      | 0.83                                   |
| $\mu_{eff}$                     | 1.76 BM                                |

The various EPR parameters were calculated for this complex and presented in Table.VI.6. The  $\mu_{eff}$  value calculated from the ESR spectra is in agreement with that obtained by Gouy balance method and the value of 1.76BM suggests a square planar structure to the complex in the zeoliteY cages.

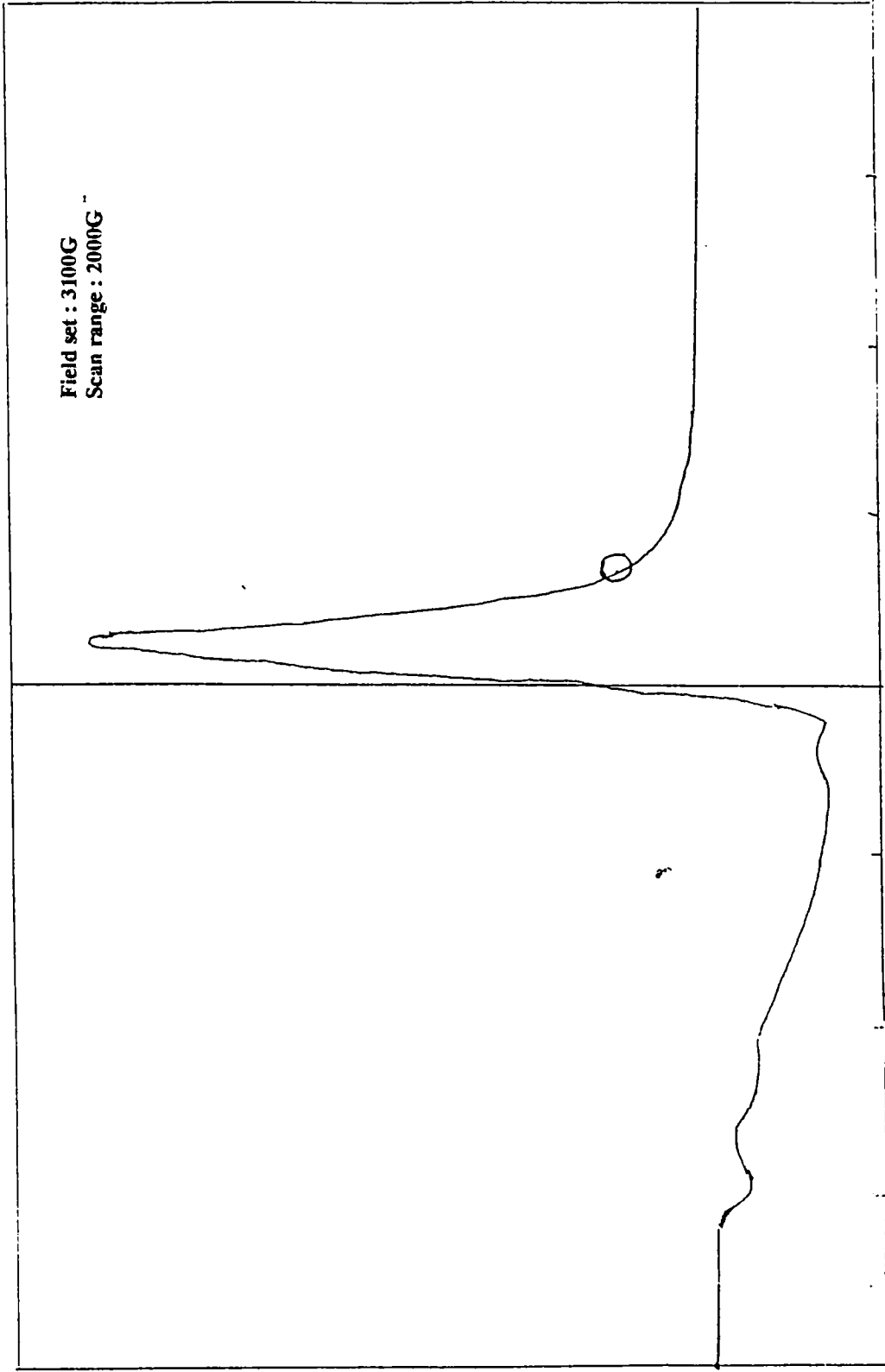


Figure. VI.6. EPR spectra of YCuVBT complex.

### 6.3.8. Thermogravimetric analysis.

**Table. VI.7**

TG data of zeoliteY encapsulated VBT complexes.

| Sample | Temperature range | % Mass loss |
|--------|-------------------|-------------|
| YMnVBT | 29-110            | 7.65        |
|        | 110-295           | 11.40       |
|        | 295-1000          | 12.60       |
| YCoVBT | 28.9-110          | 7.90        |
|        | 110-296           | 10.20       |
|        | 296-1000          | 11.20       |
| YNiVBT | 29-386            | 20.40       |
|        | 386-799           | 2.00        |

Thermal analysis reports of the complexes are given in Table.VI.7 and the TG curves are presented in Figure.VI.7. For all the three encapsulated complexes selected for this analysis, the decomposition patterns were found to be of similar type. Lattice water was removed at the initial stage followed by the decomposition of complex present in the zeolite cavities. After 400°C it can be seen that the matrix is resistant to decomposition up to the maximum temperature of 1000°C under investigation. Only 20 to 30% mass loss was recorded till 1000°C indicates the high thermal stability of zeolite matrix and low loading of the metal complex in the cavities.

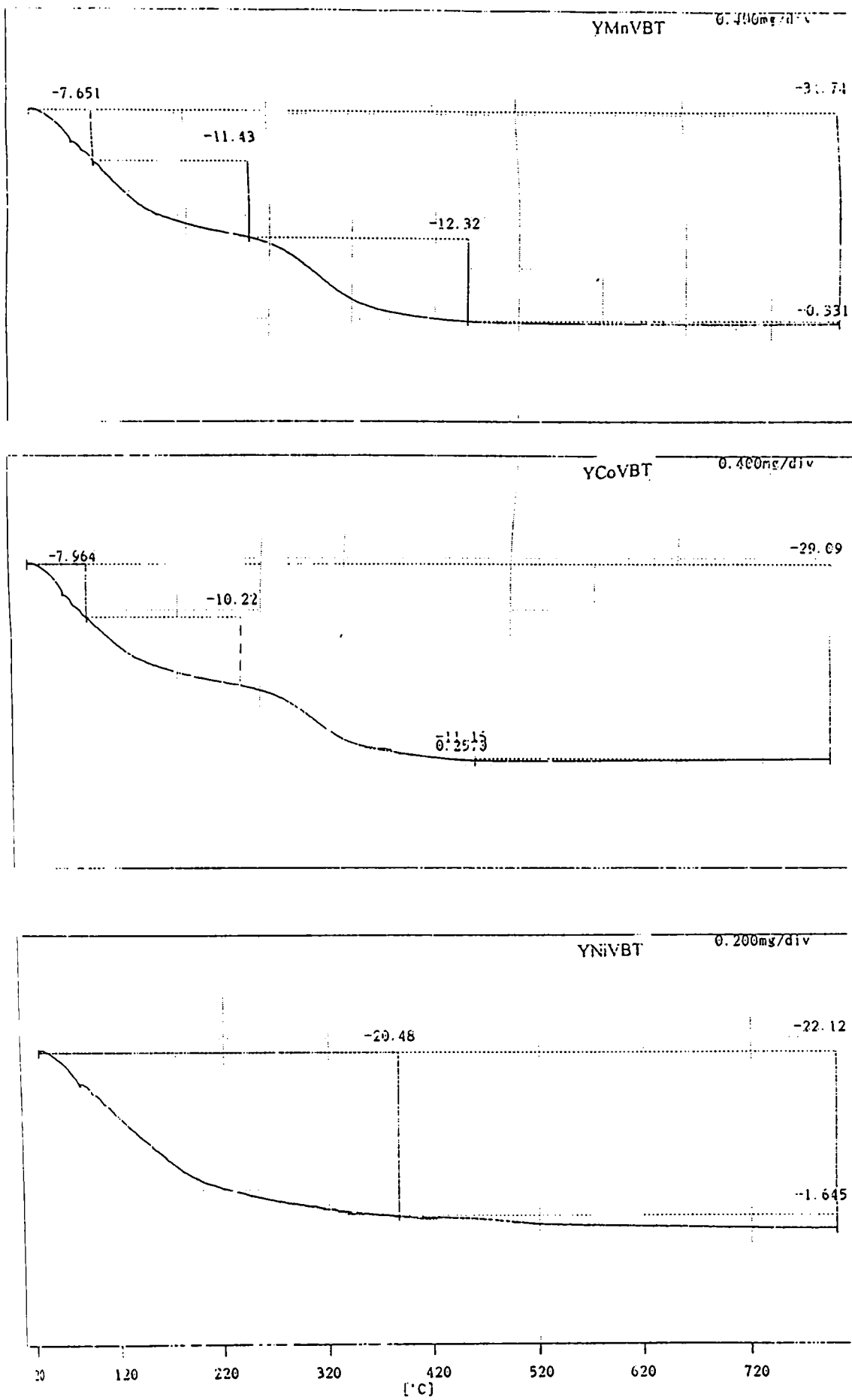


Figure. VI.7. TG curves of YMVBT complexes.

## REFERENCES

1. B.V. Romanovsky in *Proc .8<sup>th</sup> Int.Congr.Catal.*, Verlag Chemie, Weinheim, 4, (1984), 657-667.
2. Noman Heron., *Chemtech*, (1989), 542-548.
3. R. Parton, D. De Vos, P.A. Jacobs in *Zeolite Microporous Solids: Synthesis, Stucture and Reactivity*, Kluwer Academic Publishers, The Netherlands (1994), 555-578.
4. R. Raja, P. Ratnasamy., *J.Catal.* 170, (1997), 244.
5. Chandra . R. Jacob, Saji .P. Varkey, Paul Ratnasamy., *Microporous and Mesoporous Materials*, Elsevier, 22, (1998), 465 - 474.
6. K.J. Balkus Jr and A.G. Gabrielov., *J.Inclusion Phenom.Mol.Recogn.Chem*, 21, (1995), 159.
7. S.P.Varkey and C.R.Jacob., *Ind. J. Chem*, 37A, (1998), 407.
8. W.H.Quayle, G.Peeters, G.L.de Roy, E.F.Vansant and J.H.Lunsford., *Inorg .Chem*, 21, (1982), 2226.
9. Gyogygy Vanko, Zoltan Homonnay, Sandor Nagy. et.al., *JCS Chem. Comm*, (1996), 785-786.
10. A.K.Mukherjee and P.Ray., *J.Ind.Chem.Soc*, 32, (1955), 581, 604.
11. Alan Earnshaw, *Introduction to Magnetochemistry*, Academic Press, London,(1968).
12. N.N. Greenwood and A. Earnshaw, *Chemistry of the Elements*,Pergamon press,(1984).
13. K.Klier, R.Kellerman and P.J.Hutta., *J.Chem.Phys*, 61, (1974), 4224.
14. N. Ulagappan and V.Krisnasamy., *Ind. J. Chem*, 35A, (1996), 787.

14. N. Ulagappan and V.Krisnasamy., *Ind. J. Chem*, 35A, (1996), 787.
15. A.B.P.Lever., *Inorganic Electronic Spectroscopy*, Elsevier, Amsterdam, (1968).
16. Parton R., De Vos D and Jacobs P.A, in *Zeolite microporous solids synthesis, structure and reactivity*, Elsevier, Amsterdam. (1992), 553.
17. A.Syamal and M.M.Singh., *Ind. J. Chem*, (1992), 110-115.

\*

# CHAPTER VII



## ZeoliteY encapsulated Mn(II), Fe(III), Co(II), Ni(II) and Cu(II) complexes of 2-aminobenzothiazole (ABT).

### 7.1. Introduction.

Heterogeneous catalysis of isolated metal complexes encapsulated in zeolite framework shares many features in common with homogeneous and enzymatic catalysis. The high adsorption potential inside the zeolite channels raises the effective concentration of a reagent at the active sites of the catalyst and enhances their efficiency as catalytic centers. Jacobs<sup>1</sup> reported that a 200 fold increase in turn over number was found for the oxidation of n-octane using zeolite encapsulated iron phthalocyanine complex as the catalyst. This potential advantage in practical use was our guidance for synthesizing the zeolite encapsulated complexes. New intrazeolitic transition metal complexes of 2-aminobenzothiazole with metal ions Mn(II), Fe(III), Co(II), Ni(II) and Cu(II) have been prepared. Preparation and characterization of zeolite encapsulated complexes of 2-aminobenzothiazole (ABT) are presented in this chapter.

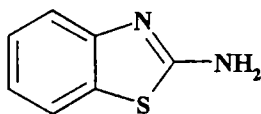


Figure. VII.1 Structure of ligand ABT

## **7.2. EXPERIMENTAL.**

### **7.2.1. Materials.**

The materials regarding the metal salts used for metal exchange, modification of commercially available zeoliteY and the synthesis of metal exchanged zeolite (MY), are given in chapter II. The ligand, 2-aminobenzothiazole, (E.Merck) was used as such for the complexation processes.

### **7.2.2. Synthesis of zeoliteY encapsulated ABT complexes.**

Flexible ligand method<sup>2</sup> was used for encapsulation of metal complexes of 2-aminobenzothiazole. Metal exchanged zeoliteY (heated to 400°C, 1g) and the ligand, 2-aminobenzothiazole (0.36g) were mixed thoroughly in a mortar, ampouled in test tube, fused and kept at 120°C for 2hrs in a muffle furnace. The change in colour of the zeolite after fusion is an indication of the encapsulation. The fused matrix was taken out and purified by soxhlet extraction first with methanol and then with dichloromethane for 5-6 days. This purification procedure was needed to remove the surface adhering complexes and excess of ligand. It was then back exchanged by magnetic stirring in 0.01M NaCl solution for 24 hrs to remove uncomplexed metal ions present in zeolite cavities. This encapsulated complex was filtered, washed several times with slightly hot distilled water to remove chloride ions until there was no precipitate formation with AgNO<sub>3</sub> and then dried in air oven. It was stored in vacuum over anhydrous calcium chloride.

### 7.3. Results and Discussion

#### 7.3.1. Elemental analysis.

Elemental analysis data for the zeolite encapsulated complexes of 2-aminobenzothiazole are presented in Table.VII.1. The data reveal the Si /Al ratio of 2.45 for the zeolite entrapped complexes, which ensures that no destruction of zeolite framework has taken place by complexation procedure. The results of elemental analysis of NaY and metal exchanged zeolites are presented in Table.V.1. Presence of carbon, nitrogen and sulphur suggests the formation of complexes within the cavities. The metal content in the encapsulated complexes was determined by atomic absorption spectroscopy, and the values indicate that very small amount of metal complexes are present in the cavities of the zeoliteY.

**Table. VII.1**

Analytical data of the zeoliteY encapsulated ABT complexes.

| Sample | Elemental Analysis |      |      |         |      |      |      |      |
|--------|--------------------|------|------|---------|------|------|------|------|
|        | % Si               | % Al | % Na | % Metal | % C  | % H  | % N  | % S  |
| YMnABT | 19.24              | 7.82 | 6.26 | 1.33    | 2.64 | 1.48 | 0.57 | 0.79 |
| YFeABT | 19.54              | 7.85 | 6.89 | 1.27    | 2.18 | 1.36 | 0.51 | 0.70 |
| YCoABT | 19.38              | 7.78 | 6.16 | 1.76    | 2.26 | 1.69 | 0.61 | 0.74 |
| YNiABT | 19.02              | 7.71 | 6.45 | 1.20    | 2.29 | 1.63 | 0.67 | 0.77 |
| YCuABT | 19.32              | 7.82 | 6.18 | 1.28    | 2.41 | 1.68 | 0.62 | 0.68 |

Ligand to metal mole ratio in the encapsulated complexes was calculated from the data available in Table.VII.1. Mn(II) , Fe(III), Co(II), Ni(II) and Cu(II) encapsulated ABT complexes in zeoliteY cages agree with 1:2 metal to ligand mole ratio. The negatively charged oxide ion in zeolite framework may be neutralizing the charge on metal ions.

### 7.3.2. Surface area and pore volume analysis.

The reports of surface area and pore volume analyses of parent NaY, metal exchanged zeolites and the zeolite encapsulated ABT complexes are presented in Table.VII.2.

**Table .VII.2**  
Surface area and pore volume of the metal exchanged zeolites and zeoliteY encapsulated ABT complexes.

| Sample | MY                                   |                    | YMABT                                |                    |
|--------|--------------------------------------|--------------------|--------------------------------------|--------------------|
|        | BET surface area (m <sup>2</sup> /g) | Pore volume (cc/g) | BET surface area (m <sup>2</sup> /g) | Pore volume (cc/g) |
| NaY    | 523                                  | 0.3045             | -                                    | -                  |
| YMnABT | 496                                  | 0.2964             | 444                                  | 0.2623             |
| YFeABT | 510                                  | 0.3013             | 458                                  | 0.2728             |
| YCoABT | 490                                  | 0.2986             | 447                                  | 0.2686             |
| YNiABT | 489                                  | 0.2934             | 435                                  | 0.2643             |
| YCuABT | 497                                  | 0.2959             | 448                                  | 0.2620             |

Decrease in surface area and pore volume of metal exchanged zeolites on encapsulation of complexes is shown diagrammatically in Figure VII.2 and VII.3 respectively.

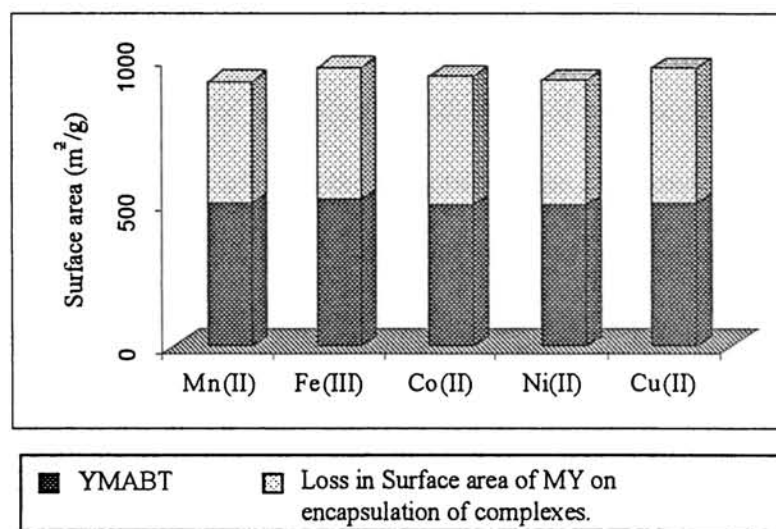


Figure. VII.2. Decrease in surface area of metal exchanged zeolites on encapsulation of ABT complexes.

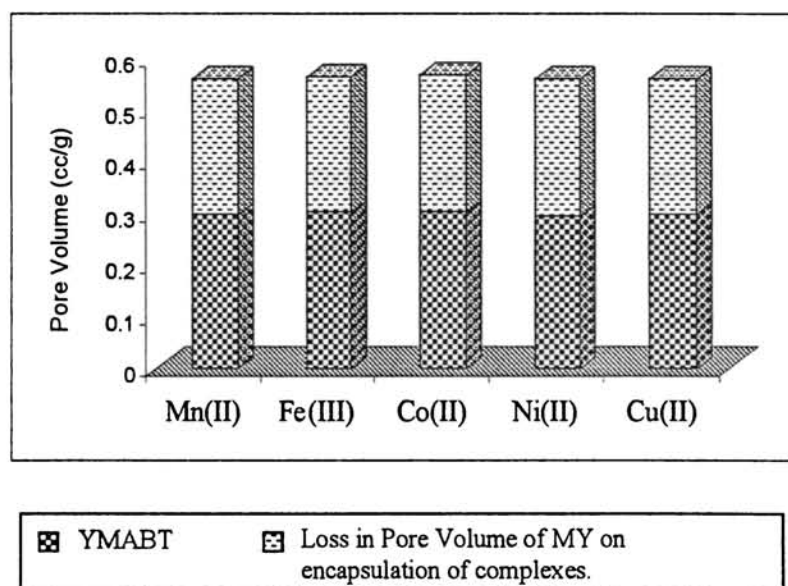


Figure. VII.3. Decrease in pore volume of metal exchanged zeolites on encapsulation of ABT complexes.

A comparison of the surface area and pore volume values of NaY, metal exchanged zeolites and zeolite encapsulated complexes reveals that the decrease in surface area of encapsulated complexes are much higher than the metal exchanged zeolites. This indicates the immobilization of complexes in the voids of zeolite cavities, which is considered as a positive indication of encapsulation of complexes<sup>2</sup>. However the decrease in surface area and pore volume is relatively smaller than that of the encapsulated SBT and VBT complexes. This shows that vacant spaces inside the cavities are greater than SBT and VBT encapsulated complexes, which may be due to smaller size of the ligand molecule when compared to SBT and VBT ligands. The vacant spaces render easy movement of reactant molecules through the voids of zeolites may be one the reason for the high catalytic activity exhibited by the encapsulated ABT complexes (see chapter VIII).

### **7.3.3. X-ray diffraction studies.**

Powder XRD patterns of zeolite encapsulated ABT complexes are presented in Figure.VII.4. Comparison of the patterns with that of the parent zeolite-NaY show that there was no change in peak positions of the diffraction patterns at the angle  $2\theta$ . This reveals that the crystallinity of the zeolite framework has been retained after encapsulation of complexes.

### **7.3.4. Magnetic susceptibility.**

Magnetic moments of the zeolite Y encapsulated ABT complexes were determined by the Gouy method. Diamagnetic contribution due to the ligand and zeolite NaY support was calculated using the unit cell formulae and subtracted from

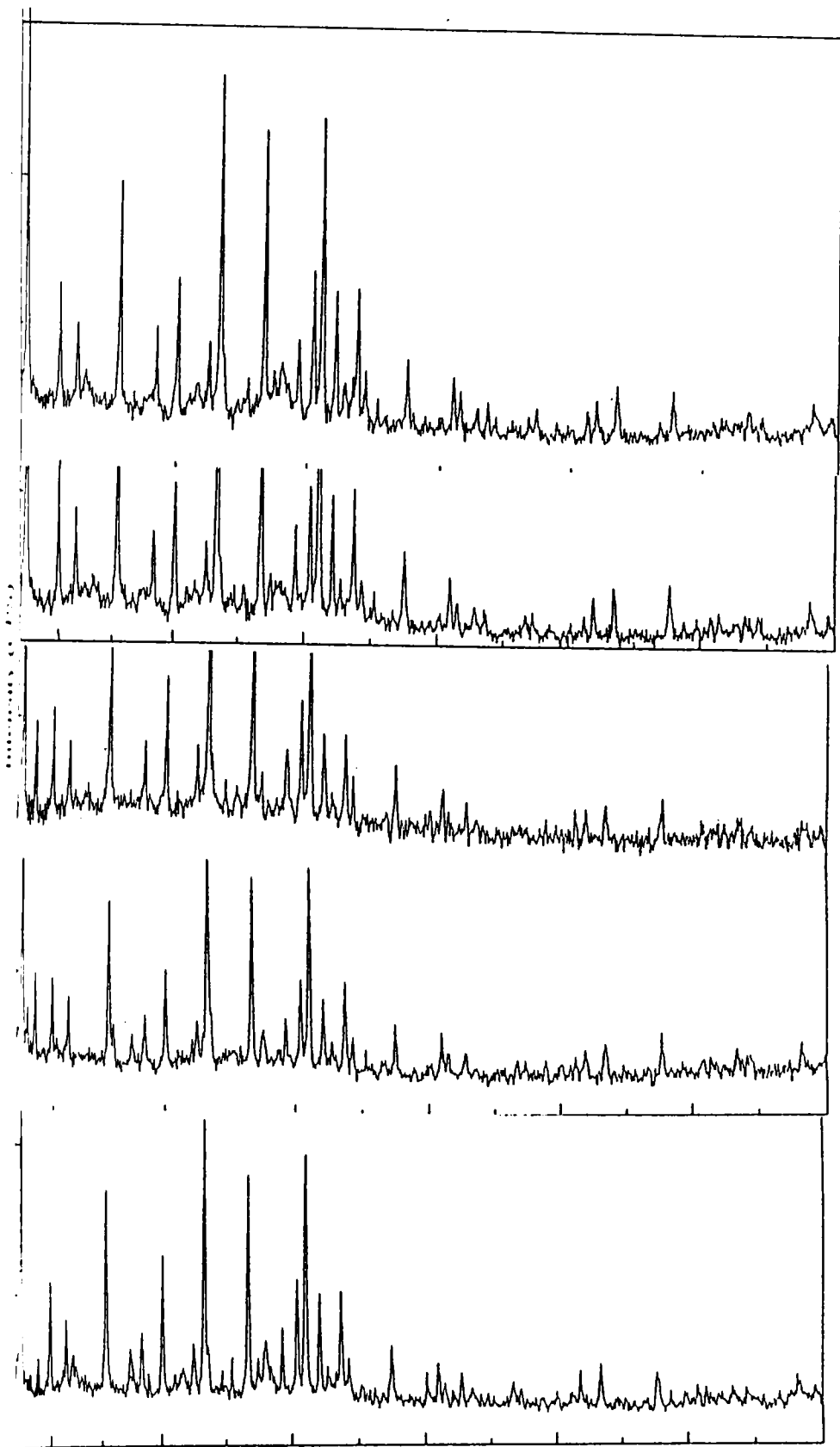


Figure VII.4. XRD Patterns of 1). YMnABT 2). YFeABT  
3). YCoABT 4). YNiABT 5). YCuABT

the molar susceptibility values of the encapsulated complexes. The values so obtained are presented in Table. VII.3.

**Table. VII.3**  
Magnetic moment data  
of the zeolite Y encapsulated ABT complexes.

| Complex | Magnetic moment.<br>$\mu_{\text{eff}}$ (BM) |
|---------|---|
| YMnABT  | 5.8   |
| YFeABT  | 5.8   |
| YCoABT  | 4.1   |
| YNiABT  | <i>diamagnetic</i>                          |
| YCuABT  | 1.8   |

The magnetic moment<sup>3,4</sup> values of 5.8 BM exhibited by the complexes of Mn(II) and Fe(III) indicate that the complexes are in high spin state. The value obtained for Co(II) complexes indicate pseudo tetrahedral arrangement of ligands around the metal ions within the zeolite pores. The diamagnetic nature of Ni(II) and the  $\mu_{\text{eff}}$  value of 1.8 BM for Cu(II) complex agree with a square planar geometry to these complexes. Square planar Cu complexes show magnetic moments near the lower end and distortion from planar structure increases the magnetic moment values.

### 7.3.5. Diffuse reflectance spectra.

Diffuse reflectance mode was used to record the electronic spectra of the encapsulated complexes of 2-aminobenzothiazole. The spectral data are presented in Table .VII.4. Representative spectra are given in Figure.VII. 5.

Spectra of Mn(II) complex exhibits a number of transitions of low intensities. Most of them can be assigned to the overtones and combination bands of stretching and bending modes of water molecules<sup>5</sup>. All the transitions in high spin  $d^5$  complexes are spin forbidden as well as Laporte forbidden. It is difficult to identify  $d-d$  bands of Mn(II) complex of organic ligand<sup>6</sup>. Charge transfer transitions and intraligand transitions of the zeolite encapsulated Fe(III)ABT complex obscures the  $d-d$  transitions and hence assignment of these bands was not possible in this case. In the electronic spectra of cobalt (II) complex two bands at  $13600\text{cm}^{-1}$  and  $12000\text{cm}^{-1}$  appear as multiple structures, which is an indication of tetrahedral geometry of this complex with in the zeolite cavities. This inference agrees with that obtained through magnetic susceptibility measurements.

The complex YNiABT exhibits bands due to  ${}^1A_{1g} \rightarrow {}^1B_{1g}$  transition expected for a square planar molecule. An absorption band in the low energy region,  $11300\text{cm}^{-1}$  exhibited by the CuABT complex indicates a square planar geometry of the complex. Usually tetrahedral Cu(II) complexes are almost invariably distorted<sup>7</sup> and a square planar complex is strongly favoured for the  $d^9$  configuration.

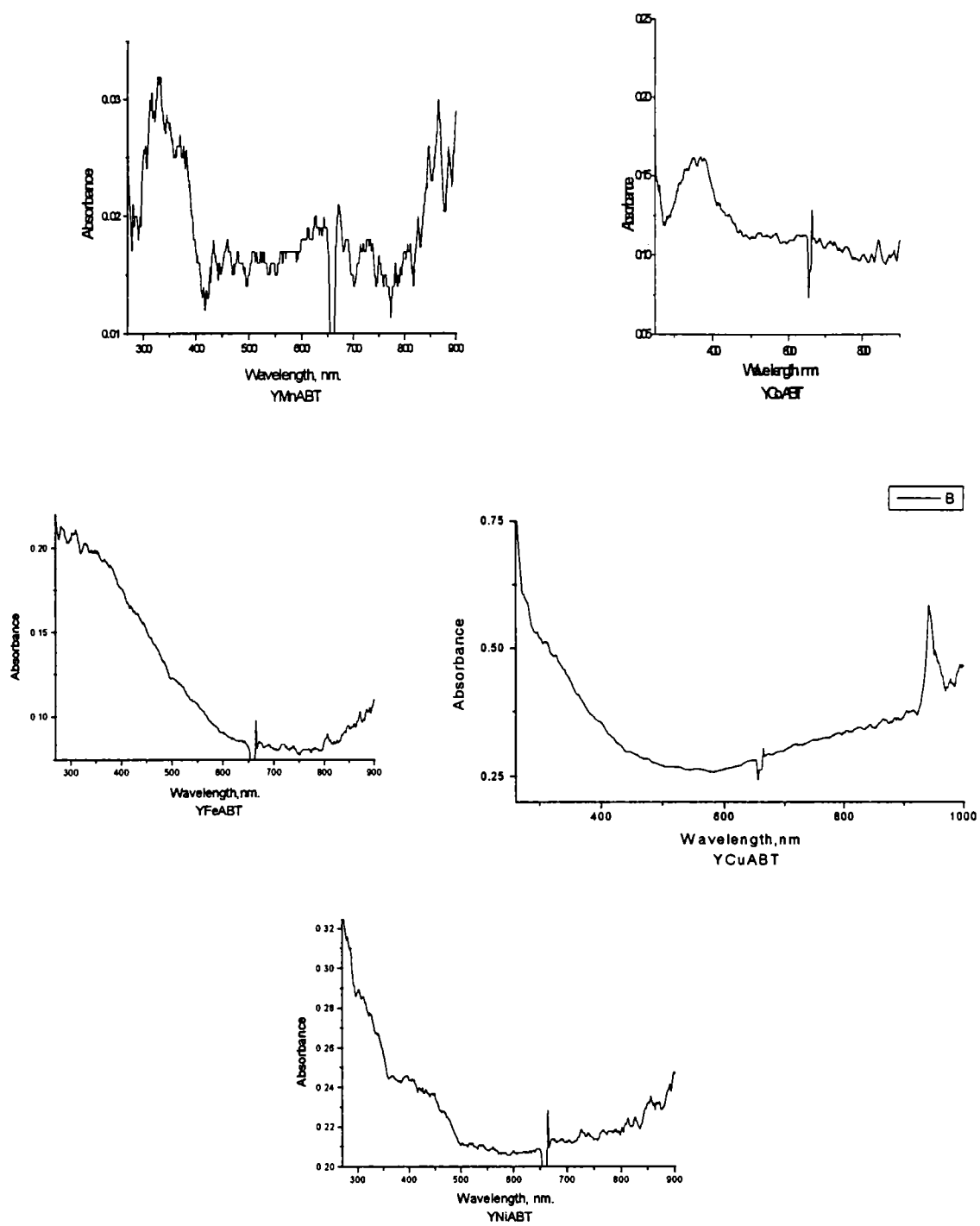


Figure. VII.5. Diffuse reflectance spectra of YMAbT complexes.

**Table. VII. 4**  
Electronic spectral data of  
zeolite Y encapsulated ABT complexes.

| Complex | Abs. Max<br>(cm <sup>-1</sup> ) | Tentative<br>Assignments                                      |
|---------|---------------------------------|---|
| YMnABT  | 31200                           | Charge transfer   |
|         | 26000                           | d-d transition  |
|         | 20000                           | "   |
|         | 16500                           | "   |
| YFeABT  | 32200                           | Charge transfer   |
|         | 15600                           | d-d transition  |
|         | 13850                           | "   |
| YCoABT  | 26320                           | Charge transfer   |
|         | 18200                           | Intra-ligand  |
|         | 13650                           | <sup>4</sup> A <sub>2</sub> → <sup>4</sup> T <sub>1</sub> (P) |
|         | 12000                           | <sup>4</sup> A <sub>2</sub> → <sup>4</sup> T <sub>1</sub> (F) |
| YNiABT  | 31200                           | Charge transfer   |
|         | 26320                           | "   |
|         | 14200                           | <sup>1</sup> A <sub>1g</sub> → <sup>1</sup> B <sub>1g</sub>   |
| YCuABT  | 31250                           | Charge transfer   |
|         | 11300                           | d-d transition  |

Note: Intra-ligand and transitions below 5000 cm<sup>-1</sup> observed in all the samples are not included in the table as they are characteristic of the zeolite lattice.

### 7.3.6. FTIR spectra.

FTIR spectra of the ligand ABT and the zeoliteY encapsulated metal complexes were recorded and given in Figure.VII.6 and Figure.VII.7 respectively. The IR spectra of metal exchanged zeolites are given in Figure.V.7. The information regarding the group frequencies is given in Table. VII.5. The spectral data reveals that most of the bands, which correspond to the ligand vibrations are present in the encapsulated system. It can be assumed that encapsulation of complexes in zeolite cavities has taken place. The two strong bands observed at  $1526\text{cm}^{-1}$  and  $3279\text{cm}^{-1}$  of 2-aminobenzothiazole could be due to  $\nu(\text{C-N})$  and  $\nu(\text{N-H})$  bending vibrations of the amino group at 2-position. A strong broad band at  $\sim 3480\text{cm}^{-1}$  in the encapsulated complexes could probably be due to N-H stretching vibrations coupled with the O-H stretching frequency of the lattice water present in zeolite framework. The band at  $1452\text{cm}^{-1}$ , which is present in the spectrum of the free ligand (due to  $\nu(\text{C-S})$  vibrations) seems to be shifted to  $1398\text{cm}^{-1}$  in all the encapsulated complexes. A sharp peak at  $1182\text{cm}^{-1}$  in the free ligand can be assigned to  $\nu(\text{C-S})$  vibrations of benzothiazole ring<sup>8,9</sup>. There is no indication of this peak in the spectra of the zeolite encapsulated complexes. Probably, the peak might have been obscured by the strong broad zeolite vibrations<sup>10</sup> in the range  $800-1013\text{cm}^{-1}$  (due to the asymmetric T-O stretching frequencies). As this band is absent, it cannot be inferred that sulphur atom of the ABT will not participate in coordination to the metal. In the neat Co(II) and Cu(II) complexes of substituted 2-aminobenzothiazole reported<sup>9</sup>, the metal ion was coordinated to the ligand through the sulphur atom of the thiazole ring. Therefore in this case also there is the possibility of coordination through the S-atom.

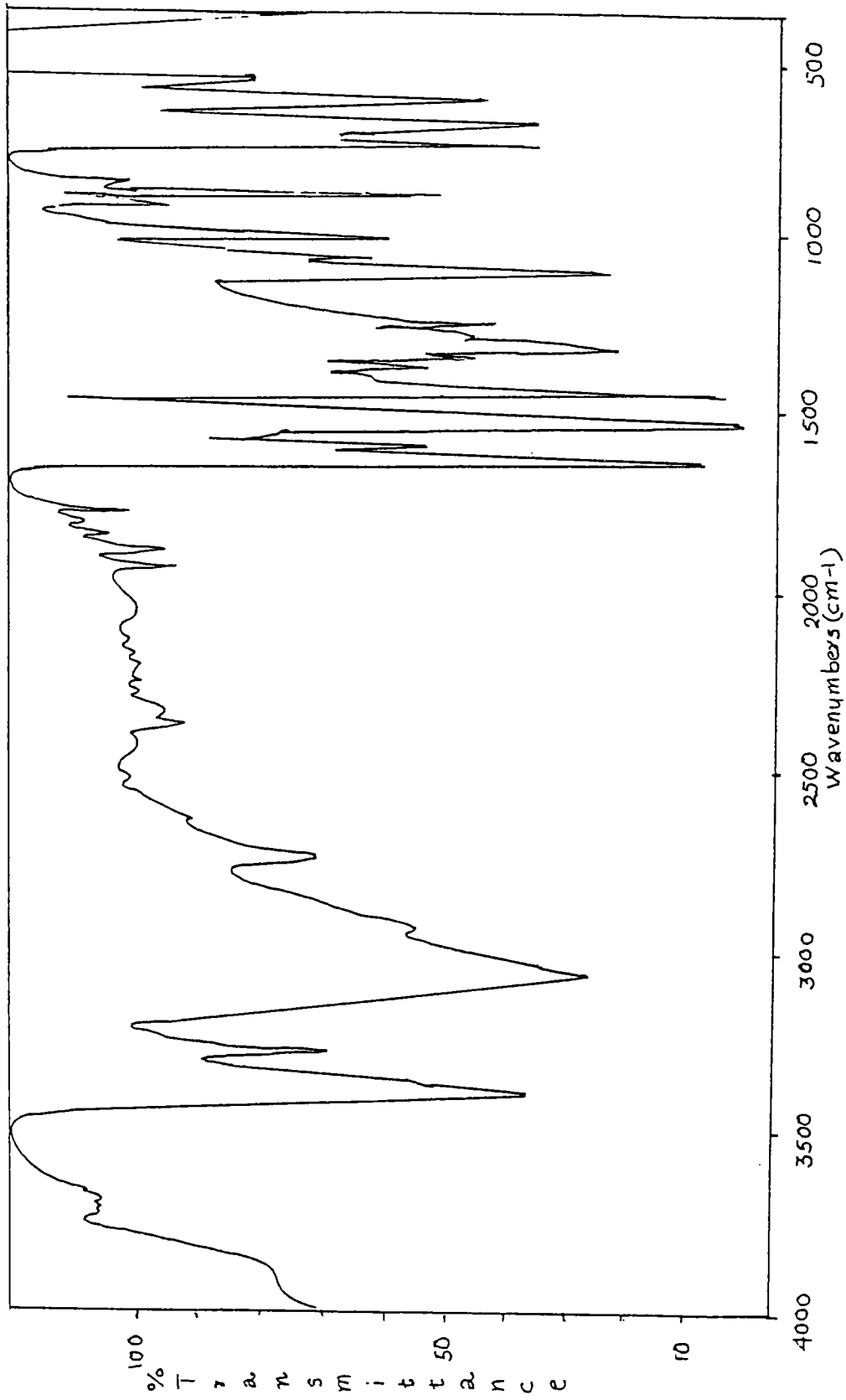


Figure. VII.6. FTIR spectra of ligand- ABT

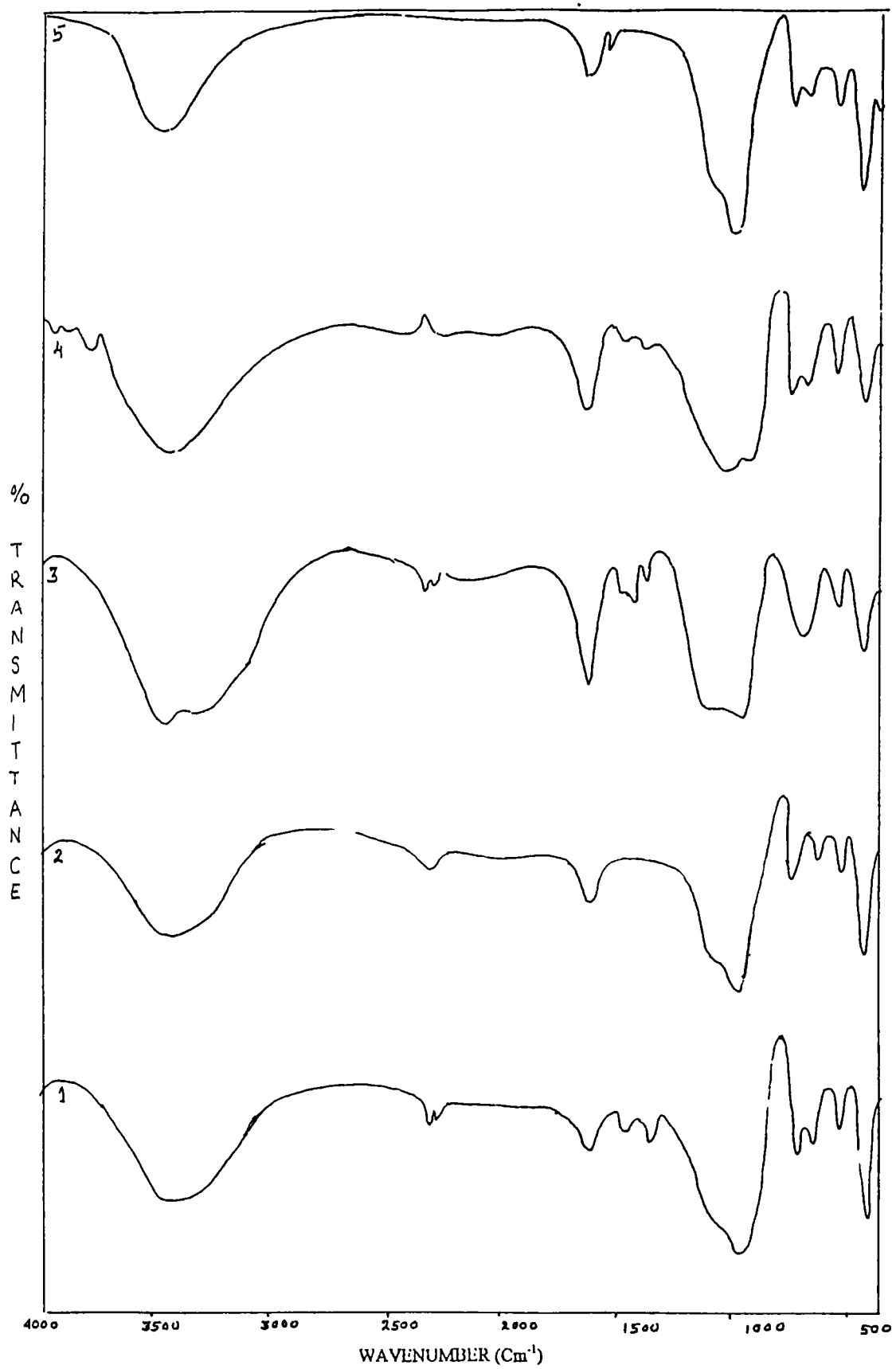


Figure. VII.7. FTIR Spectrum of (1)YMnABT (2) YFcABT (3) YCoABT (4) YNiABT (5) YCuABT.

**Table. VII.5**

Infra Red spectral data ( $\text{cm}^{-1}$ ) of  
zeoliteY encapsulated ABT complexes.

| MY   | ABT  | YMnABT | YFeABT | YCoABT | YNiABT | YCuABT |
|------|------|--------|--------|--------|--------|--------|
| 3453 | 3393 | 3481   | 3488   | 3515   | 3474   | 3462   |
| 1640 | 1647 | 1647   | 1647   | 1647   | 1647   | 1646   |
| -    | 1526 | 1542   | 1560   | 1558   | 1555   | 1566   |
| -    | 1452 | 1398   | 1398   | 1398   | 1398   | 1398   |
| 987  | 1020 | 1013   | 993    | 1007   | 1007   | 990    |
| -    | 892  | -      | -      | -      | -      | -      |
| -    | 852  | -      | -      | -      | -      | -      |
| 764  | 744  | 764    | 764    | 764    | 764    | 758    |
| -    | 636  | 690    | 683    | 697    | 697    | 698    |
| 569  | -    | 575    | 569    | 569    | 569    | 572    |
| 461  | 481  | 461    | 461    | 461    | 461    | 459    |

The bands observed around  $1526 \text{ cm}^{-1}$  and  $3393 \text{ cm}^{-1}$  in the free ligands are due to  $\nu(\text{N-H})$  bending and  $\nu(\text{N-H})$  stretching vibrations of amino group at 2- position respectively<sup>11</sup>. These bands are seen almost at the same position indicating the non-involvement of the exo-cyclic nitrogen in bonding to the metal ion. The band observed at  $1647 \text{ cm}^{-1}$  in free ligand was due to endocyclic  $\nu(\text{C=N})$  vibrations of thiazole ring.

This band remains almost as such in all the encapsulated complexes. Retention of this band at the same position conclusively proves that endocyclic nitrogen atom was not involved in the bond formation with metal ion.

### 7.3.7. EPR spectra.

The X- band EPR spectra of the zeolite supported CuABT complex at LNT was recorded and presented in Figure.VII.8. EPR parameters were calculated from the spectrum and are given in Table. VII.6.

**Table. VII.6**  
EPR spectral data of  
zeoliteY encapsulated CuABT complex.

| EPR parameter                   | YCuABT                                 |
|---------------------------------|--|
| $g_{\parallel}$                 | 2.30                                   |
| $g_{\perp}$                     | 2.05                                   |
| $A_{\parallel}$                 | $158.73 \times 10^{-4} \text{cm}^{-1}$ |
| $g_{\parallel} / A_{\parallel}$ | 144.90cm                               |
| $g_{av}$                        | 2.13                                   |
| $\alpha^2$                      | 0.76                                   |
| $\mu_{eff}$                     | 1.83 BM                                |

Qualitative idea regarding the nature of coordination in metal complexes in zeolites was obtained from EPR parameters. The  $g_{\parallel}$  value of 2.3 for

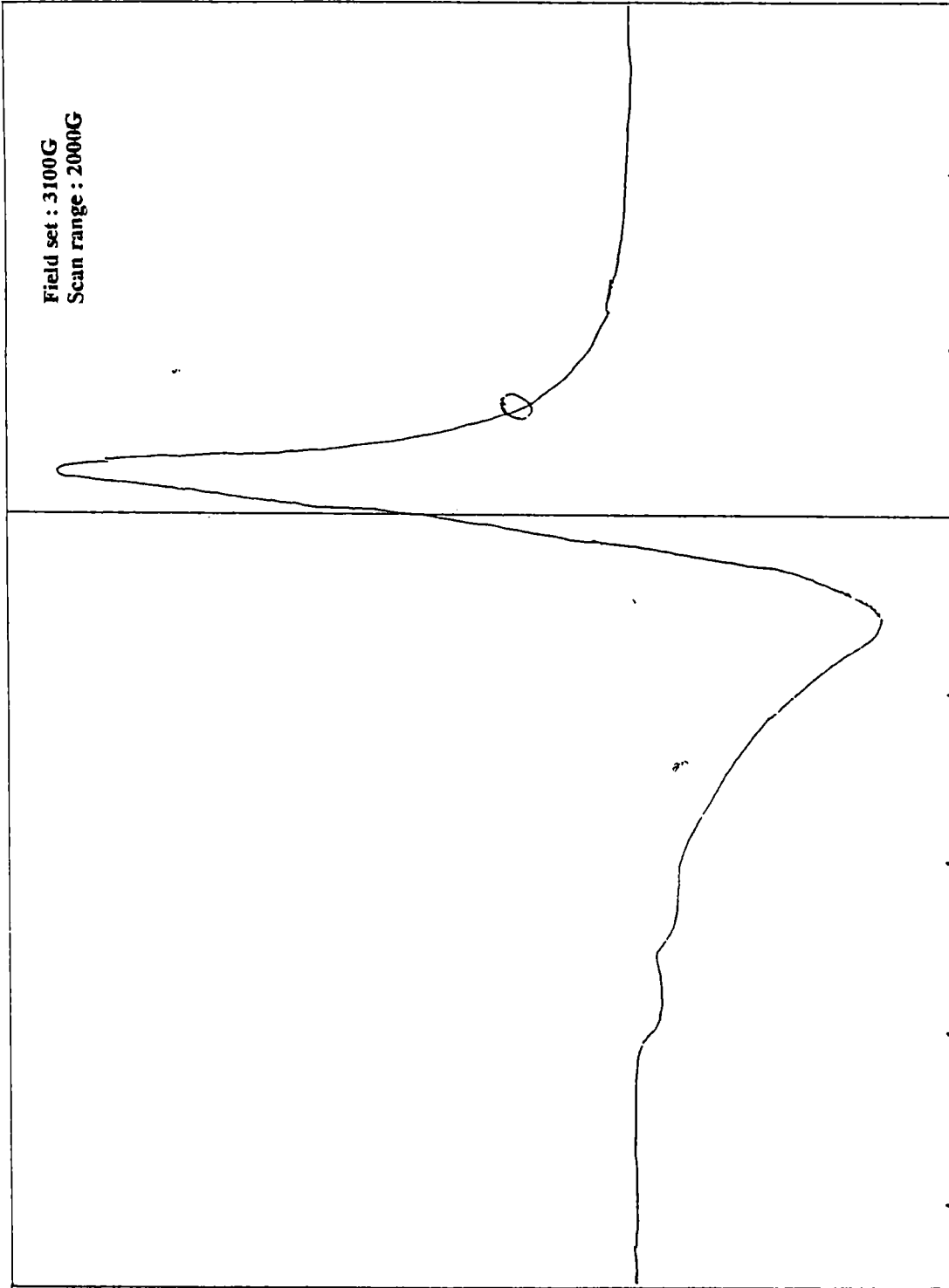


Figure. VII.8. EPR spectrum of YCuABT complex.

YC<sub>u</sub>ABT complex shows that M-L bond in the encapsulated complex is covalent in character. Since  $g_{\parallel} > g_{\perp} > 2.0023$ , the structure of encapsulated complex may be assigned as square planar geometry<sup>12</sup>. In this case,  $g_{\parallel} / A_{\parallel}$  ratio was found to be 144.9 cm<sup>-1</sup>, which is slightly greater than that for the square planar complex<sup>13</sup> and lower than that for a flattened tetrahedral structure. (The  $g_{\parallel} / A_{\parallel}$  ratio lies<sup>13-15</sup> in the range 105- 135 cm<sup>-1</sup> for square planar complexes while for flattened tetrahedral the value is reported to be in the range 150-160cm<sup>-1</sup>). The magnetic moment value calculated from EPR parameters was 1.83 BM, which lies very close to that obtained by Guoy method at room temperature. This value suggests square planar geometry to the CuABT complex in the zeolite matrix. The square planar nature of the complex with vacant coordination sites might be the reason for highest catalytic activity exhibited by this YCuABT system.

### 7.3.8. Thermogravimetric Analysis.

TG curves and data are provided in Figure.VII.9 and Table.VII.7 respectively. Similar decomposition pattern was followed by all the three zeolite encapsulated ABT complexes selected for the thermal study. Two stages of decomposition are noticed. In the first stage of decomposition lattice water was removed. Decomposition of encapsulated complex then takes place in the second stage of decomposition. After this almost nil mass loss was recorded. High thermal stability of zeolite framework and low percentage of metal complexes in zeolite cages was established by the very small (13.5 %) mass loss of the sample from 30°C upto a temperature of 1000°C.

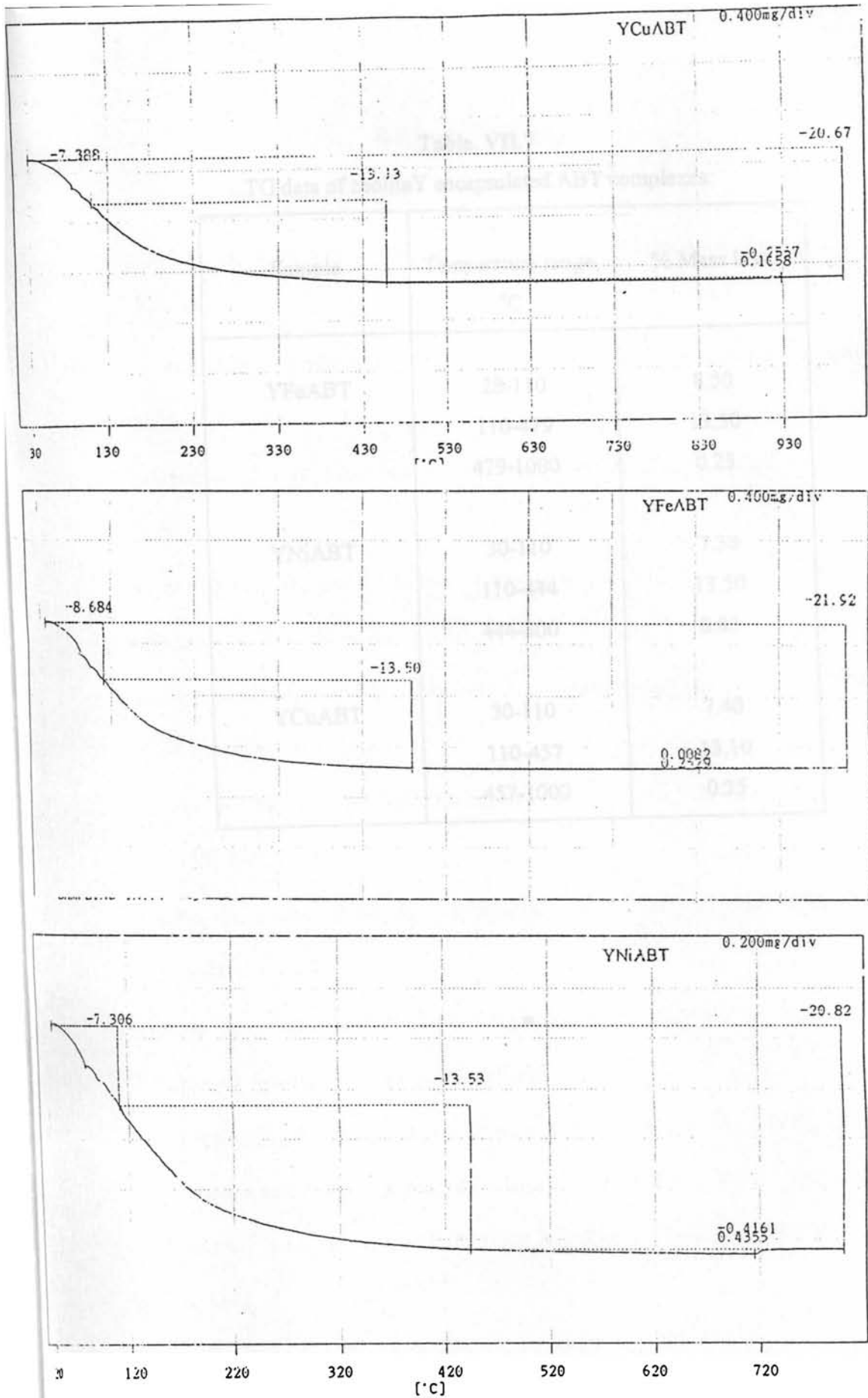


Figure. VII.9. TG curves of YMABT complexes.

**Table. VII.7**

TG data of zeoliteY encapsulated ABT complexes.

| Sample | Temperature range,<br>°C | % Mass loss |
|--------|--------------------------|-------------|
| YFeABT | 28-110                   | 8.50        |
|        | 110-479                  | 13.50       |
|        | 479-1000                 | 0.25        |
| YNiABT | 30-110                   | 7.30        |
|        | 110-444                  | 13.50       |
|        | 444-800                  | 0.85        |
| YCuABT | 30-110                   | 7.40        |
|        | 110-457                  | 13.10       |
|        | 457-1000                 | 0.35        |

\*

## REFERENCES.

1. Jacobs. P.A., *Stud Surf Sci Catal*, 59, (1991), 395.
2. K.J.Balkus Jr and A.G. Gabrieliv., *J.Inclusion Phenom.Mol. Recogn.Chem*, 21, (1995), 159.
3. A. Earnshaw.*Introduction to Magnetochemistry*, Academic press, London, (1968).
4. N.N.Greenwood and A.Earnshaw., “*Chemistry of Elements*”, Pergamon Press, (1984).
5. K.Klier, R.Kellerman and P.J.Hutta., *J.Chem. Phys*, 61, (1974), 4224.
6. J.Ferguson., *J.Chem. Phys*, 40, (1964), 3406.
7. A.B.P.Lever., ‘*Inorganic Electronic Spectroscopy*’, Second Edition, (1984), Elsevier, New York.
8. Rajendra P. Misra, Bipin B. Mahapatra and S.Guru., *J. Ind. Chem. Soc*, 56, (1979), 832.
9. Rajendra P. Misra, Bipin B. Mahapatra and S.Guru., *J. Ind. Chem. Soc*, Vol. LVIII, (1981), 808.
10. Chandra R. Jacob, Saji P. Varkey, Paul Ratnasamy., *Microporous and Mesoporous Materials*, Elsevier, 22, (1998), 465-474.
11. N.C. Mishra, B. B. Mahapatra and S.Guru., *J.Ind.Chem.Soc*, 55 , (1978), 437.
12. U.Sakaguchi and A.W. Addison., *J.Chem.Soc; Dalton Trans*, (1979), 600.
13. R.A.Palmer, W.C. Tennant, M.F. Dix and A.D.Rae., *J.Chem.Soc. Dalton Trans*, (1976), 2345.
14. H.Yokoi., *Bull.Chem.Soc.Japn*, (1974), 47, 3037.
15. H.J.Stoklosa, G.L.Seebach and J.R.Wasson., *J.Phys.Chem.*, 78, (1974), 962.

# CHAPTER VIII



## **Studies on catalytic activity of simple and zeolite Y encapsulated transition metal complexes.**

### **8.1. Introduction**

Worldwide demand for environmentally friendly chemical processes and products requires the development of novel approaches to pollution prevention. Most of these approaches make use of catalysts. Thus, the area of catalysis is often referred to as a 'foundational pillar' to the green chemistry. The search for recoverable catalysts is a challenging problem in homogeneous catalysis involving transition metal complexes. The molecular structure and the homogeneously dissolved nature of these catalysts are the most severe limitations for their application in practical catalysis. The development of innovative separation schemes is utmost importance for homogeneous catalysts. Many attempts have been made to combine the high activity and selectivity of soluble catalysts with the easy separation of them from reaction medium. Immobilization on solid support was one such approach.

Zeolite encapsulated metal complexes have been extensively studied<sup>1</sup> and their catalytic activities have been reported for the oxidation of olefins<sup>2,3</sup>, oxidation of cyclohexane<sup>4</sup>, oxidation of carbon monoxide, acid-base reactions<sup>1</sup>, hydrogen peroxide decompositions<sup>5,6</sup>, oxidation of organic compounds<sup>7,8</sup>, alkylation reactions<sup>9</sup>, epoxidations<sup>10</sup>, hydrocarbon processing and chemical synthesis<sup>11-13</sup>, selective hydrogenation reactions<sup>14</sup> and for hydroxylation reactions<sup>15</sup>.

Catalysis is predominantly known for its importance in product selectivity and process efficiency starting from large scale industrial to small-scale reactions. Today a large number of catalysts are used in all areas of chemical industries and

many national laboratories and academic institutions are pursuing research for the development of new catalysts. With the objectives to develop new oxidation catalysts, some neat and encapsulated transition metal complexes have been synthesized and characterized.

An interesting property of zeoliteY is that it has exchangeable cations allowing the introduction of cations with various catalytic properties. They have pores with one or more discreet sizes, which account for their molecular sieving properties. The encapsulated metal complexes would be expected to behave as their homogeneous analogues as they are isolated from one another on the fixed sites of the sieve.

The catalytic activity of the simple and zeoliteY encapsulated complexes was studied for the following reactions.

- A. Decomposition of hydrogen peroxide.
- B. Oxidation of benzaldehyde by acid potassium permanganate
- C. Oxidation of benzyl alcohol, propan-1-ol and propan-2-ol  
by acid potassium permanganate.
- D. Oxidation of cyclohexanol by hydrogen peroxide.

A and B were used as the test reactions to screen all the prepared complexes for catalytic activity. For convenience, this chapter is divided into the following 4 sections.

VIII-A. Catalytic activity of the simple and zeoliteY encapsulated complexes on decomposition of hydrogen peroxide.

VIII-B. Catalytic activity on the oxidation of benzaldehyde by acid potassium permanganate.

VIII-C. Catalytic activity on the oxidation of benzyl alcohol, propan-1-ol and propan-2-ol by acid potassium permanganate.

VIII-D. Catalytic activity on partial oxidation of cyclohexanol to cyclohexanone by hydrogen peroxide.

### **VIII -A. Catalytic activity of the simple and zeoliteY encapsulated complexes on decomposition of hydrogen peroxide.**

#### **8.A.1. Introduction.**

Hydrogen peroxide is widely accepted as a green oxidant as it is relatively nontoxic and breaks down readily to benign byproducts. Use of nature's major oxidants, oxygen and hydrogen peroxide, could reduce the environmental burden of pollutants based on oxidation processes. The availability of effective catalysts increases the potential of these oxidants in clean up applications for eliminating the toxic pollutants. In recent years ligand design strategy<sup>16</sup> has succeeded in attaining efficient and selective catalysts for activating hydrogen peroxide in an ideal manner for greening chemical technologies as well as for cleanup processes. Craig Jones<sup>17</sup> has written an excellent monograph on hydrogen peroxide chemistry. Hydrogen peroxide is also an important reagent in numerous enzymatic oxidations.

Decomposition of hydrogen peroxide has been investigated extensively as a homogeneous reaction catalyzed by of transition metal ions and their complexes<sup>18</sup> as well as by enzyme such as catalase<sup>19</sup>. It was used in electrolysis of water for the production of oxygen<sup>20</sup> and also in the oxidation of organic substrates<sup>21</sup>. Various copper compounds have been investigated as models for enzymes by testing their

ability to decompose hydrogen peroxide in basic aqueous solution<sup>22</sup>. The catalytic activity of ethylene diamine copper(II) complexes for this reaction and for thirteen metal ions encapsulated in zeolite Y matrix was reported<sup>5,6,23</sup>.

## **8.A.2. EXPERIMENTAL.**

### **8.A.2.1. Hydrogen peroxide solution.**

Hydrogen peroxide solution was prepared in the reaction flask itself from commercially available hydrogen peroxide solution (Merck, 30%) which was kept in a dark polyethylene bottle preserved in refrigerator to retard decomposition. The hydrogen peroxide content was determined by titration using potassium permanganate as prescribed in literature<sup>24</sup>.

### **8.A.2.2. Catalysts.**

Neat and zeolite Y encapsulated complexes of Mn(II), Fe(III), Co(II), Ni(II) and Cu(II) with the ligands, SBT and VBT and the zeolite Y encapsulated complexes of ABT were screened for the catalytic activity towards the decomposition of hydrogen peroxide. Details regarding the preparation and characterization of these complexes are presented in respective chapters. Catalysts are dried in an air oven before use.

### **8.A.2.3. Apparatus and Procedure.**

A gas burette as shown in Figure. VIII.A.1 was used for the experiment for measuring the volume of oxygen liberated during the decomposition of hydrogen peroxide in the presence of catalysts. It consists of a graduated U tube having a

stopper at the bottom. Both the arms of the gas burette were filled with ~ 20% NaCl solution, which was acidified with dilute HCl and was coloured

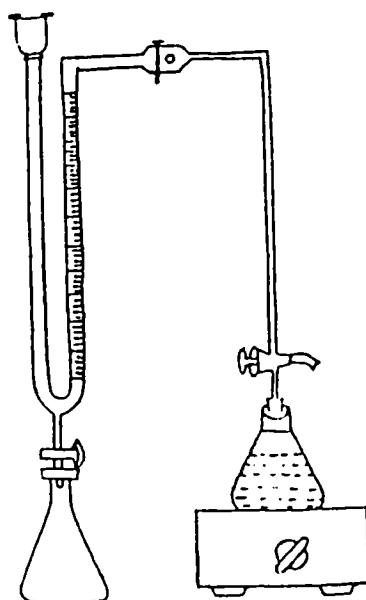


Figure.VIII.A.1. Experimental set up for monitoring the decomposition of  $H_2O_2$

orange red with methyl orange indicator. To the reaction flask of 100ml capacity containing a magnetic paddle, distilled water (18mL) and 30% hydrogen peroxide solution (2mL) were added using a graduated pipette. The reaction flask was placed in a water bath for 15 minutes to attain the equilibrium room temperature. The catalyst (50 mg) was accurately weighed into a plastic float and placed above the hydrogen peroxide solution in the reaction flask. One arm of the gas burette was connected to the reaction flask through a rubber pressure tube. The solution level in both the arms of the gas burette was equalized such that the arm attached to the reaction flask read zero by adding or withdrawing solution from the gas burette. On starting the magnetic stirring, the catalyst in the plastic float gets dispersed in to  $H_2O_2$  solution. A stopwatch was started simultaneously when the catalyst was just dispersed in  $H_2O_2$  solution. As

time passes, oxygen evolved was collected by the downward displacement of NaCl solution in the gas burette. The evolution of oxygen during the course of decomposition of hydrogen peroxide was monitored as a function of time at intervals of ten minutes after equalizing the solution level at both arms of the gas burette. The reaction was carried out for one hour. The data on the evolution of oxygen during the decomposition of hydrogen peroxide per hour is shown in Table. VIII.1.

To know the self-decomposition of hydrogen peroxide under identical conditions, a blank study was conducted. This was carried out by studying the hydrogen peroxide decomposition in exactly the same way as has been done for the catalytic activity study but with out adding any catalyst. Negligible volume of oxygen was collected in this case. Therefore evolution of oxygen (see Table.VIII.1) was obviously due to the activation of decomposition by the added catalysts. The volume of oxygen gas liberated while using NaY or metal exchanged zeolites were also negligible.

It is noted that addition of a drop of very dilute sodium hydroxide to the hydrogen peroxide solution containing catalyst increases the decomposition rate appreciably. However, addition of a drop of pyridine to the solution containing catalyst decreases the rate of decomposition. Probably, the active sites might have been blocked by pyridine and were made unavailable for interaction with hydrogen peroxide. Recycling test was also conducted with the catalysts. For this purpose, the catalyst was filtered from the reaction media usig a G4 sintered crucible, and washed with acetone, dried and was used again for the decomposition reaction. The catalyst maintained almost the same activity after recycling. The colour of the catalyst was

also seen to be preserved. This indicates that the complexes are not leached out of the zeolite cavity and the sites are active for the catalysis reaction.

### 8.A.3. Results and Discussion.

The volume of oxygen liberated during 1hr period of the decomposition reaction in the presence of complexes are presented in the Table.VIII.1. Comparison of catalytic activities of the encapsulated complexes with that of the neat complexes is shown as a bar diagram in Figure.VIII.A.2.

On comparison of the simple and zeoliteY encapsulated complexes, it can be seen that the catalytic activity of simple complexes are almost same as that of the zeoliteY complexes. However, a close examination would reveal that the zeolite encapsulated complexes are more active than the simple complexes, as the metal ion concentrations per unit mass of zeoliteY complexes in the reaction mixture are very low when compared with that of the simple complexes. On comparing the activities of different metal ions of the same ligand, it can be seen that Co(II) complexes are found to be more active than other metal ion complexes. Ni(II) complexes are least active while Mn(II) and Fe(III) are moderately active.

The activity of the metal complexes varies as, Co(II) complex > Cu(II) complex > Fe(III) complex > Mn(II) complex > Ni(II) complex. When the influence of various ligands on the activity data were analyzed, it can be seen that among the simple complexes VBT complexes are far more active than the SBT complexes.

**Table.VIII.1**  
**Catalytic activity of the complexes in the**  
**decomposition of hydrogen peroxide.**

**Reaction conditions:**

Catalyst weight = 50mg      H<sub>2</sub>O<sub>2</sub> 10% = 20ml

Temperature = 30 ± 0.1°C      Duration = 1 hour.

| Ligand/<br>Encapsulated<br>Ligand<br>(L) | Volume of oxygen liberated (mL) on interaction with the<br>complexes of L with. |         |        |        |        |
|--|---|---------|--------|--------|--------|
|  | Mn(II)  | Fe(III) | Co(II) | Ni(II) | Cu(II) |
| YVBT                                     | 1.7   | 2.2     | 6.5    | 1.6    | 6.0    |
| YSBT                                     | 1.9   | 2.6     | 6.8    | 1.3    | 3.4    |
| YABT                                     | 1.8   | 2.9     | 7.0    | 1.5    | 6.9    |
| VBT                                      | 2.8   | 2.9     | 7.5    | 1.2    | 7.2    |
| SBT                                      | 2.3   | 2.5     | 5.6    | 1.9    | 4.1    |

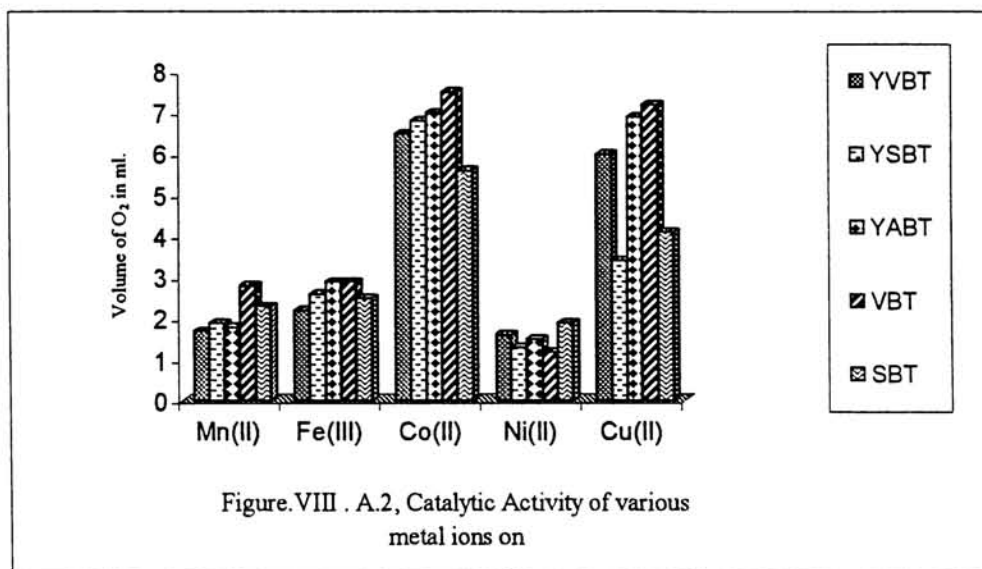
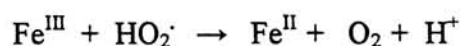
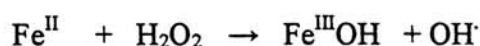


Figure.VIII . A.2, Catalytic Activity of various metal ions on

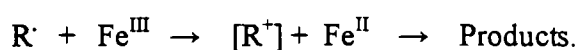
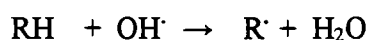
Among the zeolite Y complexes the order of activity in terms of ligands are YABT > YVBT > YSBT.

Hydrogen peroxide is a green alternative to conventional oxidants. The mild oxidizing action of hydrogen peroxide is considerably enhanced by the presence of certain metal catalysts<sup>25-27</sup> of which the best known was the Fenton's reagent. The complicated Fenton's chemistry occurs when metal ions such as ferrous or ferric iron interact with peroxides, especially in water. The reaction is characterized by the liberation of oxygen via a free radical chain process involving hydroxyl radicals as transient intermediates. The mechanism was proposed as follows:



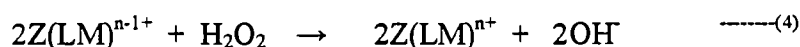
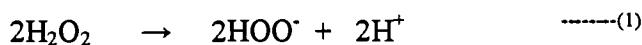
The hydroxyl radical is a potent H-atom abstractor since the O-H bond of water is much stronger than most C-H bonds. Consequently, most abstractions of H

from carbon by OH $\cdot$  are exothermic. Thus, Fenton's chemistry is superb for sterilisation purposes and for the oxidation of organic compounds. In presence of organic substrates, the hydroxyl radicals produce organic free radicals, which can undergo dimerization, oxidation by Fe(III) or reduction by Fe(II) as given below.

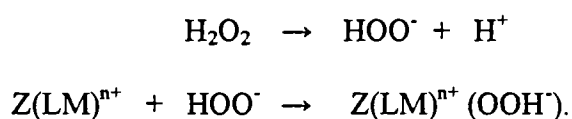


A number of metal complexes<sup>25</sup> including those of copper, cobalt, manganese and silver also decompose hydrogen peroxide by the same mechanism facilitating the homolytic fission of the peroxide bond. Probably a similar mechanism may be operating in the decomposition reaction involving the simple complexes of VBT and SBT.

For modern technological applications, one may need catalysts, which can be easily separated from the reaction systems. It is now widely recognized that one such method is heterogenising the homogeneous catalysts. Zeolite encapsulated transition metal complexes are reported<sup>28-30</sup> to be much more active than their homogeneous analogues. In this case of zeolite encapsulated complexes, the proposed mechanism involves a radical chain reaction in which the catalyst increases the rate of initiation of HOO radical as follows:



The catalytic activity of metal ion increases as its redox potential decreases within a particular range and then decreases as the rate determining step is shifted from eqn.2 to 4 as per the above mechanism<sup>31</sup>. Another mechanism involving the coordination sphere of the metal ion has also been reported<sup>25</sup>. The decomposition reaction involving the formation of intermediate peroxo species  $(LM)^{n+}(OOH^-)^{32,33}$  was also suggested as a probable mechanism for zeolite encapsulated complexes.



The information obtained from the present study was not enough to propose any mechanism. The characterization data shows that Mn(II) and Fe(III) complexes are octahedral in structure. The activities of these complexes are found to be low as expected for octahedral complexes. Co(II) complexes are tetrahedral in nature. The high activity for these complexes may be due to the availability of vacant coordination sites for interaction with  $H_2O_2$ . The lowest activity is exhibited by the Ni(II) complexes and is expected from the redox potential values; as it would be difficult to convert Ni(II) to Ni(I). The Cu(II) complexes exhibit better catalytic activity, which may be due to the availability of vacant coordination sites (square planar structure) and also due to the fact that Cu(II) can be easily converted to Cu(I).

As greater activity is observed for the ABT and VBT complexes, it is assumed that the coordination of S atom to the metal might help the redox reaction:  $M^{n+}$  to  $M^{(n-1)+}$ . YABT complexes are found to have the highest activity. Lowest steric hindrance in the case of ABT complexes (smaller in size compared to VBT and SBT)

become favourable for the easy diffusion of the reactant molecules into the cages. This may help in having greater activity compared with Schiff base complexes.

## **VIII – B. Catalytic activity on oxidation of benzaldehyde by acid potassium permanganate.**

### **8.B.1. Introduction.**

Transition metal complexes have been widely used for various oxidation reactions of industrial and environmental importance. An attempt has been made to study the effect of simple and zeoliteY encapsulated complexes of Mn(II), Fe(III), Co(II), Ni(II) and Cu(II) in the oxidation of benzaldehyde using acid potassium permanganate. Oxidation of benzaldehyde to benzoic acid by acid  $\text{KMnO}_4$  takes place at ambient temperatures. Results suggest that all the complexes undoubtedly increase the speed of oxidation of benzaldehyde to benzoic acid by acid  $\text{KMnO}_4$ . Details regarding this study are presented in this section.

### **8.B.2. EXPERIMENTAL.**

#### **8.B.2.1. Potassium permanganate solution.**

Stock solution of potassium permanganate was prepared and preserved according to the standard procedure given in the literature<sup>24</sup>. Potassium permanganate (0.1g, AR) was dissolved in 800ml distilled water taken in a 1litre beaker and boiled for 30minutes. Solution was then cooled to room temperature and filtered through a G-

4 sintered glass crucible to remove manganese dioxide present in it. The solution so obtained was preserved in a well-stoppered brown bottle in a cool and dark place to prevent further aerial oxidation. It was estimated spectrophotometrically at 546nm using the molar absorption coefficient  $2.4 \times 10^3 \text{ litre mol}^{-1} \text{ cm}^{-1}$  and was found that the concentration of the solution was above  $8 \times 10^{-4} \text{ mol dm}^{-3}$ .

#### **8.B.2.2. Perchloric acid solution.**

A stock solution of perchloric acid (0.2 M) was prepared by diluting the required volume of commercially available 60% aqueous solution of perchloric acid. This solution was standardized by using standard  $\text{Na}_2\text{CO}_3$  solution as given in literature<sup>24</sup>. This was then diluted directly in the reaction flask to get 0.05M solution in the reaction mixture.

#### **8.B.2.3. Benzaldehyde.**

Commercially available benzaldehyde was of analar grade and was used as such for the catalytic activity study.

#### **8.B.2.4. Catalysts.**

All the simple and zeolite Y encapsulated transition metal complexes of the metal ions; Mn(II), Fe(III), Co(II), Ni(II) and Cu(II) with the Schiff base ligands, SBT and VBT and the zeolite Y encapsulated complexes of ABT were screened for the catalytic activity towards the oxidation of benzaldehyde. The catalytic activities of these were also compared with that of the metal ion exchanged zeolite Y matrix.

Information regarding the preparation and characterization of these complexes is given in earlier chapters. Catalysts were dried in an air oven before use.

#### **8.B.2.5. Apparatus.**

A Shimadzu double beam spectrophotometer UV-160A (Japan) with 1 cm quartz cuvette was used for absorption measurements.

#### **8.B.2.6. Procedure.**

The reaction was carried out at a constant temperature of  $30.0 \pm 0.1^\circ\text{C}$ . In a reaction flask, distilled water (2.5mL), perchloric acid (2.5mL,  $0.2 \text{ mol dm}^{-3}$ ), potassium permanganate solution (5mL,  $8 \times 10^{-4} \text{ mol dm}^{-3}$ ) were taken and shaken well for uniform concentration and the solution was placed in a thermostat. After the solution had attained the temperature of the bath, 3mL of the solution was pipetted out into the quartz cuvette in the spectrophotometer. The reaction was initiated by transferring 2mg of the catalyst into the cuvette. A stopwatch was started when the catalyst just touches the solution. Benzaldehyde (0.5mL) was then added into the cuvette. The oxidant substrate mole ratio was 1/100. The stopwatch was stopped when the first reading was monitored on the screen of the spectrophotometer. This was needed to know the time of the initial reading monitored in the spectrophotometer. The absorbance at this time was noted. The spectrophotometer was initially adjusted to get the value of absorbance at every one minute at 546nm. The progress of the reaction with respect to time was monitored spectrophotometrically by measuring the absorbance of  $\text{KMnO}_4$  at 546nm, where  $\text{KMnO}_4$  has maximum absorbance and all

other reactants and the product involved have negligible absorbance. It is found that the absorbance decreases with time.

Absorbances versus time plots were computed by curve fitting method. A software called 'Axum' (Trimetrix,1989) was used for this purpose. The initial rate method was employed to determine the rate of oxidation of benzaldehyde. The absorbance versus time data were fitted into a polynomial of the form

$$C = a_0 + a_1t + a_2t^2 + \dots$$

using polynomial regression method. From the plots so obtained, initial slopes were computed. Initial slopes were divided by molar absorption coefficient of  $\text{KMnO}_4$  to get the initial rates. The initial rates so obtained were then converted to the initial rates per metal ion concentration (metal ion concentration of various catalysts in the reaction mixture were obtained from the analytical data for the complexes) in the reaction mixture, for comparing the catalytic activity of the simple and zeoliteY encapsulated complexes. These values for various catalysts are presented in Table. VIII.2.

A blank study was carried out between acid  $\text{KMnO}_4$  and benzaldehyde in the absence of the catalyst to compare the rate of oxidation. The initial rate of the blank reaction is also given in the table. The initial rate of this reaction was found to be very much low in the case of blank when compared with the reaction in presence of catalyst.

### 8.B.3. Results and Discussion.

The simple  $\text{Mn(II)}$ ,  $\text{Fe(III)}$ ,  $\text{Co(II)}$ ,  $\text{Ni(II)}$  and  $\text{Cu(II)}$  complexes of SBT and VBT and the zeoliteY encapsulated complexes of the above two Schiff bases and 2-

aminobenzothiazole was screened for catalytic activity for the oxidation of benzaldehyde by acid potassium permanganate. The results so obtained are given in Table.VIII.2.

**Table.VIII. 2.**

**Catalytic activity of the complexes for oxidation of benzaldehyde by acid potassium permanganate.**

**Reaction conditions:**

$$[\text{KMnO}_4] = 4.0 \times 10^{-4} \text{ mol dm}^{-3}; \quad [\text{HClO}_4] = 5.0 \times 10^{-2} \text{ mol dm}^{-3}$$

Benzaldehyde = 0.5 ml; Catalyst = 2 mg, temperature =  $30.0 \pm 0.1^\circ \text{C}$ .

| Ligand/<br>Encap<br>sulated<br>ligand | Initial rate $\times 10^4 \text{ mol dm}^{-3} \text{ min}^{-1}$ |         |        |        |        |
|---------------------------------------|---|---------|--------|--------|--------|
|                                       | Mn(II)  | Fe(III) | Co(II) | Ni(II) | Cu(II) |
| Y ABT                                 | 6.3   | 6.5     | 7.6    | 4.4    | 8.2    |
| Y SBT                                 | 4.5   | 5.2     | 5.5    | 3.3    | 6.4    |
| Y VBT                                 | 3.9   | 4.5     | 4.9    | 3.1    | 5.0    |
| Y ZY                                  | 2.0   | 3.5     | 2.7    | 1.5    | 3.1    |
| VBT                                   | 1.3   | 1.2     | 1.5    | 1.1    | 1.6    |
| SBT                                   | 1.1   | 1.0     | 1.1    | 0.9    | 1.1    |
| BLANK                                 | 0.7   |         |        |        |        |

## Catalytic activity of Mn(II) complexes.

All the five Mn(II) complexes (two sets of simple and three sets of zeolite Y systems) are detected to be catalytically active towards the oxidation of benzaldehyde. The catalytic activities of zeolite Y encapsulated complexes were compared with that of their homogeneous analogues as well as with that of the metal exchanged zeolite Y matrix. All the three sets of heterogeneous zeolite Y encapsulated complexes exhibit more catalytic activity than that of the simple complexes. YMnABT has highest catalytic activity among the manganese(II) complexes (Figure VIII.B.1)

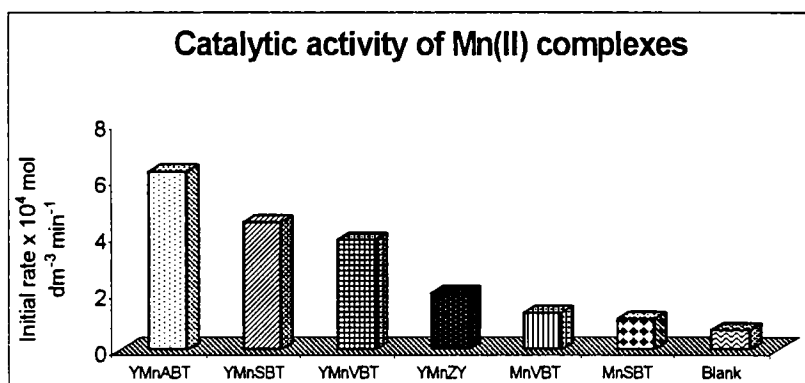


Figure. VIII.B.1. Catalytic activity of Mn(II) complexes.

It can be seen from the figure that the encapsulated complexes could enhance the catalytic activity to higher extent than the metal exchanged zeolite Y system. The order of catalytic activity among the five complexes and the metal exchanged zeolite Y is,



The study shows that heterogeneous Mn(II) complexes are effective catalysts for the oxidation of benzaldehyde by acid potassium permanganate. In the case of homogeneous catalysts MnVBT is more active than SBT complexes.

### Catalytic activity of Fe(III) complexes.

Initial rates of catalytic activity of simple Schiff base complexes and encapsulated complexes of Fe (III) are given in Table.VIII.2. The complex FeABT, is the most active among the Fe(III)complexes. All the simple complexes and the encapsulated complexes exhibit enhanced rate of oxidation of benzaldehyde

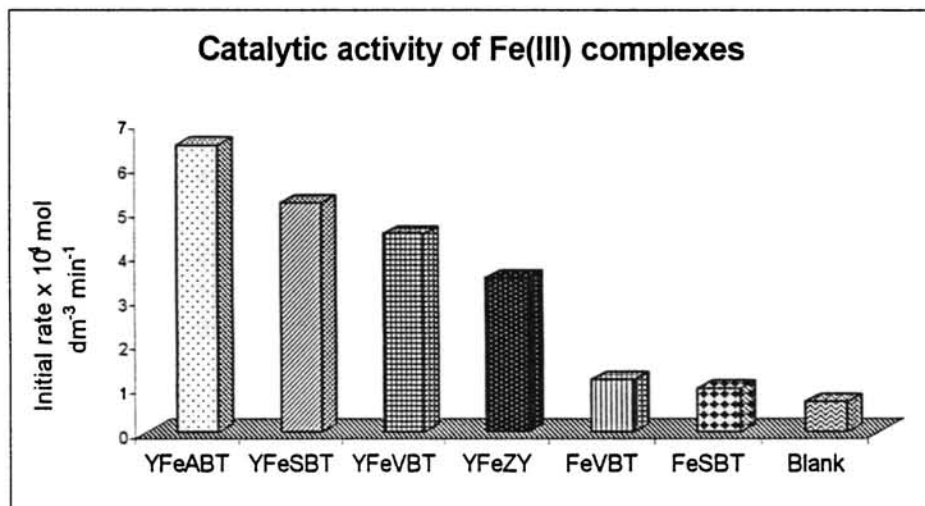


Figure VIII.B.2. Catalytic activity of Fe(III) complexes.

compared to the uncatalysed blank reaction. The catalytic activity can be expressed in decreasing order as:



## Catalytic activity of Co(II) complexes.

Encapsulated Co(II) complexes have higher catalytic activity than the encapsulated complexes of Mn(II), Fe(III) and Ni(II) and the simple complexes of cobalt. They have far higher catalytic activity than the metal exchanged zeolites and hence the ligand has a crucial role in tuning the catalytic nature of the complexes. The order of activity is,

YCoABT > YCoSBT > YCoVBT > YCoZY > CoVBT > CoSBT.

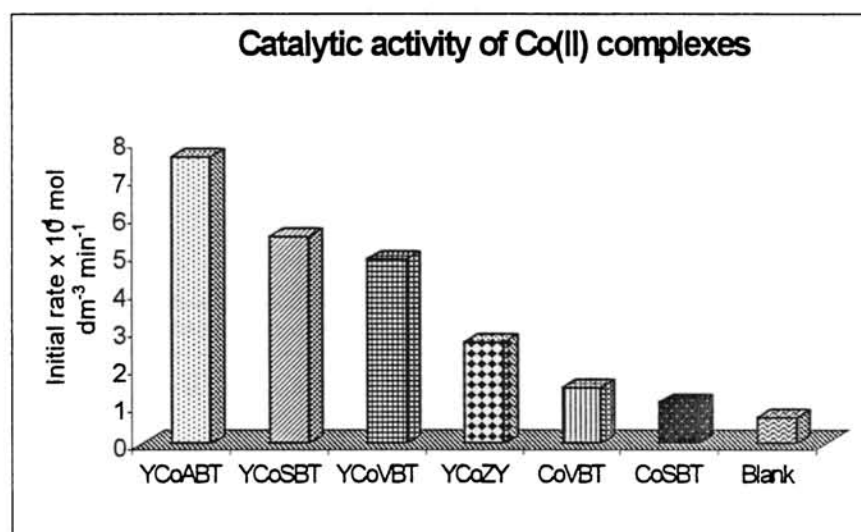


Figure VIII.B.3. Catalytic activity of Co(II) complexes.

Of all the encapsulated complexes, the encapsulated complex YCoABT, exhibit higher activity than all the thirty catalysts screened for catalytic activity, except YCuABT.

### Catalytic activity of Ni(II) complexes.

All the Ni(II) complexes exhibit unexpected catalytic activity for the oxidation reaction. Here also YNiABT is the highest active among Ni(II) complexes. The activity of the complexes is seen to be modified by the presence of ligands on metal ion in the molecular sieve. Their catalytic activity is lower than that of the other metal ion complexes in the zeolite cage.

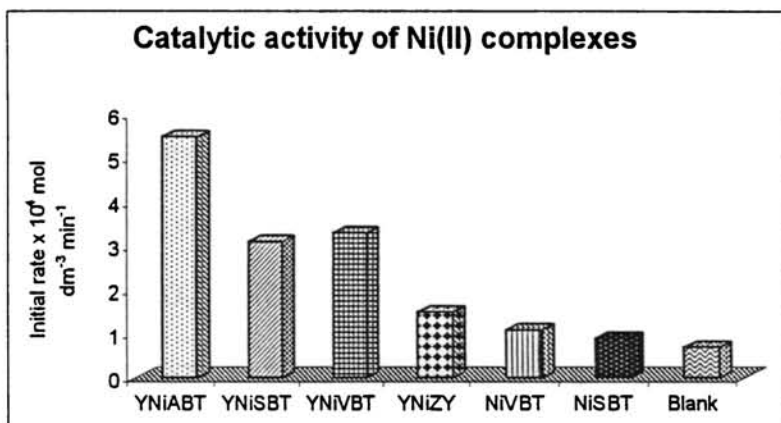


Figure. VIII.B.4. Catalytic activity of Ni(II) complexes.

The order of activity based on initial rate measurement is,



### Catalytic activity of Cu(II) Complexes.

ZeoliteY encapsulated Cu(II) complexes have greater catalytic activity than that of the other metal ions. Among all the five Cu(II) complexes and the Cu(II) exchanged zeoliteY, YCuABT is more active (~1.5 fold times) than the other complexes in enhancing the oxidation of benzaldehyde by acid potassium permanganate

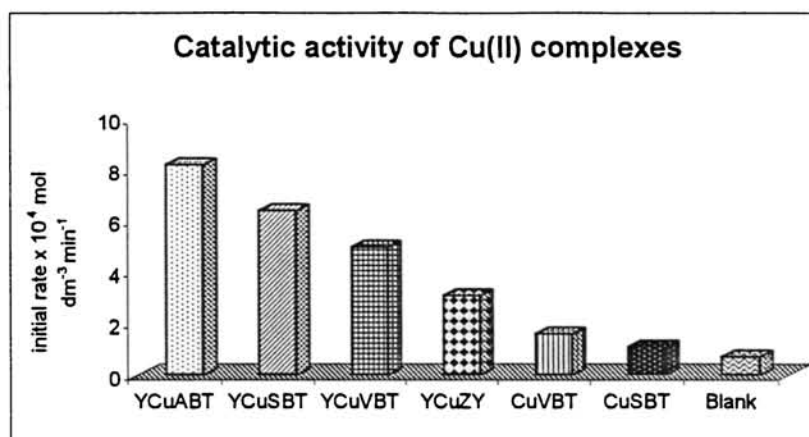


Figure. VIII.B.5. Catalytic activity of Cu(II) complexes.

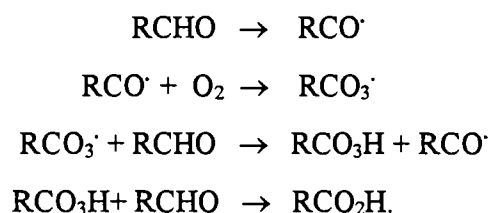
The order of catalytic activity based on initial rate measurements is:



Aldehydes undergo apparent oxidation even at ambient temperatures. Although the reaction occurs in the absence of a catalyst, Cr(VI) compounds, permanganate ion,  $\text{MnO}_2$ , Co(III) or Cu(II) salts are often added to catalyze the reaction<sup>34,35</sup>. Metal catalyzed oxidation of benzaldehyde gives benzoic acid in virtually quantitative yields.

Transition metal complexes are used as homogeneous catalysts in a variety of organic oxidation reactions. Attempts have been made to immobilize these complexes on insoluble support such as zeolite cavities for the purpose of industrial applications. These supports are believed to induce specific control over the catalytic activity of the metal ion present in these complexes. Moreover, this encapsulation is found to be effective for solving the practical problems such as catalyst recovery, product selectivity and environmental safety.

The mechanism<sup>21</sup> of catalytic oxidation of benzaldehyde involves the formation of perbenzoic acid and free peroxy radical through the following chain process:



The metal catalyst initiates the oxidation via a one electron process such as:



The substrate activation by the metal ion catalyst takes place and the aldehyde molecule is converted into a precursor of the final product. It is not possible to say that such a mechanism is operative in the case of present complexes.

The present study is not adequate enough to provide a mechanism for the catalytic activity. The greater activity of all the YABT complexes may be attributed to the easy diffusion of the aldehyde molecule through the pores of the zeolite framework. ABT ligand is smaller in size than VBT and SBT. Another factor to point out in this case of ABT is that, the sulphur atom present in it is coordinated to the metal atom (see Chapter-VII). Coordinated sulphur atom may tune the redox potentials of the oxidized and reduced forms of the metal ions taking part in the reaction.

The highest catalytic activity is facilitated by the Cu(II) complexes. The complexes are found to be square planar in nature and the vacant coordination sites available for the attachment of substrate molecule might be the reason for the increased activity in these cases. Mn(II) and Fe(III) complexes are characterized as octahedral complexes from their magnetic and DRS data. The lower catalytic activities

of these complexes might be due to the absence of vacant coordination sites. However, the removal of the coordinated H<sub>2</sub>O (as evidenced from the IR spectrum) may be responsible for the moderate activity shown by the zeoliteY encapsulated Mn(II) and Fe(III) complexes. The zeoliteY encapsulated SBT complexes are more active than the VBT complexes, which might be due to the steric effect of the –OCH<sub>3</sub> group present in VBT ligand. This effect may reduce the diffusion of benzaldehyde through the “windows” of zeolite cages, and lower the catalytic activity. In the case of simple complexes, VBT complexes are more active than SBT complexes. Here the –OCH<sub>3</sub> group with +I effect, being an activating group, might be fine tuning the redox potentials of metal ions and thus enhancing the catalytic activity of MVBT complexes.

### **VIII.C. Catalytic activity on the oxidation of benzyl alcohol, propan-1-ol and propan-2-ol by acid potassium manganate.**

#### **8.C.1. Introduction.**

Oxidation of alcohols to carbonyl compounds or carboxylic acids over Pt metals or Au has been thoroughly investigated in the past decades<sup>36-38</sup>. The reactions are generally carried out below 100°C under mild conditions and aqueous medium. Instead of aqueous medium an organic solvent has also been proposed<sup>39</sup> but the explosion risk hinders the practical application in these cases. Recently the application of “supercritical” carbon dioxide was reported<sup>40-42</sup> as a substitute for organic solvents in liquid phase oxidation of alcohols.

Oxidation of primary alcohols by acid potassium permanganate was known to be autocatalytic<sup>43</sup>. Acid permanganate being an oxidizing agent oxidizes almost all

simple organic compounds. Oxidation of organic substrates like cinnamic acid<sup>44,45</sup> acetylenic compounds<sup>46</sup> and alcohols<sup>47,48</sup> by acid permanganate has been studied and mechanisms were suggested on the basis of the oxidation and reduction product of permanganate. Oxidations of organic substrates were environmentally essential with respect to pollution control and these reactions are found to be eco-friendly with an inorganic oxidant. Partial oxidation of benzyl alcohol to benzaldehyde<sup>49,50</sup> has been chosen as a model reaction for the synthesis of aromatic aldehydes, which is an important compound for fine chemical synthesis. From both environmental and economic view points there is an urgent demand, for greener and more efficient methods that employ oxidants and recoverable catalysts. Hence, this investigation is aimed at maximizing the conversion of the reactants into the final product, employing recoverable catalysts.

## **8.C.2. EXPERIMENTAL.**

### **8.C.2.1. Potassium permanganate solution.**

A stock solution of potassium permanganate was prepared as given in section 8.B.2.1. for the oxidation of benzaldehyde.

### **8.C.2.2. Perchloric acid solution.**

A stock solution of 0.2 M perchloric acid was prepared as given in the oxidation of benzaldehyde.

### **8.C.2.3. Benzyl alcohol, Propan-1-ol and Propan-2-ol**

The alcohols (benzyl alcohol, propan-1-ol and propan-2-ol) used were of analar BDH grade and were distilled before use.

### **8.C.2.4. Catalysts.**

From the oxidation reaction study on benzaldehyde, it was found that

simple as well as zeoliteY encapsulated cobalt and copper complexes are much more active than that of Mn(II), Fe(III) and Ni(II). Hence the complexes of Co(II) and Cu(II) were selected to study their catalytic activity for the oxidation of benzyl alcohol, propan-1-ol and propan-2-ol by acid potassium permanganate.

### **8.C.2.5. Apparatus and Procedure.**

Apparatus, procedure and reaction conditions used were similar to that of the oxidation of benzaldehyde and the reaction was monitored as a function of absorbance versus time at 546nm. Initial rate method was employed here also to determine the initial rate of oxidation of alcohols (see section 8.B.2.6). Reaction was carried out at a constant temperature of  $30.0 \pm 0.1^\circ\text{C}$ . In a reaction flask distilled water (2.5 ml), perchloric acid (2.5ml, 0.2 M), potassium permanganate solution (5ml,  $8 \times 10^{-4} \text{ mol dm}^{-3}$ ) were taken and shaken well. A small volume (3mL) of this solution was pipetted into the quartz cuvette in the spectrophotometer. Reaction was initiated by transferring 2mg of the catalyst into the cuvette. A stopwatch is started simultaneously. Alcohol (0.5 mL) was then added into the cuvette. Oxidant substrate

mole ratio of 0.01 was maintained through out the experiment. The spectrophotometer was initially adjusted to get the absorbance at every one minute. The progress of the reaction with respect to time was monitored spectrophotometrically, by measuring the absorbance of  $\text{KMnO}_4$  at 546nm, where  $\text{KMnO}_4$  has maximum absorbance and all other reactants and products involved have negligible absorbance. The reaction was monitored for one hour. The initial rates were obtained from the initial slopes of the plots of the absorbance versus time data. This was determined using the polynomial regression method on the software called "AXUM". The initial rates were then obtained by dividing the initial slopes with the molar absorption coefficient of the permanganate. For the comparison of catalytic activities of the simple and zeoliteY encapsulated complexes, the initial rates were then converted to that for unit metal ion concentration in the reaction mixture. This was done by calculating the metal ion concentration in the reaction mixture from the percentages of metal ions in the catalysts (obtained from the elemental analysis data). This calculation is required because the metal ion loading in zeolite system is very small when compared to the simple complexes. The higher rates shown by the simple complexes will be erroneously taken as the greater activity of these complexes. The initial rates so obtained were presented in Table.VIII.3.

In a blank study, the reaction was carried out between acid potassium permanganate and alcohol in the absence of the catalyst. The initial rate of this reaction was very low in the case of blank when compared with their activity in the presence of catalysts. The initial rates obtained for these reactions are also shown in the Table.VIII.3. Two other blank studies were carried out. The first study was on reaction between the acid potassium permanganate and catalysts monitored in the

absence of alcohol. The initial rate values are found to be varying and hence these values are not included in the table. The second study was to see any self-decomposition of acid permanganate in the absence of alcohol and catalysts. There was practically no change in absorbance after monitoring the reaction for one hour, which suggest that self-decomposition of permanganate is nil under the present reaction conditions.

### **8.C.3. Results and Discussion.**

A number of alcohols such as methanol, ethanol, 1-propanol, 2-propanol, butanol, pentanol, cyclohexanol, cresols and benzyl alcohol, and other substrates like toluene, xylenes, benzyl chloride were tried for screening the synthesized samples for the catalytic activity. Enhancement of initial rates of oxidation was observed in all the cases when compared with that of the blank reaction. Even though a number of substrates were used for screening studies, many of them could not be studied due to one or more reasons. In case of methanol and ethanol, the reaction rate was too fast to monitor while that for butanol and pentanol it was too slow. Some others masked the walls of cuvet with a brown deposit. Nevertheless, 1-propanol, 2-propanol and benzyl alcohol were found ideal for monitoring the initial rates of reaction spectrophotometrically. Spectrophotometric study was considered as an easier, reliable and accurate method for monitoring the reactions in which one of the substrate or product have maximum absorption in the UV-Vis region of electromagnetic spectrum preferably in the visible region. The initial rates of reaction so obtained for the oxidation of selected alcohols are given in Table .VIII .3.

The selected catalysts were screened for their catalytic activity in the oxidation of benzyl alcohol, propan-1-ol and propan-2-ol. Oxidant-substrate mole ratio was maintained in all reactions. These reactions were carried out to see whether the catalysts were active for the oxidation of other organic substrates.

**Table. VIII.3**

**Catalytic activity on the oxidation of  
benzyl alcohol, propan-1-ol and propan-2-ol**

**Reaction conditions:**

$$[\text{KMnO}_4] = 4.0 \times 10^{-4} \text{ mol dm}^{-3}; \quad [\text{HClO}_4] = 5.0 \times 10^{-2} \text{ mol dm}^{-3}$$

Benzaldehyde = 0.5 ml; Catalyst = 2 mg, temperature =  $30.0 \pm 0.1^\circ \text{C}$ .

| Catalysts | Initial rate $\times 10^4 \text{ mol dm}^{-3} \text{ min}^{-1}$ |             |             |
|-----------|---|-------------|-------------|
|           | Benzyl alcohol  | Propan-1-ol | Propan-2-ol |
| YCoABT    | 4.8   | 5.5         | 2.6         |
| YCoSBT    | 3.9   | 4.6         | 2.5         |
| YCoVBT    | 3.4   | 4.5         | 2.4         |
| CoVBT     | 1.9   | 1.0         | 1.2         |
| CoSBT     | 1.2   | 0.6         | 1.1         |
| YCuABT    | 7.3   | 7.7         | 3.7         |
| YCuSBT    | 4.9   | 5.3         | 2.6         |
| YCuVBT    | 4.1   | 5.0         | 2.3         |
| CuVBT     | 1.6   | 1.0         | 1.1         |
| CuSBT     | 1.0   | 0.8         | 0.91        |
| Blank     | 0.6   | 0.5         | 0.54        |

Initial rates per metal ion concentration are represented in table.

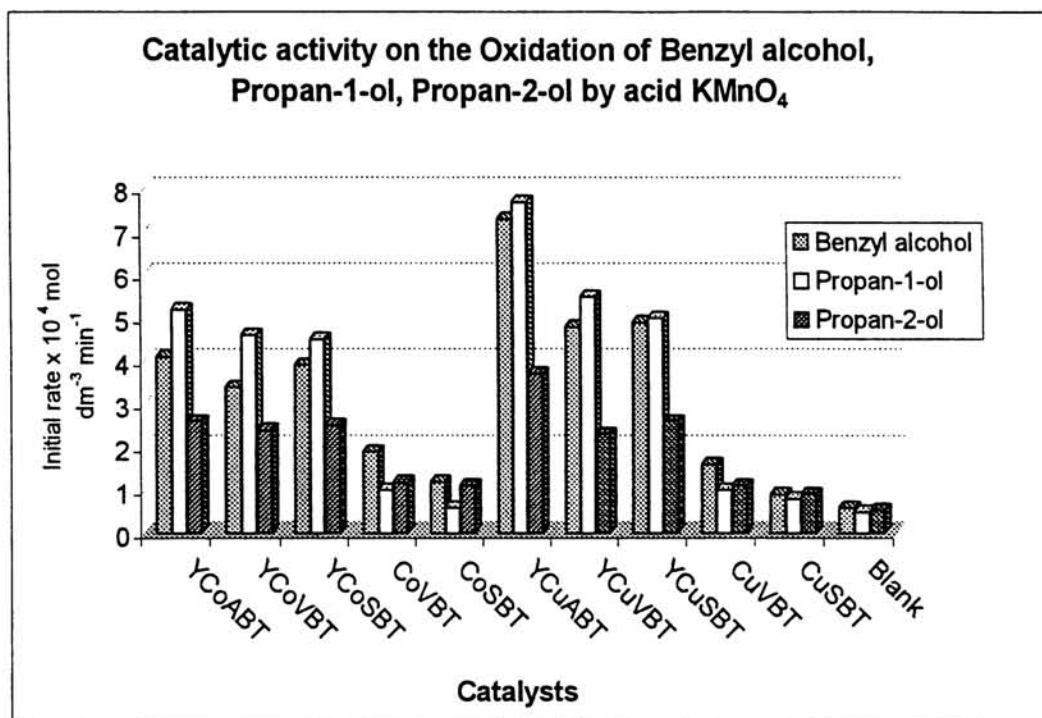


Figure.VIII.C.1. Initial rates of oxidation of alcohols by acid  $\text{KMnO}_4$ .

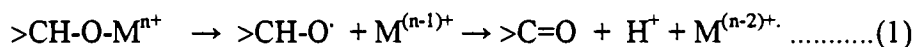
Substantial activities are shown by the catalysts for the oxidation of alcohols. The copper complexes are the most active catalysts for the oxidation reaction. Further, the zeolite encapsulated complexes are found to be highly active than their homogeneous counter parts. The activity for the encapsulated complexes was in the order  $\text{YABT} > \text{YSBT} > \text{YVBT}$ . However, simple complexes show the activity in a different order  $\text{CoVBT} > \text{CuVBT} > \text{CoSBT} > \text{CuSBT}$ . Interestingly it was noted that zeoliteY encapsulated complexes have the substrate preference for greater activity in the order  $\text{Propan-1-ol} > \text{Benzyl alcohol} > \text{propan-2-ol}$ . All the six encapsulated complexes exhibited the same preference order irrespective of the metal ion present in the cavities and irrespective of the ligand coordinated to the central

metal ion. Simple complexes on the other hand have greater activity towards benzyl alcohol. The order of activity of simple complexes in the oxidation of alcohols is as follows:

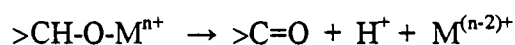


A bar diagram showing the gradation in the initial rates of oxidation of acid potassium permanganate on various alcohols in presence of the selected simple and encapsulated catalysts is given in Figure. VIII.C.1. Since only a small quantity (2mg) of the catalyst was used for a reaction that it was not possible to collect it after use and hence recycling test was not carried out for the reaction. Even then, the insoluble catalyst settled at the bottom has the same colour and texture of the complex, which indicate that no decomposition or leaching of metal ion might have taken place to the complex on usage as the catalyst.

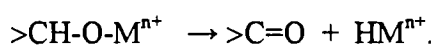
The oxidation of primary and secondary alcohols to aldehydes or carboxylic acids and ketones, respectively, is a pivotal reaction in organic synthesis<sup>51</sup>. Traditionally, such transformations have been performed with stoichiometric inorganic oxidants, notably chromium(VI) reagents. Stoichiometric oxidations of alcohols to carbonyl compounds with oxochromium<sup>52</sup>, manganese(VII)<sup>53</sup> and vanadium(V)<sup>54</sup> reagents are well known. These reactions probably involves<sup>21</sup> the formation of an inner sphere alkoxymetal intermediate that can decompose by either a hemolytic,



or a heterolytic pathway.

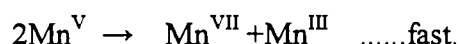
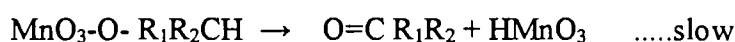
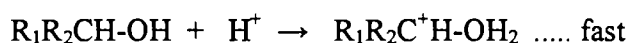


Metals such as Pt(II), Pd(II), Ru(III) and Rh(III) readily oxidize alcohols to carbonyl compounds by a process involving the  $\beta$ -hydride elimination of a metal alkoxide intermediate<sup>55</sup>.



This reaction is often employed for the synthesis of hydrides of the above mentioned metals, but it can also be used as a preparative procedure for the oxidation of alcohols. For example, when  $\text{PtCl}_2(\text{PEt}_3)_2$  is refluxed in ethanol solution of potassium hydroxide, the platinum hydride is obtained together with acetaldehyde.

Suryanarayanamurthy. et al<sup>48</sup> have studied the oxidation of alcohols by acid permanganate and suggested the mechanism on the basis of the oxidation products and reduction product of permanganate as given below.



According to them, the reaction is found to be first order each in substrate and the oxidant and proposed that an “encumbered carbonium ion” be involved in the transition state involving protonation of alcohol. The same suggestion was put forward by early workers<sup>56,57</sup>. The hydride ion may be transferred to permanganate in the rate-determining step through a five membered cyclic transition state.

In the present investigation, attention was virtually focused on the activities of simple and zeolite Y encapsulated complexes to probe the possibilities offered by these catalysts on the oxidation of organic substrates. It can be seen from Table VIII.3. that

all the prepared catalysts show almost drastic enhancement in the initial rate of oxidation of alcohols when compared with that of the blank study in the absence of catalysts. The highest conversion was observed for the YABT complexes, which may be due to the easier diffusion of alcohols through the pores of zeolite cavities. Pore volume and surface area present inside the zeolite cavities of YABT complexes are found to be larger than that of the encapsulated Schiff base complexes. The vacant space inside the pores is greater for these complexes through which the substrate can diffuse at faster rate. The lower conversion over YVBT to that of YSBT complexes was also expected on account of the same reason. The greater activity of Cu(II) complexes may be due to the distorted square planar geometry of the complex. This distortion in zeolite has been thought to arise from the constraints imposed by the cavity and its participation in coordination sphere<sup>58</sup>.

Substrate selectivity of zeoliteY encapsulated complexes was found to be in the order propan-1-ol > benzyl alcohol > propan-2-ol. Shape and size of the substrate greatly influence the easier diffusion of organic molecules through the pores of zeolites. The conformational changes leading to the arc-like shape of propan-2-ol increase the overall strain of the molecules and hence their diffusion through pores becomes difficult<sup>59</sup>. This can be further confirmed by the molecular graphics analysis and textural characteristic measurements. Due to lack of facility, such characterization studies could not be carried out. Over the simple complexes, the order of activity was benzyl alcohol > propan-2-ol > propan-1-ol. The formation of 'carbonium ion' intermediate may be more stabilized by the hyperconjugative effect of the alkyl groups attached to the secondary carbon atom of propan-2-ol over these catalysts. Similarly,

resonance stabilization of benzyl carbonium ion explicates the greater reactivity of benzyl alcohol.

## **VIII-D. Catalytic activity on partial oxidation of cyclohexanol to cyclohexanone by hydrogen peroxide.**

### **8.D.1. Introduction.**

Partial oxidation of cyclohexanol to cyclohexanone is an industrially important reaction extensively used for the production of polyamides, nylon 6,6, urethane foams, adipic acid, lubricating additives etc. The present commercial process for the conversion of cyclohexanol to cyclohexanone involves, passing the substrate over a Cu-SiO<sub>2</sub> catalyst at around 300°C. Since the selectivity is not sufficient with the usual processes, a lot of study was made to enhance the selectivity. Recently zeoliteY encapsulated metal complexes have been extensively used for carbonylation reactions as well as for hydroformylation<sup>60-62</sup> reactions. The [Cu(Salen)] complex encapsulated in supercages of zeoliteY was used for the selective oxidation of cyclohexanol to cyclohexanone using hydrogen peroxide as the oxidant<sup>63</sup>. A selectivity of 98% and conversion rate of 50% were recorded for this reaction. Hydrogen peroxide is recognized as a superior and benign oxidizing agent, which yields only water and oxygen as the decomposition products. Various oxidation reactions have been reported using hydrogen peroxide as oxidant over diversified heterogeneous catalysts such as metal oxides<sup>64</sup>, molecular sieves<sup>63,65</sup>, clays<sup>66</sup>, spinels<sup>67</sup>. It was therefore considered worthwhile to do the oxidation of cyclohexanol to cyclohexanone at a much milder condition using the synthesised catalysts. Two

zeoliteY encapsulated transition metal complexes have been selected as catalysts. The reaction was studied at two different temperatures and at two different time intervals. Both the catalysts were found to be effective in converting cyclohexanol to cyclic carbonyl compound up to 30 to 40% conversion at 70°C.

## **8.D.2. EXPERIMENTAL.**

### **8.D.2.1. Hydrogen peroxide solution.**

Commercially available 30% aqueous solution (Merck) of hydrogen peroxide was used as such for the reaction.

### **8.D.2.3. Cyclohexanol.**

Cyclohexanol (BDH) was obtained commercially.

### **8.D.2.4. Catalysts.**

YCoVBT and YCuVBT are the catalysts selected for the study of their catalytic activity for the oxidation of cyclohexanol by hydrogen peroxide. The catalysts were dried in an air oven before use.

### **8.D.2.5. Apparatus.**

Chemito 8510 GC fitted with Carbowax column, 5% mesh size with FID detector, coupled with PC was used for monitoring the reaction.

### 8.D.2.6. Procedure.

The experimental set up used for monitoring the oxidation reaction is shown in Figure.VIII.D.1.

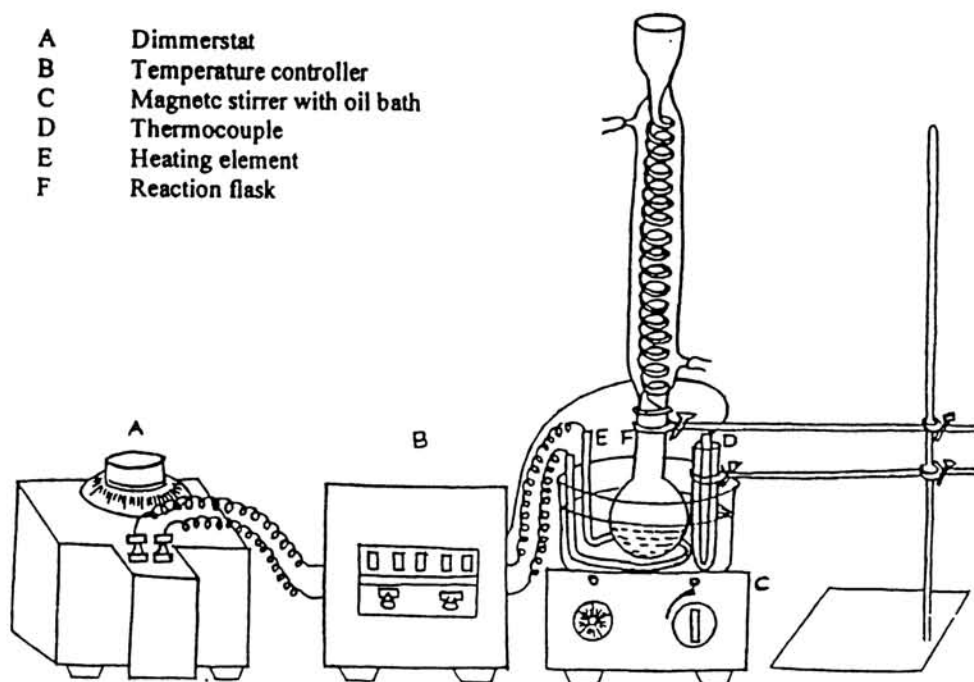


Figure.VIII.D.1. Experimental set up for the oxidation of cyclohexanol.

The catalytic activity of YCoVBT and YCuVBT towards the oxidation of cyclohexanol was carried out by GC method. Cyclohexanol (2mL) was pipetted into a reaction flask (25 mL capacity) fitted with a reflux condenser containing magnetic paddle. A mixture of 30% hydrogen peroxide (3mL) and distilled water (5ml) was used as the oxidant. A catalyst (50mg) was added. The reaction flask was then placed in a water bath over magnetic stirrer to maintain constant room temperature. The reaction mixture in the flask was stirred magnetically. A septum was used to withdraw solution from reaction flask after one hour and after 4hours of stirring. The solution so withdrawn was then extracted with ether. Cyclohexanol and cyclohexanone in the

ether solution were then injected to GC. A similar GC analysis was conducted at 70°C in an oil bath previously set to 70°C using thermo coupled thermostat to maintain the constant temperature. (See Figure.VIII. D.1) Blank studies without catalyst was also carried out at both the temperatures to see whether any oxidation occurs in the absence of catalysts. The results obtained are presented in Table VIII.4. The composition of the mixture was obtained by comparing their gas chromatographs with those of their authentic samples injected to the column.

### **8.D.3. Results and Discussion.**

Oxidation of cyclohexanol to cyclohexanone using hydrogen peroxide as the oxidant was carried out in liquid phase using CuVBT and CoVBT. The reactions were carried out at room temperature and at 70°C. The products were analyzed at two different time intervals (1hr and 4hrs). The catalytic activity was expressed in terms of the percentage conversion of cyclohexanol. The only product identified by GC was cyclohexanone. As can be seen from the Table. VIII.4 that the catalysts show good conversion and excellent selectivity towards the product of interest. It was observed that with the increase of time cyclohexanol conversion was increased upto one hour and thereafter equitable change in conversion was not perceived. The temperature dependence of cyclohexanol conversion was also depicted in the table. It indicates that the increase of temperature increases the cyclohexanol conversion appreciably with a marginal decrease in the cyclohexanone selectivity. The recyclability of the catalysts was tested using the

**Table. VIII.4**

**Catalytic activity on oxidation of cyclohexanol.**

**Reaction conditions:**

Catalysts = 50mg, Cyclohexanol = 2ml (BDH)

Hydrogen peroxide = 3ml (30% aqueous, Merck).

| Catalysts   | Cat/Cyclo Hexanol<br>wt/wt | Reaction temp.<br>K | Time<br>hours | Conversion of cyclo hexanol<br>Wt% | Product selectivity<br>% |        |
|-------------|----------------------------|---------------------|---------------|------------------------------------|--------------------------|--------|
|             |                            |                     |               |                                    | Cyclo hexanone           | Others |
| Y-<br>CuVBT | 0.025                      | 303                 | 1             | 2.18                               | 100                      | -      |
|             |                            |                     | 4             | 3.15                               | 100                      | -      |
|             |                            | 343                 | 1             | 27.05                              | 98.25                    | 1.75   |
|             |                            |                     | 4             | 33.2                               | 97.7                     | 2.3    |
| Y-<br>CoVBT | 0.025                      | 303                 | 1             | 7.57                               | 100                      | -      |
|             |                            |                     | 4             | 11.43                              | 100                      | -      |
|             |                            | 343                 | 1             | 11.04                              | 98.00                    | 2.00   |
|             |                            |                     | 4             | 39.40                              | 97.51                    | 2.49   |

spent catalysts. After the reaction the catalysts were filtered, washed, dried and reused for the another batch of reaction. It was found that the catalysts were still active for the reaction and only a slight decrease in conversion was noticed. YCuVBT was found more active than YCoVBT which, may be attributed to the structural features of this complex with in the zeolite cavities.

\*

## REFERENCES

1. H.F. Leach, *Ann. Rep.*, 68A, (1971),195.
2. I. Mochida, S.Hayata, A.Kato and T. Seiyama. *J.Catal.* 15, (1969),314.
3. J Rouchand and J Mawaka, *J. Catal*, 19, (1970),172 .
4. I Mochida, T. Jitsumatsu, A.Kato and T. Seiyama. *Bull. Chem. Soc. Jap.*44, (1971),2595.
5. Isao Mochida and Kenjiro Takeshita. *J. Phys.Chem* , 78, (1976), 16.
6. Isao Mochida, Akio Kato and Tetsuro Seiyama. *Bull. Chem. Soc. Jap*, 45, (1972),2230.
7. Chandra Ratnasamy, Anupa Murugkar and Subhash Padhye.  
*Ind. J.Chem*, 35A, (1996), 1-3.
8. Trissa Joseph, C.S. Sajanikumari, S.S Desh Pande and Sarada Gopinathan. *Ind. J.Chem*, 38A, (1999), 792-796.
9. D. Bhattacharya, A.K Pandey and A.D Singh. *Recent advances in Basic and Applied aspects of Industrial Catalysis*, Vol.113,(1998)Elsevier Science (BV).
10. Bowers.C and Dutta.P.K., *J.Catal*, 122, (1990), 271.
11. Gellin.P, Naccache.C and Tarrit.Y.B, *Pure Appl. Chem.* 8 ,(1988), 1315.
12. Auroux.A, Bolis.V, Wierachoski.P, Grzvelle.P and Vedrine.J, *J. Chem. Soc. Faraday. Trans* , (1979) 2544
13. Iwamoto.M, Kusano.H and Kagawa.S, *Inorg.Chem.*22, (1983), 3366.
14. Kowalak.S., Weiss R.C. and Balkus.K.J.Jr, *J.Chem.Soc., Chem Commun.* (1991), 57.
15. N.Ulgappan and V.Krishnasamy . *Ind.J.Chem*, 35A ,(1996), 787-789.

16. Terrence J. Collins., *Acc. Chem. Res* 27,, (1994), 279-285.
17. Jones C.W., *Applications of Hydrogen Peroxide and Derivatives*, Royal Society of Chemistry, Cambridge, (1999).
18. V.S.Sharma and J.Schubert, *J.Am.Chem.Soc*, 91,(1969), 6291.
19. N. Uri, *Chem. Rev.* 50, 375 (1952), J.H.Baxendale, *Advan. Catal. And Related Subjects* ,4, (1952),31.
20. S.K.Sengupta and L.Preethi, *Ind.J.Tech.*, 30, (1992), 172.
21. R.A.Sheldon and J.K.Kochi. *Metal Catalysed Oxidations of Organic Compounds*, Academic Press, New York (1981)
22. J. Peisavh, P.Aisen and W.E. Blumberg, "*The Biochemistry of Copper*", Academic Press, New York (1966)
23. H. Sigel and T.Kaden, *Helv. Chim. Acta*, 51, (1968),947.
24. A.I. Vogel., *A Text Book of Qualitative Inorganic Analysis*; Longmans –Green; London. (1978).
25. G. Sosnovsky, in "*organic peroxides*", D. Swern.ed., Wiley Interscience, New York, (1971).
26. C.Walling., *Accts. Chem. Res.*, 8, (1975), 125.
27. Collins T.J., Designing ligands for oxidizing complexes, *Accts. Chem. Res*, 27, (1994), 279-285.
28. H. Sigel., *Angew. Chem. Int Ed.Engl*, 8, (1969), 167.
29. Geoffrey A. Ozin and Carolin Gil., *Chem.Rev*, 89, (1989), 1749-1764.
30. M.L.Kremer and G.Stein., *Trans Faraday Soc*, 55, (1959), 595, M.L.Haggett, P.Jones and W.F.K.Wynne-Jones *Trans Faraday Soc*, 56, (1960), 153.
31. Isao Mochida and Kenjiro Takeshita. *J. Phys.Chem* , 78, (1976),16.

32. R.V.Prasad and N.V.Thakkar, *Ind.J.Chem*, 33A, (1994), 861.
33. K.O.Xavier, Ph. D Thesis submitted to Cochin University, Kochi, (2000).
34. Khandval. N.C. and Nayak. P.L., *J. Ind.Chem. Soc*, 50, (1973), 317.
35. Cooper. T.A. and Waters.W.A., *J.Chem. Soc*, (1964), 1536.
36. T. Mallat and A. Baiker., *Catal Today*.,19, (1994), 247.
37. M.Besson and P.Gallezot., *Catal Today*. 57, (2000), 127.
38. J.H.J. Kluytmans, A.P. Markusse, B.F.M. Kuster, and G.B.Marin., *Catal Today*. 57, (2000), 143.
39. K.Heyns and L.Blazejewicz., *Tetrahedron*, 9, (1960), 67.
40. G. Jenzer, D. Sueur, T. Mallat and A. Baiker.,*J.Chem.Soc. Chem.Commun*, (2000), 2247.
41. G. Jenzer, T. Mallat and A. Baiker., *Catal. Letters*., 73,(2001), 1, 5-8.
42. Steele, J.Zhu and S.C.Tsang., *Catal. Letters*.,73, (2001),1, 9-13.
43. Benarjee K.K, *J.Chem.Soc. B*(1973) 435.
44. Lee.D.G and Brownridge J.R, *J.Am.Chem.Soc*,95, (1973), 3033.
45. Wiberg K.B, Deutsch C.J and Rocek J, *J.Am.Chem.Soc.*, 95, (1973), 3034.
46. Jaky. M. and Simandi L.I., *J.Chem.Soc.*, B,(1972) ,1481.
47. Fariza , Banoo and Ross Stewart, *Can.J.Chem*, 47,(1969) ,3199.
48. N. Suryanarayana Murthy and E.V Sundaram, *Ind.J.Chem* ,16A ,(1978), 806.
49. R Sumati K Johnson, B Viswanathan and T.K. Varadarajan. *Ind.J.Chem*,38A, (1999),40.
50. M.M. Heravi, R.Kiakojoori and M.M Mojtahedi,*Ind.J.Chem*, 40B,(2001) 329.
51. Hudlicky. M., "*Oxidations in organic chemistry*", *J. Am. Chem. Soc*,(1990).

52. K.B.Wiberg.,in "*Oxidations in Organic Chemistry*", (K.B.Wiberg,ed.), Part .A, P.69, Academic press, New York,(1965).
53. R.Stewart., in "*Oxidations in Organic Chemistry*"(K.B.Wiberg,ed.), Part .A, p.2, Academic press, New York,(1965).
54. W.A. Waters and J.S. Littler., in "*Oxidations in Organic Chemistry*"(K.B.Wiberg,ed.), Part .A, p.186, Academic press, New York,(1965).
55. H.D.Kaesz and R.B. Saillant, *Chem. Rev.*,72,(1972), 231.
56. Boyd. R.H, Taft. (Jr), R.W.Wolf and Chrisyman . D.R., *J.Am. Chem.Soc.*, 82, (1960), 4729.
57. Schubert.W.M, Lamm.B and Keefee.J.R., *J.Am. Chem.Soc.*, 86, (1964), 4727.
58. Bhadbhade. M.M and Srinivas .D., *Inorg Chem*, 32, (1993), 5458.
59. S.P. Katare, S.B.Waghmode, R.Vetrivel, Veda Ramaswamy, and S.Sivasanker., *Recent Trends in Catalysis*.V.Murugesan(Eds.), Narosa Publishing House, New Delhi, (1999).
60. Auroux.A, Bolis.V, Wierzchowski. P, Grzielle.P and Vedrine.J., *J.Chem.Soc.Faraday Trans*, (1979),2544.
61. Iwamoto.M, Kusano.H and Kagawa.S., *Inorg.Chem*, 22, (1983), 336.
62. Mantooani.E, Palladino. N and Zarrobi.A.,*J.Molec. Catal*, (977), 285.
63. Chandra Ratnasamy, Anupa Murugkar and Subhash Pandhye., *Ind.J.Chem*, (1996), 1-3.
64. S.Goldstein,G. Czapski and J.Robani., *J.Phys.Chem*, 98, (1994), 6586.
65. J.S. Reddy and S.Sivasankar., *Catal.Lett*, 11, (1992), 241.
66. M.A.Camblor, A.Corma, A.Martinez, and J.Perez-Pariener., *J.Chem. Soc.Chem.Commun.*, (1992), 589.

67. Y. Yang, J.F. Yu, T.H. Wu and J.Z. Sun., *Chin. J. Catal*, 18, (1997), 126.

\*

## SUMMARY AND CONCLUSIONS.

This thesis deals with studies on the synthesis and characterizations of some simple and zeoliteY encapsulated complexes of Mn(II), Fe(III), Co(II), Ni(II) and Cu(II) and on the catalytic activity of these complexes on some oxidation reactions. Simple complexes were prepared from the Schiff base ligands SBT derived from 2-aminobenzothiazole and salicylaldehyde and the ligand VBT derived from 2-aminobenzothiazole and vanillin (4-hydroxy-3-methoxybenzaldehyde). ZeoliteY encapsulated Mn(II), Fe(III), Co(II), Ni(II) and Cu(II) complexes of Schiff base ligands SBT and VBT and also of 2-aminobenzothiazole were synthesized. All the prepared complexes were characterized using the physico-chemical techniques such as chemical analysis (employing AAS and CHN analyses), magnetic moment studies, conductance measurements and electronic and FTIR spectra. EPR spectra of the Cu(II) complexes were also carried out to know the probable structures and nature of Cu(II) complexes. Thermogravimetric analyses were carried out to obtain the information regarding the thermal stability of various complexes. The successful encapsulations of the complexes within the cavities of zeoliteY were ascertained by XRD, surface area and pore volume analysis. Assignments of geometries of simple and zeoliteY encapsulated complexes are given in all the cases. Both simple and zeoliteY encapsulated complexes were screened for catalytic activity towards oxidation reactions such as decomposition of hydrogen peroxide, oxidation of benzaldehyde, benzyl alcohol, 1-propanol, 2-propanol and cyclohexanol.

The thesis consists of 8 chapters. **Chapter I** of the thesis gives a general introduction to the simple and zeoliteY encapsulated Schiff base complexes. The chapter also includes information regarding the development in the field of homogeneous and heterogeneous catalytic systems and the scope of the present investigation.

**Chapter II** is on the experimental techniques used for the preparation and purification of ligands, simple complexes and encapsulation procedure of zeoliteY complexes. The various physico-chemical techniques used for the characterization of simple and zeoliteY encapsulated complexes are presented in this chapter.

In **Chapter III**, details regarding the studies on the synthesis and characterization of SBT complexes of Mn(II), Fe(III), Co(II), Ni(II) and Cu(II) are presented. All the complexes are coloured and crystalline. They are soluble in methanol, ethanol, acetone, and nitrobenzene and are found to be stable for a long period. Analytical data shows that the complexes have the empirical formulae  $[M(SBT)_2(H_2O)_2]$  for Mn (II) complex,  $[M(SBT)(NO_3)_2(H_2O)_2]$  for the Fe(III) complex and  $[M(SBT)(Cl)(H_2O)]$  for the Co(II), Ni(II), and Cu(II) complexes. The complexes are nonelectrolytes in nitrobenzene. FTIR spectra suggest that the ligand SBT is acting as a bidentate ligand, coordinating through the nitrogen atom of the azomethine group and oxygen atom of the phenolic group. Magnetic moment values and electronic spectral analyses have been carried to arrive at the structure of the complexes. Mn(II) and Fe(III) SBT complexes are octahedral, CoSBT is tetrahedral and Ni(II) and Cu(II) SBT complexes are square planar in nature. The EPR parameters for copper(II) complex also suggest a square planar geometry for this complex.

**Chapter IV** deals with the synthesis and characterization of Mn(II), Fe(III), Co(II), Ni(II) and Cu(II) complexes of the Schiff base ligand VBT. Complexes have the empirical formulae,  $[\text{Mn}(\text{VBT})_2(\text{Cl})_2]$  for the Mn(II) complex,  $[\text{Co}(\text{VBT})(\text{H}_2\text{O})_2]\text{Cl}_2$  for the Co(II) complex and  $[\text{M}(\text{VBT})\text{Cl}_2]\cdot\text{H}_2\text{O}$  for Cu(II) and Ni(II) complexes. The Fe(III) complex has the empirical formula  $[\text{Fe}(\text{VBT})(\text{NO}_3)_2(\text{H}_2\text{O})(\text{OH})]$ . The molar conductance data suggest that the Mn(II), Fe(III), Ni(II) and Cu(II) complexes exist as non-electrolyte in methanol, while Co(II) complex exists as 1:2 electrolyte. Electronic spectra and magnetic moments of complexes suggest octahedral structures for the Mn(II) and Fe(III) complexes. Tetrahedral structure for the Co(II) complex and square planar structures for Cu(II) and Ni(II) complexes. The EPR parameters for the CuVBT complex suggests that the complex is more ionic and has square planar structure. FTIR spectra of complexes suggest that ligand VBT is bidentate and coordinates to the metal through the nitrogen atom of the azomethine group and the sulphur atom of the thiazole ring in all the complexes.

**Chapter V** presents studies involving the preparation and characterization of zeolite Y encapsulated SBT complexes of Mn(II), Fe(III), Co(II), Ni(II) and Cu(II). The analytical data shows that the Si /Al ratio is 2.43 for NaY, which corresponds to the idealized unit cell formula of  $\text{Na}_{56}[\text{AlO}_2]_{56}(\text{SiO}_2)_{136}\cdot n\text{H}_2\text{O}$  for the parent zeolite-NaY. The Si /Al ratio of parent, metal exchanged zeolites and encapsulated complexes are found to be the same indicating that dealumination has not taken place during ion exchange and complexation process. Surface area, pore volume analyses, XRD patterns and FTIR also indicate the retention of zeolite framework and the encapsulation of complexes within the cavities. SEM of one zeolite encapsulated

complex (YCoSBT) before and after soxhlet extraction indicates that complexes adsorbed on the surface of zeolite framework has been removed by soxhlet extraction. Analytical data, magnetic moment measurements and DRS spectra show that zeolite encapsulated Mn(II) and Fe(III) complexes have octahedral, Co(II) has tetrahedral and Ni(II) and Cu(II) complexes have square planar structures. EPR spectral data also suggest a square planar structure to the YCuSBT complex. Ligand SBT is coordinated to the metal ion through the nitrogen atom of the azomethine group and oxygen atom of phenolic group. TG data indicate that the decomposition temperature for the encapsulated complexes is higher than that of the simple complexes suggesting the higher thermal stability for the encapsulated complexes.

**Chapter VI** contains the details of preparation and characterization of zeoliteY encapsulated complexes of Mn(II), Fe(III), Co(II), Ni(II) and Cu(II) with the Schiff base VBT. Magnetic moments and DRS spectral data suggests octahedral geometry to Mn(II) and Fe(III) complexes, distorted tetrahedral structure to Co(II) complex and square planar geometries to Ni(II) and Cu(II)VBT complexes. FTIR spectral data indicate that the coordination of ligand VBT through sulphur atom of thiazole ring and nitrogen atom of the azomethine group. High thermal stability and low loading of the metal complexes in voids of zeoliteY are suggested by thermal analysis.

In **Chapter VII**, details regarding the preparation and characterization of zeoliteY encapsulated 2-aminobenzothiazole (ABT) complexes of the metal ions Mn(II), Fe(III), Co(II), Ni(II) and Cu(II) are presented. The analytical data indicate 1:2 metal to ligand mole ratio. Assignment of geometries was not possible in the case of Mn(II) and Fe(III) complexes. Tetrahedral structure is assigned to Co(II) complex and

square planar structures is assigned to the, Ni(II) and Cu(II) complexes. The ligand ABT acts as a monodentate ligand coordinating through the S-atom of the thiazole ring.

**Chapter VIII** deals with the application of all the synthesised complexes as catalysts for the decomposition of hydrogen peroxide, oxidation of benzaldehyde, benzyl alcohol, propan-1-ol and propan-2-ol by acid potassium permanganate and for the oxidation of cyclohexanol by hydrogen peroxide. All the prepared complexes are found to be effective for these oxidation reactions. Catalytic activity of simple complexes are compared with that of zeoliteY encapsulated complexes. In all the cases zeoliteY encapsulated complexes are found to be far more active than simple complexes. Encapsulated Cu(II) complexes are the most active catalysts. Vacant coordination sites in the square planar geometry of the Cu(II) complex in both simple and zeoliteY cavities may be the reason for the high activity exhibited by these complexes. Fine tuning of the redox potentials of this metal ion might be taking place in this geometry than in complexes of other metal ions. Among the simple and zeoliteY encapsulated complexes, encapsulated ABT complexes are catalytically more active than the encapsulated as well as the simple Schiff base complexes. The small size of this ligand might help the easy diffusion of reactant molecule through the windows of zeoliteY matrix. The encapsulated SBT complexes are second in position for the highest catalytic activity. The VBT complexes exhibit the highest catalytic activity among the simple complexes. The activating groups –OH and –OCH<sub>3</sub> present in VBT ligand, which is in conjugation with the coordinate bond may enhance the activity of these complexes. In both VBT and ABT complexes S-atom is coordinated

G 8498

to the metal ion. This may help the metal ion in tuning the redox potentials. Geometry of the complexes also plays vital role in variation of catalytic activity.

\*\*\*